ASSOCIATION, ROUTING AND SCHEDULING ALGORITHMS FOR ENHANCING THROUGHPUT AND FAIRNESS IN WIRELESS MESH NETWORKS

BY LIN LUO

A dissertation submitted to the

Graduate School—New Brunswick

Rutgers, The State University of New Jersey

in partial fulfillment of the requirements

for the degree of

Doctor of Philosophy

Graduate Program in Electrical and Computer Engineering

Written under the direction of

Prof. Dipankar Raychaudhuri

and approved by

_____

_____

_____

_____

New Brunswick, New Jersey

October, 2010

ABSTRACT OF THE DISSERTATION

Association, Routing and Scheduling Algorithms for Enhancing Throughput and Fairness in Wireless Mesh Networks

by Lin Luo

Dissertation Director: Prof. Dipankar Raychaudhuri

Wireless mesh networks (WMNs) have emerged as a promising step towards the goal of ubiquitous broadband wireless access due to the ease of deployment and its low cost. Current research on WMNs aims at a number of challenges, including capacity limitation and poor fairness.

In this thesis we carefully design association, routing and scheduling algorithms to enhance throughput and fairness in WMNs. The association mechanism specified by the IEEE 802.11 standard is based on the received signal strength. Employing this mechanism in WMNs may only achieve low throughput and low user transmission rates. We develop a new association framework in order to provide optimal association and network performance in WMNs. In this framework, we first propose two new access link metrics that are aware of channel condition, channel access contention as well as AP load. We then extend association mechanisms based on such metrics in a cross-layer manner taking into account information from the routing layer, in order to fit it in the operation of WMNs. We evaluate the performance of our system through simulations, and show that WMNs that use the proposed association mechanism can achieve up to 100% improvement in throughput and delay.

Contention-based MAC protocols such as 802.11 greatly limit the throughput and fairness of WMNs. Significantly higher throughput and fairness are achievable if bandwidth is carefully allocated and transmissions are scheduled. To study the performance limits of WMNs, we first optimally allocate bandwidth to each data flow, jointly computing the user-router association and backbone routing solutions, such that network throughput can be maximized while certain fairness is achieved. We then focus on the integral association, single-path routing case and investigate the optimal performance of a WMN on a given tree topology. We also develop an efficient scheduling algorithm to coordinate channel access and to enforce the allocated bandwidth. Our evaluation shows that association and routing have a great impact on bandwidth allocation, namely constructing a good topology can improve throughput while enhancing fairness.

Finally, multiple channel and Multiple-Input-Multiple-Output (MIMO) are two technologies being introduced into WMNs to mitigate interference and increase network capacity. Higher layer protocols need to be aware of these techniques in order to fully leverage their benefits, which makes cross-layer approach desirable. We first formulate a cross-layer optimization framework for maximizing an aggregate utility, which jointly allocates link bandwidth for data flows, and determines channel assignment and MIMO stream selection. We then present an efficient MIMO-aware scheduling algorithm called stream controlled multiple access (SCMA). SCMA determines a baseline schedule in the channel assignment stage where a set of non-interfering links are scheduled on each channel. The second stage of SCMA, link pairing, takes advantage of the performance gain of MIMO stream control. SCMA also incorporates a congestion control scheme at traffic sources to prevent the network from being overloaded. Simulation results show that the MIMO-aware scheduling algorithm leads to about 50%$\sim$100% higher throughput while preserving fairness than the MIMO-oblivious algorithm. It achieves close-to-the-optimal performance in certain scenarios.

Acknowledgements

This thesis is the end-of-journey harvest of years of hard work whereby I have been inspired and encouraged by many people. It is my greatest pleasure to express my deepest and sincerest gratitude for all of them.

This thesis would not exist without my advisor, Professor Dipankar Raychaudhuri. His enlightening guidance, colossal support and sincere friendship helped me from day one and throughout my graduate study. I am grateful that he gave me enough freedom in selecting my topics and for trusting me with my work. I would also like to disclose my sincere gratitude to my co-advisor, Dr. Hang Liu, for his great guidance and direction for my research, for his patience with me and for being not only my advisor but also my friend. I would also like to express my gratitude to Professor Roy Yates and Professor Wade Trappe for their expertise and valuable feedbacks on this work. I further present my gratefulness to all of my colleagues in WINLAB.

I'm deeply indebted to my parents, whose unconditional love and support has accompanied me throughout my life. There can never be enough words to express how much I appreciate them for their trust in me, their patience and everything else they have done for me. I owe my thanks to my dear sister who helps me fulfill my obligation to take good care of my parents when I am far away from home. My husband, Xiaojun Tang, has always been the source of strength, love and confidence. I owe my deepest appreciation to him. Finally, but not least, I would like to express my thanks to my lovely daughter, Chloe, who makes me happier and stronger.

Table of Contents

List of Figures

Chapter 1

Introduction

With the widespread use of mobile devices such as laptop computers, cellular phones, and PDAs, wireless access to the Internet has become important. Wireless Internet access has been mainly achieved via a single wireless hop, either to base stations for cellular data, or to access points for wireless LAN access. Recently wireless mesh networks (WMNs) [84] [44] have emerged as a promising step towards the goal of ubiquitous broadband wireless access, and quickly become an intensive research topic. The leading exponents of this increased interest in WMNs are the provision of a low cost and reliable extension to the wired infrastructure [43].

A typical WMN has a hierarchical architecture, as shown in Figure 1.1. The upper layer is based on gateways, which are special wireless routers with a high-bandwidth wired connection to the Internet backbone. The middle layer employs wireless mesh routers that provide network access to mobile users (e.g., laptops, PDAs) and interconnect with each other via wireless links. Gateways and mesh routers form a wireless backbone communication system, providing each mobile user with a low-cost, high-bandwidth, and seamless multi-hop connectivity. In WMNs, most users wish to connect to the Internet, though some of them are beyond transmission range of a mesh router that has Internet connection (i.e., gateway). This happens where wireline Internet access and/or existing one-hop wireless access is too expensive to set up because of low utilization. Mesh routers are required to forward others' packets in a peer-to-peer mode, while they communicate to the Internet via a gateway [44]. A path in wireless mesh networks thus typically includes multiple router to router hops and a single router to user hop.

A distinguishing feature of wireless mesh networks, especially large-scale urban mesh

networks, is the presence of a large number of mesh routers, each with relatively small coverage. This contrasts cellular networks that have far fewer infrastructure nodes, each with large regions of coverage. Compared with mobile ad hoc networks (MANETs), wireless sensor networks (WSNs), and infrastructure-based mobile cellular networks, WMNs offer several distinct features:

- The mesh routers in a mesh network are powered, and hence the energy is not a critical concern.
- Unlike nodes in MANETs, mesh routers are commonly stationary. This allows the mesh routers to make intense measurements of the environment. For example, it is possible for mesh routers to make detailed channel measurements and estimate the channel model parameters. Since this estimation can proceed continuously, detailed channel models are feasible.
- In general MANETs, the common assumption is that any node is equally likely to be the source or the destination of a traffic flow, while in WMNs most of the traffic is expected to flow between the users and the Internet (via the gateways).

Despite recent advances in WMNs, there is still a wide range of different open research issues. First, the user-router association is an important issue, which greatly affects the network throughput, fairness, and the provision of user quality-of-service (QoS) requirements. In current implementations of WLANs, each user station (STA) scans the wireless channel to detect the access points (APs) nearby and associate itself with the AP that has the strongest received signal strength indicator (RSSI). With this approach, it is expected that an STA associates itself with the closest/strongest AP. However recent studies have shown that this policy can lead to inefficient use of the network resources [93] [14] [99]. The most important disadvantage of RSSI-based user association is that RSSI does not provide any information about the current load of the AP. Moreover, the association problem in wireless mesh networks must be dealt with differently compared to the problem in conventional infrastructure wireless networks without wireless backbones. In particular, the packet routing performance on

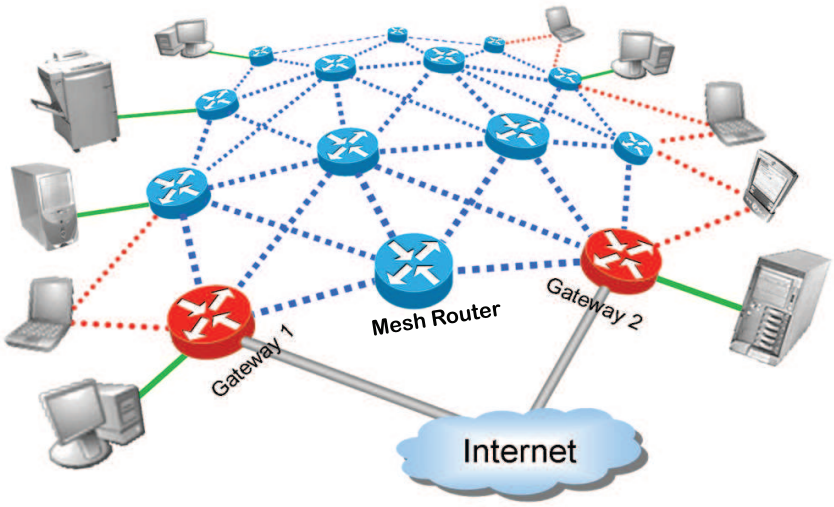

Figure 1.1: Illustration of a wireless mesh network

the backbone can no longer be considered negligible due to lower physical transmission rates and wireless channel contention.

In this thesis, we develop an easy-to-implement user association framework for wireless mesh networks in order to provide optimal association and network performance. The proposed mechanism is designed to be compliant with the current 802.11 standards, and it is shown to significantly improve the network performance in terms of throughput and end-to-end delay under different operational scenarios. In this framework, we first propose two new access link metrics that are aware of channel condition, channel access contention as well as AP load. We then extend association mechanisms based on such metrics in a cross-layer manner taking into account information from the routing layer, in order to fit it in the operation of WMNs. Specifically, the user combines information about links between itself and candidate routers as well as information about the routing of the packets from those routers to the gateway. In such a way, the association decision is based on the end-to-end transmission capability of mesh routers and thus it has the promise to increase the overall throughput of the mesh network. We evaluate the performance of our system through simulations, and show that WMNs that use the

proposed association mechanism can achieve up to 100% improvement in throughput and delay.

Interference and collisions greatly limit the throughput and fairness of wireless mesh networks that use contention-based MAC protocols such as 802.11. It is widely believed that significantly higher throughput and fairness are achievable if bandwidth is carefully allocated and transmissions are scheduled. On one hand, we would like to improve the overall network utilization by maximizing the total throughput from all data flows. On the other hand, fairness among flows must be maintained to guarantee the performance of individual flows. Therefore, an important goal of bandwidth allocation is to maximize the utilization of network resources while sharing the resources in a fair manner among network flows. To strike a balance between fairness and throughput, max-min fairness [15] has been proposed and become a widely studied criterion in the network community.

In this thesis, we attempt to find the performance limits of the target wireless mesh networks by optimally allocating bandwidth to each data flow and enforcing the allocated bandwidth via scheduled channel access. We first optimally allocate bandwidth to each data flow, jointly computing the user-router association and backbone routing solutions, such that network throughput can be maximized while max-min fairness is achieved. Two scenarios are considered: (1) fractional association and multi-path routing and (2) integral association and single-path routing. The reason for the joint optimization is that bandwidth allocation is dependent on the user-router association and the backbone routing. Association and backbone routing organize the physical links into a logical communication topology. The logical topology accordingly determines the traffic flows for each link and have an impact on the extent to which link transmissions interfere, which certainly affects bandwidth allocation to individual flows. We then focus on the integral association, single-path routing case and investigate the optimal performance of a WMN on a given tree topology. We also develop an efficient scheduling algorithm to coordinate channel access and to enforce the allocated bandwidth. Our evaluation shows that association and routing have a great impact on bandwidth allocation, namely constructing a good topology can improve throughput

while enhancing fairness.

To reduce interference and improve network capacity, some techniques such as multi-channel and Multiple-Input-Multiple-Output(MIMO) are being introduced into wireless mesh networks. By exploiting multiple channels, we can achieve a higher network throughput than using one channel, because multiple transmissions can take place in a neighborhood without interfering. The IEEE 802.11b standard and IEEE 802.11a standard [2] [3] offer 3 and 12 non-overlapping channels respectively. Multiple channels introduce the issue of channel assignment, that is, which of the 3 or 12 radio channels should be assigned to a given interface? On one hand, for two nodes to communicate with each other, their interfaces need to be assigned to a common channel. On the other hand, if the sending interface of one transmission is in the interference range of the receiving interface of another transmission and if the two interfaces are assigned to the same channel, then the former transmission would interfere with the latter one. Channel assignment aims to ensure the connectivity for intended transmissions while minimizing the interference. MIMO employs multiple antenna elements to offer multiple Degrees of Freedom (DOFs) for communications in a node. A transmitting node can divide the incoming data flow into multiple independent data streams and transmit them simultaneously over multiple antenna elements. The intended receiving node is able to separate and decode the received data streams based on their spatial signatures. This special feature is referred to as spatial multiplexing [56]. In addition, one or more antenna elements in a receiving node can also be used to suppress the interference from other links in a common neighborhood. Due to spatial multiplexing and interference suppression, MIMO links can significantly improve network throughput. Therefore, they are especially desirable for multihop wireless networks with heavy traffic demands, such as wireless mesh networks. Use of MIMO in WMNs also poses a new challenge: how should the DOFs of each node be allocated (transmit, receive or suppress interference) at certain times? This is referred to as the stream control problem in [56] [16].

To fully leverage the benefits of multi-channel and MIMO, higher layer protocols need to be aware of these techniques, which makes cross-layer approach desirable. In Chapter 4 of this thesis, We first formulate a cross-layer optimization framework for

maximizing an aggregate utility, which jointly allocates link bandwidth for data flows, and determines channel assignment and MIMO stream selection. We then present an efficient MIMO-aware scheduling algorithm called stream controlled multiple access (SCMA). SCMA determines a baseline schedule in the channel assignment stage where a set of non-interfering links are scheduled on each channel. The second stage of SCMA, link pairing, takes advantage of the performance gain of MIMO stream control. SCMA also incorporates a congestion control scheme at traffic sources to prevent the network from being overloaded. We present simulation results to show that the MIMO-aware scheduling algorithm leads to about 50%$\sim$100% higher throughput while preserving fairness than the MIMO-oblivious algorithm. It achieves close-to-the-optimal performance in certain scenarios.

The rest of the thesis is organized as follows. Chapter 2 presents the end-to-end performance based association mechanism, in which information from the routing layer is incorporated in a cross-layer manner. We present the simulation results to show that WMNs that use the proposed association mechanism can achieve up to 100% improvement in throughput and delay. In Chapter 3 we formulate the topology optimization and fair bandwidth allocation problem to find the performance limits of WMNs in different operational scenarios. We also provide a scheduling algorithm to coordinate the channel access and enforce the allocated bandwidth. In Chapter 4 we study multi-channel MIMO mesh networks. We first give the performance bound by jointly allocating link bandwidth for data flows, and determining channel assignment and MIMO stream selection, and then present an efficient MIMO-aware scheduling algorithm called SCMA. We show that SCMA leads to 50%$\sim$100% higher throughput while preserving fairness than the MIMO-oblivious algorithm. It achieves close-to-the-optimal performance in certain scenarios. Chapter 5 concludes this thesis work and outlines the future work.

Chapter 2

End-to-End Performance Based Association Protocol

User-router association is a critical problem in wireless mesh networks. It determines the per-AP traffic load as well as the traffic distribution on the mesh backbone. It therefore has a great impact on the network performance.

2.1 Background and Related Work

Although receiving a lot of criticism due to its performance inefficiency in wireless multihop networks, 802.11 MAC protocol has been adopted as the de facto standard for first-generation WMNs due to its wide popularity. Recently, the IEEE 802.11s task group was formed to work on an infrastructure mesh amendment (802.11s [5]) to allow 802.11 access points or cells to self-configure into multi-hop wireless topologies. In WMNs, Backbone routing and user-router association both have great impacts on the network performance. Routing algorithms and routing metrics for the wireless multihop networks have been extensively researched, but association mechanism for WMNs has been left untouched. In this chapter we try to fill this void.

2.1.1 Wireless Multi-Hop Routing

Traffic routing for wireless mesh backbone plays a critical role in determining the performance of a wireless mesh network. It has received extensive attentions in recent studies.

AODV-ST [55] is a hybrid routing protocol designed for WMNs. It uses proactive tree formations by using a beaconing protocol initiated at the gateways to form spanning trees rooted at the gateway. For intra-mesh routing, it uses AODV [19] to discover routes that bypass the gateways. The main assumption in AODV-ST is that

the common-case traffic is to and from the gateway, and, thus, uses the proactively constructed trees.

IEEE 802.11s [5] draft standard defines a default mandatory routing protocol (Hybrid Wireless Mesh Protocol, or HWMP) to provide both on-demand routing for predominantly mobile topologies and proactive tree-based routing for predominantly fixed infrastructure networks. The on-demand routing protocol is based upon AODV which uses a simple hop count routing metric. HWMP makes the same assumption as AODV-ST that mesh traffic is predominantly forwarded to and from gateway nodes forming a logical tree structure. It then uses hierarchical/tree-based routing to exploit this tree-like logical structure. In the hierarchical/tree-based routing, the root announcement is periodically broadcast by the root (commonly gateway) with a sequence number assigned to each broadcast round and a path cost field initialized to zero. During the propagation of the announcement, each intermediate router updates the path cost and then rebroadcasts the message if the announcement carries a larger sequence number than it has seen or if the sequence number is the same but the path cost is better. The mesh router chooses the best parent and caches other potential parents. The topology thus builds away from the gateway, and a path is proactively established between each mesh router and the gateway. In addition, periodic RREQs are sent from each mesh router to its parent to maintain the path to the root. If the connection to the parent is lost (3 consecutive RREQs), the mesh router will notify its children of the failure, then find a new parent, and send a gratuitous RREP to the root, which all intermediate routers use to update their next-hop information about the source.

In many routing protocols for the Internet and wireless multihop networks, *Hop Count* is the most commonly used routing metric. It provides minimum hop count routing. Link quality for this metric is a binary concept; either the link exists or it doesn't. The primary advantage of this metric is its simplicity. Once the topology is known, it is easy to compute and minimize the hop count between a source and a destination. On the other hand, the primary disadvantage of this metric is that it does not take link quality or bandwidth into account. A path that minimizes the hop count does not necessarily maximize the throughput of a flow.

The *ETX* routing metric, proposed by De Couto *et al.* [23], is defined as the expected number of MAC layer transmissions for successfully delivering a packet through a wireless link, i.e., for link l, $ETX_l = \frac{1}{1-E_l}$ where E_l denotes the packet loss rate on link l. ETX reflects the difficulty of MAC layer to send a packet to its destination. The weight of a path is defined as a summation of the ETX of all links along the path. In this way, ETX considers both path length and packet loss ratio. However, ETX fails to capture the link transmission rate and also ignores the interference from other links because of the nature of CSMA/CA mechanism used in the MAC layer.

The *ETT* routing metric, put forward by Draves *et al.* [76], is improved from ETX by considering the differences in link transmission rates. ETT is defined as the amount of time that is needed to transmit a packet through the link, i.e., for link l, $ETT_l = \frac{1}{1-E_l}\frac{s}{r_l}$, where r_l denotes the link data rate and E_l denotes the packet loss rate. The weight of a path is a summation of the ETT of all links on this path. Despite the improvement from ETX, ETT still fails to capture the interferences among different links.

The WCETT routing metric, proposed by Draves *et al.* [76] , introduces enhancement over ETT by taking into account the intra-flow interference. WCETT tries to reduce the number of nodes along a path of a flow that transmit on the same channel. It captures the intra-flow interference of a path since it gives low weights to the paths that have more diversified channel assignments on their links or in other words, that have lower intra-flow interference. Although WCETT can capture the intra-flow interference, it fails to consider explicitly the effects of inter-flow interference. Hence, WCETT could route traffic to congested areas.

RALA [103] was proposed to improve ETT by incorporating the impact of traffic load on the path performance [103]. In addition RALA uses a quantization technique to improve route stability while achieving quick responses to link state and network topology changes. Let λ denote channel idleness ratio (the ratio of time that the channel is idle) and the RALA for a link l can be formulated as

$$\mathrm{RALA}_l = \frac{s}{r_l} \times \frac{1}{1-E_l} \times \omega(\lambda)$$

where s denotes the test packet size (e.g., 1024 bytes), r_l is the link data rate, and E_l the packet loss rate. $\omega(\lambda)$ is a weight function of the channel idleness ratio λ, which is defined:

$$\omega(\lambda) = \begin{cases} 1 & \lambda \geq \lambda_u \\ \frac{1}{\lambda} & \lambda_l \leq \lambda < \lambda_u \\ M & \lambda < \lambda_l \end{cases}$$

where M is a very large constant. In the definition of $\omega(\lambda)$, links with λ greater than λ_u are weighted equally because channel is idle most of the time for these links. Links with λ between λ_l and λ_u are given weights decreasing with the channel idleness ratio, i.e., links with light traffic load are preferred. Links with λ less than λ_l are generally not considered in the path selection to avoid creating hotspot in the network.

Since RALA is a load dependent metric, it may cause the self-interference problem [24] [57], in which a flow constantly switches between two alternative paths. To combat this problem, RALA uses a quantization technique and also decreases the frequency with which a mesh router updates its routing metric to the gateway. After quantization, if the change in link cost is small, the quantized value of the link cost will be the same. The quantized RALA for a link l can be formulated as

$$\text{QRALA}_l = \lceil N \times RALA_l / Q \rceil$$

where N is the number of quantization levels and Q is the quantization range.

Compared to ETT, RALA takes link available bandwidth instead of physical layer data rate into account. It yields more accurate link throughput and delay estimation than ETT.

2.1.2 MAC Layer Association

In the IEEE 802.11 [2] standard, the association procedure consists of three phases. In the first phase, the unassociated stations (STAs) scan the medium and listen to the beacons of the available access points (APs) (passive scanning). The STAs use the information broadcasted by the APs (in their beacon frames or Probe Response

frames) to make their association decisions. Similarly, an STA may choose a more active approach and send Probe Request frames, to which available APs respond by Probe Response frames (active scanning). During the second phase, the STA determines the AP that is the most appropriate to associate with. Finally, in the third phase, STA sends an Association Request frame to the selected AP (Association phase). Then after successful authentication, the STA becomes part of the network and is able to communicate with other STAs.

The state of the art mechanism for the second phase, implemented in the majority of 802.11 wireless adaptors, relies on measurements of received signal strength (RSSI); the STA associates with that AP that is heard at the highest signal strength. Such an affiliation algorithm has received significant criticism [93] [14] [99] due to its ignorance of AP load. Sole consideration of link quality in the AP affiliation process can lead to the overload of APs with high STA concentration, while other APs remain unused due to their slightly longer distance from the majority of the STAs. As a consequence, new algorithms have been proposed that incorporate AP load in the selection process [25] [8]. Some of these algorithms rely on passive measurements collected from Beacon frames, while a recent approach advocates the use of active measurements for the identification of the best AP [81]. In [51] the authors demonstrated why the use of signal-to-noise ratios in selecting APs is not appropriate. Both [51] and [22] consider techniques to allow the STA to estimate the AP workload before connecting, while [81] considers the use of available bandwidth in AP selection. A more holistic solution encompassing factors such as the number of connected users and mean RSSI was proposed in [71]. [100] incorporates both the total number of users associated with the AP and the average packet loss rate on the access link into the association metric. [61] proposes a beacon assisted discovery protocol to address the relay node selection for hierarchical ad hoc networks. The scheme simply uses RSSI to select the relay node and employs *hop count* to establish the path between a relay node and the gateway. In [99], the authors study a new user association policy that ensures network-wide max-min fair bandwidth allocation to the users. The work in [13] presents self-configuring algorithms that provide improved user association and fair resource sharing in the wireless network. The authors in [69]

propose a new handoff mechanism that is based on the monitoring of the wireless links. In [58], the problem of optimal user association to the available APs is formulated as a utility maximization problem. The multihoming scenario is introduced in [80], where the traffic is split among the available APs. In [80], the throughput is maximized by constructing a fluid model of user population that is multihomed by the available APs in the network. In [98], the authors propose new protocols applied in a new architecture called SMesh. This architecture supports fast handoff introducing collaboration between the APs in the network. The authors in [27] and [26] present a dual-association approach in wireless mesh networks, where the APs for unicast traffic and the APs for broadcast traffic are independently chosen by exploiting overlapping coverage. In this way, they optimize the overall network load. The last three approaches [98] [27] [26] are applied in wireless mesh networks, and so, they are closely related to our work. The first one of them try to speed up the handoff process introducing collaboration between the APs. It is clear that they do not work in the direction of improving the performance of the association decision of the users in the network. Our work optimizes the association decision, taking into account channel quality, AP load, and backbone routing performance. In the last two approaches, the authors improve the network load using traffic categorization and dual association on top of the RSSI-based user association process. Our approach is different wherein we incorporate the channel quality, AP load and backbone routing performance in the association process, replacing in this way the RSSI-based association procedure.

To overcome the ignorance of AP load of RSSI and incorporate more link attributes in the association process, we first propose two new link metrics in this chapter. The two metrics take into consideration the quality of the channel, the AP load as well as the contentions between multi-rate users, and can be applied as association metrics for 802.11 WLANs and WMNs. Furthermore, motivated by the observation that the common-case traffic in wireless mesh networks is to and from the gateway, so the user satisfaction can be significantly improved if the user can associate itself with an access point (collocated with a mesh router) that can provide the best path to the gateway, we then extend the first proposed schemes by combining information about the links

between the users and the candidate mesh routers as well as the information about the routing of the packets from those routers to the destination. In summary, we make the following contributions in this chapter:

1. To overcome the inefficiency of RSSI, we design two new metrics to measure the access link quality, (a) Contention Aware Expected Transmission Time (CAETT), and (b)Load Aware Expected Transmission Time (LAETT). In contrast to previously proposed link metrics, CAETT takes into account the impact of 802.11 MAC layer contentions between multi-rate stations. It yields more accurate link throughput estimation. LAETT further captures the impact of traffic load on the shared medium. Like RSSI, CAETT and LAETT can both be used as user association metrics. The corresponding association mechanisms are called CAETT- and LAETT-based association mechanisms, respectively.

2. Considering the unique characteristics of wireless mesh networks, we propose a new end-to-end performance based association mechanism. The new mechanism combines information about the links between the users and the candidate routers as well as the information about the routing of the packets from those routers to the destination (commonly gateway). In such a way, the association is based on the end-to-end transmission capability of the candidate routers, and thus it has the promise to increase the overall throughput of the mesh network.

3. In order to reduce the association time, we develop an analytical model and propose a hybrid measurement and estimation method to enable a station to quickly determine the cost of CAETT and LAETT.

4. We present detailed simulation results to evaluate the performance of the proposed association mechanisms. We show that the end-to-end performance based association mechanism can significantly improve the network performance in terms of throughput and delay by up to 100%.

2.2 New Access Link Metrics: CAETT and LAETT

The two proposed link metrics are called Contention Aware Expected Transmission Time (CAETT) and Load Aware Expected Transmission Time (LAETT), respectively. In the following we refer to mesh routers as mesh access points (MAPs) to emphasize their functionality of providing access to users. A MAP together with its associated users form a basic service set (BSS).

2.2.1 Contention Aware Expected Transmission Time (CAETT)

CAETT is defined as the expected transmission time for a user to successfully deliver a data packet to a MAP under the contention with other users associated with the same MAP. For a new user n, its CAETT metric with respect to MAP i is formulated as

$$CAETT_{n,i} = \frac{1}{1 - E_{n,i}} \sum_{j \in C_i \cup n} \frac{s}{r_{j,i}} \tag{2.1}$$

where C_i denotes the set of users currently associated with MAP i; s denotes the test packet size (e.g, 1024 bytes) and $r_{j,i}$ is the link data rate between user j and MAP i; $E_{n,i}$ denotes the packet loss rate on the link between the scanning user n and the MAP i if user n transmits packets of size s at data rate $r_{n,i}$.

Previous works [7] [66] have shown that the distributed coordinate function (DCF) of 802.11 MAC tends to provide equal transmission opportunity to all associated users under saturated traffic. If all users transmit packets of equal length and the transmissions are error free, per-user throughput is upper bounded by $\frac{1}{\sum_{j \in C_i \cup n} \frac{1}{r_{j,i}}}$ [7].In other words, $\sum_{j \in C_i \cup n} \frac{s}{r_{j,i}}$ is the lower bound of the time needed for a user to acquire the channel and transmit a packet of size s onto the channel. If the transmission is unsuccessful due to channel error, the packet has to be retransmitted. Given the packet loss rate $E_{n,i}$, the average number of transmission attempts to successfully deliver a packet to the receiver is $\frac{1}{1-E_{n,i}}$. Then $\frac{1}{1-E_{n,i}} \sum_{j \in C_i \cup n} \frac{s}{r_{j,i}}$ represents the lower bound of the expected transmission time for a user to send a packet successfully.

To determine CAETT, a user requires the information of its own access link data

rate and packet loss rate, as well as the data rates of other users currently associated with the MAP. The MAP measures the link date rates of current associated users, and advertises the rate information (in the form of $\sum_{j \in C} \frac{1}{r_j}$) in the enhanced beacon and probe response frames. This information is carried in one of the Information Elements (ISs) of the beacon and probe response frames. A new user retrieves the rate information from the received beacon or probe response frames, and evaluates its own data rate and packet loss rate to calculate the CAETT to a candidate MAP. If CAETT is directly used as the association metric, the user then selects the MAP with the smallest CAETT to associate with.

Probing packets have been used for measuring the packet loss rate on a wireless link [76] (previous work [75] has shown that direct measurement of expected transmission time does not work well because of self-interference). However probing-based measurement techniques need certain samples to obtain accurate results, which requires a long measurement time. When a user determines a MAP to associate with at its bootup or hand-off to a new MAP due to quality deterioration of its current MAP, it desires to make a fast decision. In addition, it is inaccurate to use broadcast packets such as beacons to measure the packet loss rate, since broadcast packets are always transmitted at a fixed and low data rate, which is more tolerant of channel errors, and which may differ from the actual data transmission rate. Therefore to reduce the scanning time at bootup and hand-off, we propose to use a hybrid approach of measurement and estimation for a new user to obtain the packet loss rate and link date rate.

Given a radio technology and physical layer mode, the packet loss rate can be estimated from the channel SNR γ. As an example, in IEEE 802.11b with a PHY mode m, where m=1, 2, 3, and 4 for 1, 2, 5.5, and 11 Mbps PHY rates, respectively, the packet loss rate can be calculated by [73],

$$E(m, s, \gamma) = 1 - (1 - P^m_{e\_data}(s, \gamma)).(1 - P^m_{e\_ack}) \tag{2.2}$$

where s is the packet size. $P^m_{e\_data}(s, \gamma)$ is the error probability for data packets of size s in PHY mode m and P_{e_ack} the error probability for ACK. Since ACK frames are

always transmitted at the lowest rate (i.e., PHY mode 1) and is only 14 bytes long, the error probability for ACK is negligible compared to the data packet. Hence we approximate the packet error probability as:

$$E(m, s, \gamma) = 1 - (1 - P^m_{e\_data}(s, \gamma)) = P^m_{e\_data}(s, \gamma) \tag{2.3}$$

The error probability for a data frame of size s in PHY mode m is given by [73]:

$$P^m_{e\_data}(s, \gamma) = 1 - (1 - P^1_e(24, \gamma)) \cdot (1 - P^m_e(28 + s, \gamma)) \tag{2.4}$$

where $P^1_e(24, \gamma)$ is the error probability for the PLCP preamble that is always transmitted with PHY mode 1, and $P^m_e(28+s, \gamma)$ is the error probability for the s-byte data plus the MAC header. $P^m_e(s, \gamma)$ can be further expressed in terms of bit error rate (BER) $P^m_b(\gamma)$ as:

$$P^m_e(s, \gamma) = 1 - (1 - P^m_b(\gamma))^{8s} \tag{2.5}$$

Given the received SNR per bit γ, the BER $P^m_b(\gamma)$ can be derived for each PHY mode m based on the modulation scheme and channel coding rate used in the PHY mode. The detailed analysis on BER can be found in [52], [105], and [10].

In our proposed hybrid measurement and estimation method, MAP beacon and probe response frames also carry the transmit power. The new user measures the received signal power and obtains the channel SNR. The new STA then selects the PHY mode m that minimizes the CAETT cost using the above analytical model, that is,

$$\min(CAETT_{n,i}) = \min_m \{CAETT_{n,i}(m, s, \gamma)\} \tag{2.6}$$

This $\min(CAETT_{n,i})$ is used as the access link CAETT with respect to the given MAP.

2.2.2 Load Aware Expected Transmission Time (LAETT)

CAETT is easy to determine. It captures channel quality and MAC contentions between multi-rate users under saturation. The insufficiency of the CAETT lies in its ignorance

of real traffic load imposed on the target MAP. As a result, the MAP with a smaller CAETT value might be overloaded. In this section, we propose another access link metric that factors in real traffic, called Load Aware Expected Transmission Time (LAETT). The determination of LAETT depends on the estimation of the *effective bit rate* (EBR). EBR represents the bandwidth/throughput that a user is likely to receive after affiliating with a particular MAP. Many aspects of link quality, such as data rate, packet loss rate, channel access contention and traffic load can all be incorporated in EBR.

To estimate the EBR with respect to a given MAP i, we differentiate two cases. First, when the traffic load of the scanned BSS i is far from saturation and the channel is idle most of the time, we assume that the probability of collisions is negligible and that the addition of the new user's traffic will not affect the current transmissions in this BSS. Let T_{idle} be the average amount of channel idle time during a measurement interval T_p. Channel idleness ratio of the scanned MAP i is defined as

$$\lambda_i = \frac{T_{idle}}{T_p}$$

This idle part of the channel is sufficient to support the transmissions between the new user and MAP i without conflicting with other users channel occupation time. Therefore, in the light traffic case, the EBR of user n with respect to MAP i is

$$EBR_{n,i} = (1 - E_{n,i})\lambda_i r_{n,i} \tag{2.7}$$

where $E_{n,i}$ and $r_{n,i}$ are the packet loss rate and data rate of the access link between user n and MAP i, respectively.

Second, when MAP i is heavily loaded, new user's traffic would saturate the target BSS if new user associated with MAP i. As explained above, associated users of a MAP will fairly share the bandwidth under saturation and get equal throughput upper bounded by $\frac{1}{\sum_{j \in C_i \cup n} \frac{1}{r_{j,i}}}$ [7] [66]. Due to contentions, collisions and protocol overhead, a user can actually never achieve this throughput bound. To avoid the complicated derivation of the accurate per-user throughput under saturation, we use a simulation

based method in this thesis. We simulate a BSS with saturated traffic. We vary the number of associated users from 5 to 40. For each number of users we generate 10 scenarios in which the users are randomly located around the MAP. We calculate the ratio of achieved per-user throughput to upper bound for each scenario. The results are shown in Figure 2.1, where the x-axis is the number of the users and the 10 points corresponding to each x value are the calculated ratios from the 10 scenarios. We observe that the ratio stays around 0.6 and is insensitive to the number of associated users. Therefore, we set $\theta = 0.6$ for our EBR estimation in this thesis. Now, given the

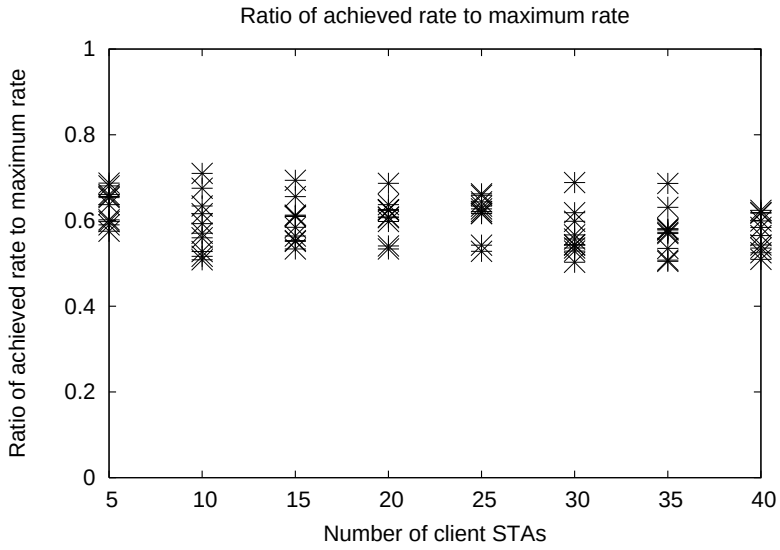

Figure 2.1: Ratio of achievable per-user throughput to the upper bound

throughput bound $K = \frac{1}{\sum_{j \in C_i \cup n} \frac{1}{r_{j,i}}}$, we can reasonably assume that a user can only achieve the throughput of θK, where $\theta = 0.6$. Based on this throughput estimation, the EBR of the new user under heavy traffic load is approximated by

$$EBR_{n,i} = (1 - E_{n,i})\theta \frac{1}{\sum_{j \in C_i \cup n} \frac{1}{r_{j,i}}} \tag{2.8}$$

Combining the light and heavy load situations, the EBR of the new user with respect

to MAP i is heuristically estimated as

$$EBR_{n,i} = \begin{cases} (1 - E_{n,i})\lambda_i r_{n,i} & \lambda_i \geq \lambda_0 \\ (1 - E_{n,i})\theta \frac{1}{\sum_{j \in C_i \cup n} \frac{1}{r_{j,i}}} & \lambda_i < \lambda_0 \end{cases} \tag{2.9}$$

where λ_0 is a threshold. When the channel idleness ratio is greater than λ_0, we assume that the traffic in the considered BSS is far below saturation; otherwise the traffic is assumed saturated or near saturation. It should be mentioned that the optimal choice of λ_0 depends on many factors such as link capacity and traffic volume of the new user. However, for simplicity we fix λ_0 as a predefined parameter in our EBR estimation in this thesis.

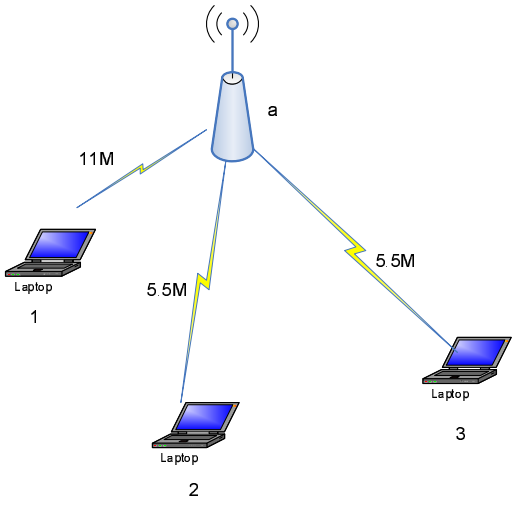

Figure 2.2: An example to illustrate calculation of the effective bit rate in a BSS

As an example to illustrate the EBR estimation, we consider the network shown in Figure 2.2, where user 1 and user 2 are currently associated with MAP a. Links $(1, a)$ and $(2, a)$ have data rates of 11Mbp and 5.5Mbps, respectively. If user 3 joins, the data rate of its access link to a is 5.5Mbps. If the channel is lightly loaded, say the channel idleness ratio is 0.8 before user 3 joins, the part of the channel not occupied by users 1 and 2 is sufficient for user 3's transmissions. The EBR of the access link $(3, a)$ is thus estimated as $0.8 \times 5.5 = 4.4Mbps$. On the other hand, if the current traffic is nearly saturated or already saturated, the channel will be fairly shared by the three users. Each of them get equal throughput that is bounded by $\frac{1}{\frac{1}{11}+\frac{1}{5.5}+\frac{1}{5.5}} = 2.2Mbps$. The

estimated EBR for user 3 is then $0.6 \times 2.2 = 1.32Mbps$. Note that we only consider the access link between the user and the MAP here. The wireless mesh backbone operates on another non-overlapped channel.

Finally, the traffic load aware expected transmission time (LAETT) is defined as

$$LAETT_{n,i} = \frac{s}{EBR_{n,i}} \tag{2.10}$$

where s is the test packet size. $LAETT_{n,i}$ represents the time needed by a user to successfully transmit a packet of size s over the access link under current contention and traffic load conditions.

LAETT incorporates more information elements and can better reflect the link quality. However it requires each MAP constantly measuring the channel idle time. Such measurement may sometimes need special hardware support.

For a new user to determine the value of LAETT, it requires four pieces of information, 1) the traffic load under a MAP, 2) the data rates of the users currently associated with the MAP, 3) its own access link date rate and 4) the packet loss rate on the access link. The latter two are determined locally, e.g., packet loss rate can be measured either through periodic probing or based on the channel SNR [73] [52] [105] [10], as described in last section. The MAP has the complete information of the channel state (busy or idle), so it measures the channel idleness ratio and makes this information available to the users through enhanced beacon and probe frames. The MAP also measures the link date rates of the currently associated users, and advertises the rate information in the form of $\frac{1}{\sum_{j \in C_i \cup n} \frac{1}{r_{j,i}}}$. Such enhanced information is carried in the Information Elements (IEs) of the beacon and probe response frames. Note that CAETT is determined in the same way except that the traffic information is not needed.

2.3 End-to-End Performance Based User Association

Although CAETT and LAETT provide significant improvement in user throughput as demonstrated in the forthcoming section, it is not adequate for wireless mesh networks. As stated, mesh traffic is predominantly destined to a gateway node and thus the level

of the end-to-end performance provided to the users is the most important performance criterion. In a typical 802.11-based wireless mesh network, it is expected that there will be a large population of mesh access points (MAPs) connected to each other. Among several MAPs that a user can associate with, it should choose the one that provides the best end-to-end performance. Motivated by this observation, we present a new association framework for WMNs in this section. The proposed association mechanism combines information about the links between the users and the candidate MAPs as well as the information about the routing of the packets from those MAPs to the destination. In such a way, the association is based on the end-to-end transmission capability of the candidate MAPs, and thus it has the promise to increase the overall throughput of the mesh network.

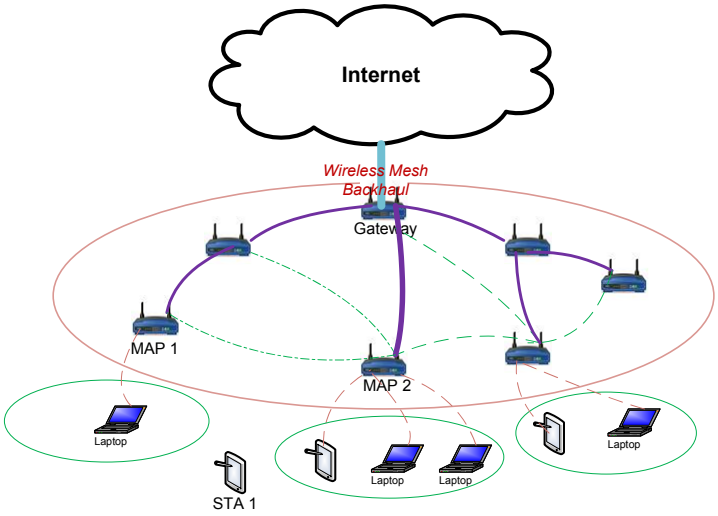

Figure 2.3: A motivating example of end-to-end performance based association

Our approach is better motivated with an example. In Figure 2.3, we give a sample wireless mesh network, where the tree topology is illustrated as the solid purple lines. The thickness of a line represents the corresponding link quality. The thicker, the better quality. Assume that STA1 has the option of associating with MAP1 or MAP2. Following the approach that we described, STA1 receives from MAP1 and MAP2 the necessary information to calculate the association metrics for each MAP. According to the CAETT and LAETT based association schemes, STA1 associates with the MAP that provides the minimum association metric, say MAP1. However, according to our

end-to-end performance based approach, the association decision of STA1 is affected by the respective routes between MAP1-gateway and MAP2-gateway. During the association phase, if MAP1 and MAP2 inform STA1 about the expected path quality to the gateway, then STA1 can use this information to determine the MAP with the better end-to-end performance, which is MAP2. Moreover, the variability of the network conditions can affect the provided end-to-end routing quality. Therefore, STA1 is periodically informed about the routing quality during the data transfer in order to initiate a reassociation when needed.

2.3.1 JSEL Association Metric

The main feature of the end-to-end performance based association mechanism is to incorporate information about the backbone routing from candidate MAPs to the gateway. During the scanning phase, the new user sends a probe request message to candidate MAPs. The MAPs that are in the transmission range of the user receive this message. MAPs advertise their minimum path cost in an extra field in the Probe Response frame or Beacon frame. The path cost is then combined with information about the access link between the user and the MAP to get a total association cost. The total association cost, called *JSEL*, is a weighted sum of the access link metric and the backbone path cost, and reflects the end-to-end transmission capability that can be provided by the network in case that the user associates with a specific MAP. Specifically, *JSEL* is formulated as:

$$JSEL = (1 - \beta)Q_{al} + \beta C_{bp} \tag{2.11}$$

where Q_{al} is the access link metric that reflects the access link quality between the user and a candidate MAP. C_{bp} is the backbone path cost from the candidate MAP to the gateway. β is a tunable parameter ($0 \leq \beta \leq 1$). We can view the expression in (2.11) as a balance between the access link quality and backbone path quality. The impact of β on the end-to-end communication performance is investigated in Section 2.4.2. In the following, we also refer to the end-to-end performance based association mechanism as

joint MAP association mechanism.

2.3.2 Association Protocol

The association mechanism allows a user to determine and update the MAP that it associates with. In Figure 2.4 we depict the association protocol. When a user joins the network, it discovers the MAPs in its neighborhood through active or passive scanning. In active scanning a user sends a "probe request" frame and the MAP replies with a "probe response". Alternatively, in passive scanning, a user listens to "beacon" frames which are periodically transmitted by MAPs. The MAP beacon and probe response frames are enhanced in our end-to-end performance based association mechanism to carry: 1) the path cost between the MAP and the gateway, 2) the information of the link data rates of the users that are currently associated with the MAP, and 3) the information of current traffic load in the BSS served by this MAP. The last two information elements are used by the new user to estimate its access link quality with respect to a given MAP based on the proposed CAETT or LAETT metric (refer to the next section for details of CAETT and LAETT), wherein the third element is only for LAETT. Such enhanced information is carried in the vendor specific Information Elements (IEs) in the beacon and probe response frames. The legacy users that do not support the proposed association mechanism simply discard the unrecognized IEs as specified in IEEE 802.11 and use conventional RSSI method to associate with a MAP. This achieves backward compatibility.

After scanning, the user evaluates the quality of its access link to each candidate MAP based on its own measurements and the information delivered in the beacon or probe response frames. Then it computes the joint association cost *JSEL* according to (2.11) and selects the MAP with the best *JSEL* cost.

Due to the variability of the network conditions, the provided end-to-end routing quality may vary. Therefore the user needs to perform periodic re-scanning after association. If the joint cost of the current MAP is above a threshold T_1 or the joint cost of another MAP is below the cost of its current MAP by at least a threshold T_2, the user initiates the re-association process with the new MAP. The thresholds T_1 and T_2

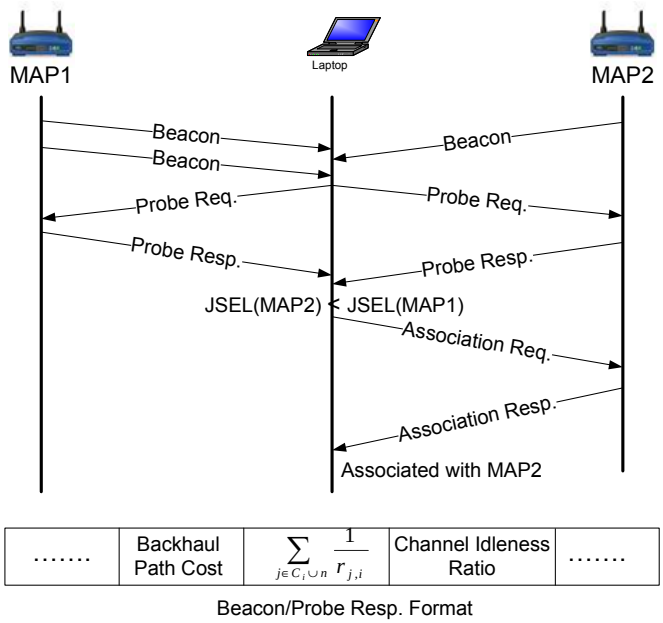

Figure 2.4: Association Protocol

as well as the background scanning interval are used to prevent the oscillations between selected MAPs.

2.3.3 Discussions

In the presence of multiple gateways, a routing tree rooted at each gateway is established. A MAP chooses to join one tree by comparing the minimum path cost to each reachable gateway. It then broadcasts the path cost to the selected gateway. User association proceeds as described before.

If MAPs are equipped with multiple relay radios and these radios work on different channels, a high-quality path between each MAP and a gateway can be better established based on some routing metric specially designed for multi-radio, multi-channel networks, e.g., WCETT [76]. Obtaining path cost from each candidate MAP, the user selects the best MAP as before.

2.4 Performance Evaluation

For the evaluation, we have implemented the proposed mechanisms in ns2 [1]. We have modified the beacon and probe frames in order to incorporate the information

elements that our system needs, such as the rate information of the associated users, the measured channel idleness ratio, and the path cost from a MAP to the gateway.

First we study and compare the performance of four access link metrics, RSSI, potential bandwidth (PB) [81], CAETT and LAETT, in a single-hop WLAN setting where each AP is directly connected to a high-speed wired backbone. Second we investigate the impact of the tunable parameter β on the system performance when the *JSEL*-based association mechanism is used in the context of wireless mesh networks. Then we present results that compare different association mechanisms (joint, non-joint) with various combinations of access link metrics (RSSI, PB, CAETT, LAETT) and backbone routing metrics (Hop Count, ETT, RALA) in muni mesh networks.

2.4.1 Performance of CAETT and LAETT

RSSI, PB [81], CAETT and LAETT are four metrics to measure the access link quality. They have different notions of what constitutes a good link to an access point. As RSSI and PB, CAETT and LAETT can be used as association metrics, where a user selects the AP with the smallest CAETT or LAETT value. To compare their performance in a single-hop WLAN setting, we simulate a multi-cell 802.11b network that consists of 5 different overlapping cells. We use a simple wireless channel model in which a user's data rate depends only on its distance to the AP. Specifically, the distance thresholds for 11Mbps, 5Mbps, 2Mbps and 1Mbps are 80m, 150m, 200m and 250m, respectively. 5 APs are located at the four corners and the center of a $500m \times 500m$ area, and are directly connected to a high-speed wired backbone. The number of users is either 30 to simulate a moderate-sized network or 60 to simulate a dense network.

We consider various user distributions ranging from uniform distribution to hot-spot scenarios. In Figure 2.5 and Fig. 2.6, we show the average total throughput and average packet delay with 30 users and 60 users, respectively. The X axis is the offered load injected into the network. Fig. 2.5(a) and Fig. 2.6(a) depict the total throughput of the users while the offered load increases. Compared to RSSI, we observe throughput improvement by using PB, CAETT and LAETT, and that LAETT achieves the highest throughput. In RSSI based association, a user associates with the AP that

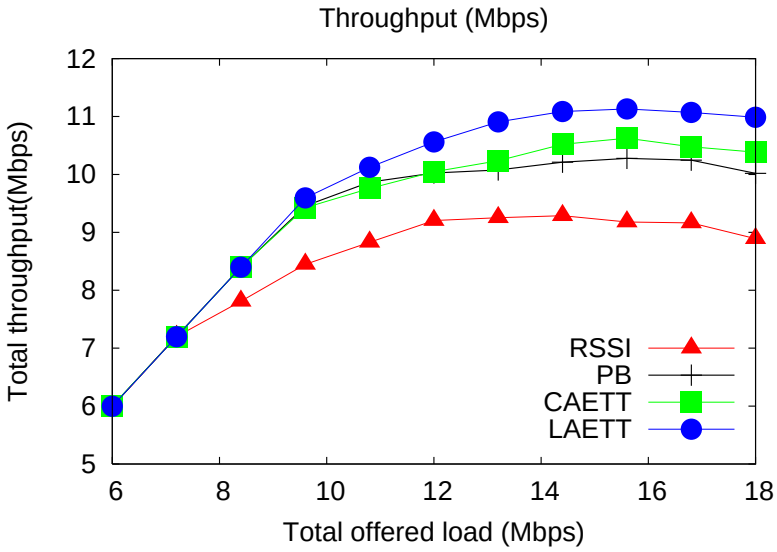

(a) Aggregate throughput

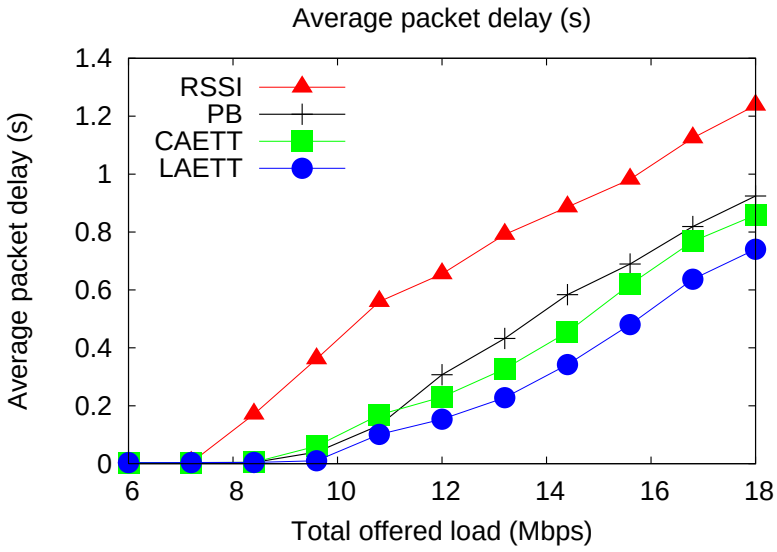

(b) Average packet delay

Figure 2.5: Aggregate throughput and average packet delay of 30 users

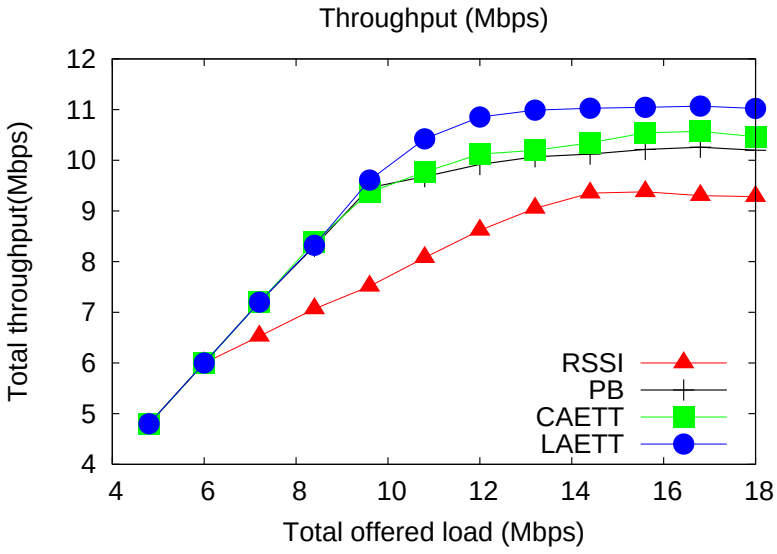

(a) Aggregate throughput

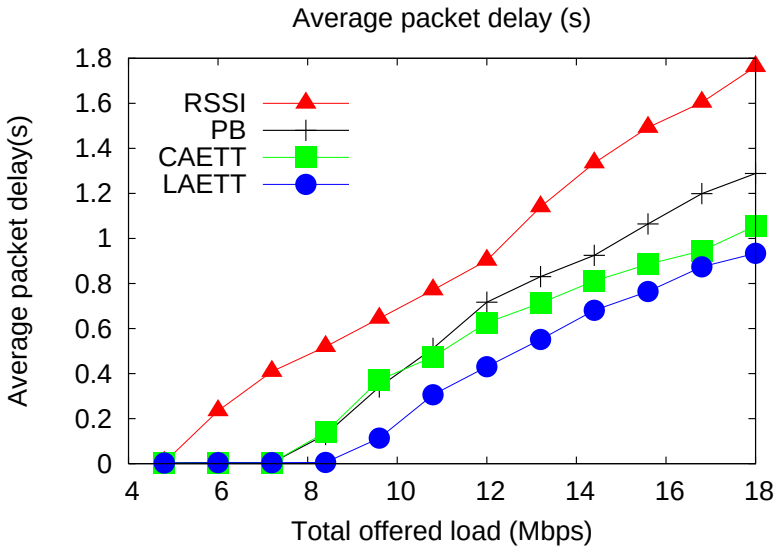

(b) Average packet delay

Figure 2.6: Aggregate throughput and average packet delay of 60 users

has the highest signal strength. This policy easily creates hot-spots especially when the users are not uniformly distributed. On the other hand, PB, CAETT and LAETT associate users in more intelligent manners and lead to higher throughput. PB captures traffic load and contentions, but the bandwidth estimation quality is constrained by its measurement techniques, especially under heavy load. CAETT offloads users from the cells that are either crowded or with lower transmission rates or with poor channel conditions. It achieves much better performance than RSSI and outperforms PB in most cases (especially under heavy load, because CAETT assumes saturated traffic). LAETT incorporates the factors of link SNR, user contention and real traffic load. It outperforms RSSI, PB and CAETT. Comparing Figures 2.5(a) and 2.6(a), we observe more throughput increase with 60 users than with 30 users by employing PB, CAETT and LAETT. This is because more severe hot-spots are likely to exist in a denser network.

Figure 2.5(b) and Figure 2.6(b) depict the average packet delay in the network. We can see that the average transmission delay is quite low for all the four schemes when the network is lightly loaded. When the offered load in the network increases the average packet delay gets higher as well. However, CAETT and LAETT can achieve lower transmission delay than RSSI and PB. For example, CAETT and LAETT keep the average delay at a very low level (near 0) when the network is lightly and moderately loaded (less than 10 Mbps).

2.4.2 Performance of JSEL-Based Association with respect to β

As shown in (2.11), the joint cost (*JSEL*) of a MAP is the weighted sum of the access link metric and the backbone path cost. In this section we investigate the relationship of the joint MAP association mechanism with the weighting parameter β.

We simulate a mesh network with 31 MAPs (one as the gateway) and 120 users. The MAPs and the users are both randomly deployed in a 750m×500m area. All the users are sending CBR traffic to the gateway. We use the physical model of IEEE 802.11a/g that supports 8 data rates up to 54Mbps. As above, we assume that the data rate of a link depends only on the distance between the two endpoints. Each MAP has two

Table 2.1: Number of users at different access link data rates with respect to β

β	54M	48M	36M	24M	18M	12M	9M	6M
0	7	15	14	37	16	15	13	2
0.3	4	16	12	34	21	18	12	3
0.6	3	11	10	28	25	20	17	6
0.9	1	0	2	11	17	30	28	31
1.0	1	0	0	7	14	27	32	39

radio interfaces working on orthogonal channels. One is for user-MAP communications and the other is for MAP-MAP communications in the backbone. CAETT and ETT are used in this section as the access link metric and the backbone routing metric, respectively.

We vary β from 0 to 1 to study how the weighting parameter β impacts the performance of the joint association mechanism. Figure 2.7 shows the aggregate access link throughput (from users to the associated MAPs) and aggregate end-to-end throughput (from users to the gateway) with different β. The results are averaged over 10 runs of simulations. In table 2.1, we list the number of users at different access link data rates with respect to β for one of the 10 runs.

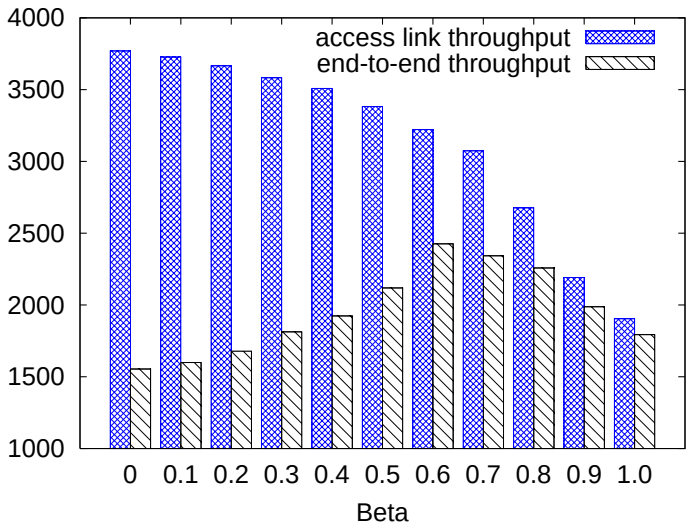

Figure 2.7: Access link throughput and end-to-end throughput under different β

When β is small, the access link metric is prevalence and users tend to select the

MAPs which can provide the highest access link throughput. However, injecting more traffic into the associated MAP does not necessarily imply high end-to-end throughput. As shown in Figure 2.7, most of the traffic arriving at the MAPs can not get to the gateway through the backbone when β is small. The difference between the access link throughput and end-to-end throughput is huge. On the other hand, when β is large, more weight is given to the backbone path cost. In such cases, the access link is more likely to become the bottleneck, where a lot of traffic cannot be delivered across the access link to reach the associated MAP. At $\beta = 1$, the access link throughput is just a half of that for $\beta = 0$. Figure 2.7 shows that choosing a middle value (0.6, 0.8) for β is a good tradeoff between access link quality and backbone path cost, and leads to high end-to-end performance. In table 2.1 it is shown that as β increases, more users shift from the MAPs providing high access link data rates (24M and above) to the MAPs with low access link data rates (18M and below). When β is increased to 0.9 and 1, majority of users (106 out of 120 and 112 out of 120, respectively) select the MAPs which provide the data rates of 18M and below.

2.4.3 Performance Comparison of User Association Schemes

In this section, we conduct a comparative study to show that the joint association mechanism can significantly improve the performance of the end-to-end communications in wireless mesh networks. Similar to last subsection, we simulate a mesh network with 31 MAPs (one as the gateway) and 120 users. The same physical model of IEEE 802.11a/g is used.

In a network some users may be idle and have no traffic to send, while others are actively transmitting. To capture this, we consider three scenarios with different ratios of active users, 0.3 (36 users are active), 0.6 (72 users are active) and 1 (120 users are active). In the following simulations, we set β to 0.6 and all the traffic flows are CBR with 1000-byte packet size.

We consider 8 schemes with different combinations of access link metrics and backbone routing metrics in our simulations. First, as the baseline, a user associates to the

MAP with the highest RSSI and the backbone uses hop count as the routing metric. The combination is denoted with "RSSI, HOP". Then we change access link metrics and routing metrics, but association still depends purely on the access link quality, regardless of the backbone path cost, that is, no joint MAP association is employed. We first keep RSSI as the association metric and use ETT for the backbone routing. We denote it with "RSSI, ETT". Since ETT is an improved routing metric over hop count, "RSSI, ETT" is used to demonstrate the possible performance gain by employing a better routing metric in the backbone. Next we keep ETT for the backbone routing and base user association on the access link quality measured with PB, CAETT and LAETT, respectively. The three combinations are denoted with "PB, ETT", "CAETT, ETT" and "LAETT, ETT". They are used to show the impact of access link metrics on the network performance. Through "PB, ETT" we can also observe the performance of the existing association approach (PB) in wireless mesh networks. Finally we consider the schemes employing the proposed joint MAP association. A user makes association decision based on the $JSEL$ metric that combines the access link quality and the backbone path cost. The joint association mechanism can use various combinations of access link metrics and routing metrics. We denote such combinations in the form of "access-link metric, backhaul routing metric" followed by "J" to represent the joint association. In our simulations, we study three combinations of this kind, "CAETT, ETT(J)", "LAETT, ETT(J)" and "LAETT, RALA(J)".

By varying the sending rate of each flow, we compare the throughput and delay performance of the eight schemes under different offered load. Figures 2.8, 2.9 and 2.10 show the end-to-end throughput and end-to-end packet delay with different ratios of active users.

We see that when the network is lightly loaded, all the eight schemes perform almost equally well. The aggregate throughput matches the offered load and the resulting end-to-end delay is quite small. On the other hand, under moderate and heavy load, they achieve different performance. RSSI and hop count are the conventional metrics for association and routing, respectively. Their combination is incapable of finding a

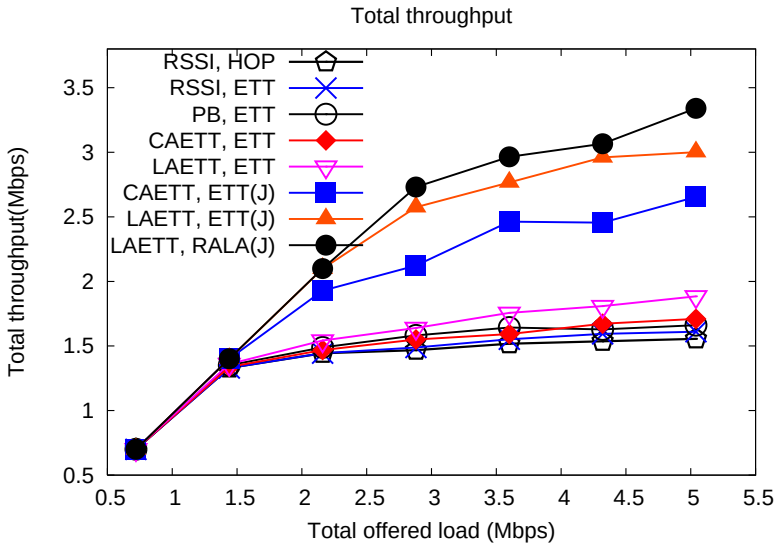

(a) Total end-to-end throughput

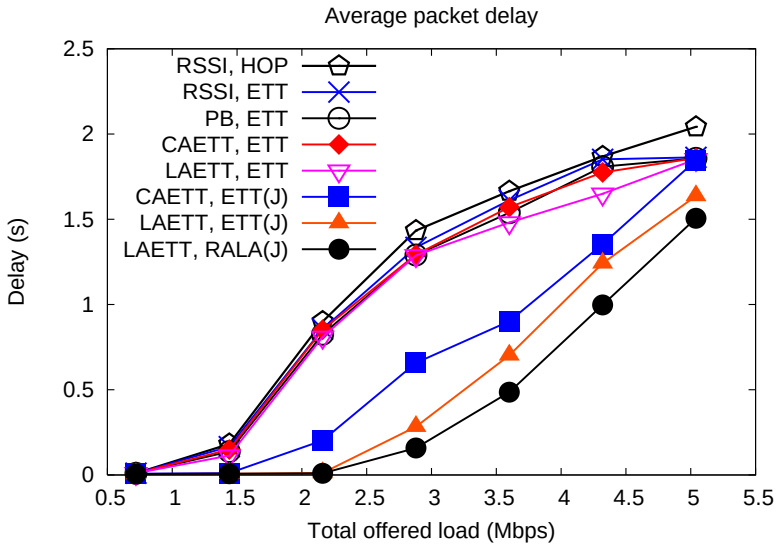

(b) Average transmission delay

Figure 2.8: 30% users are active: end-to-end throughput and delay

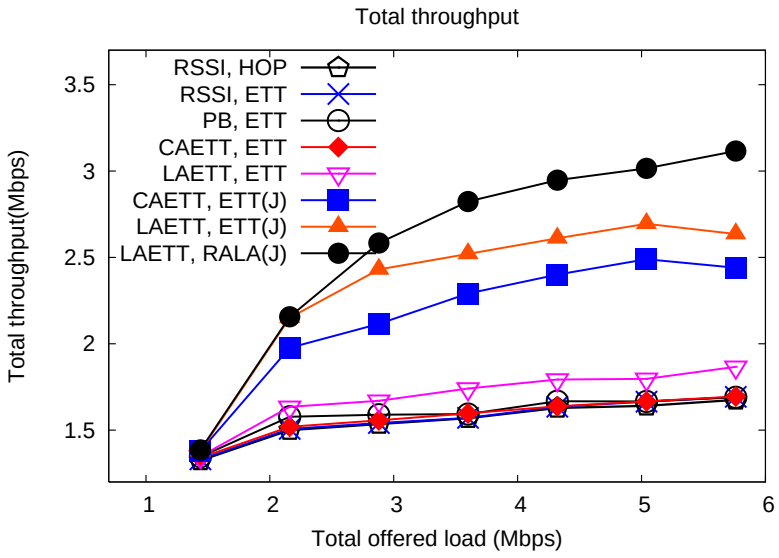

(a) Total end-to-end throughput

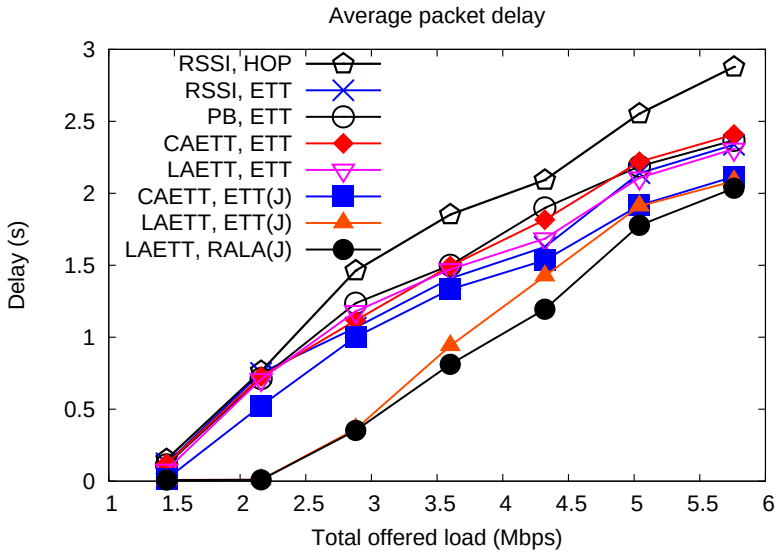

(b) Average transmission delay

Figure 2.9: 60% users are active: end-to-end throughput and delay

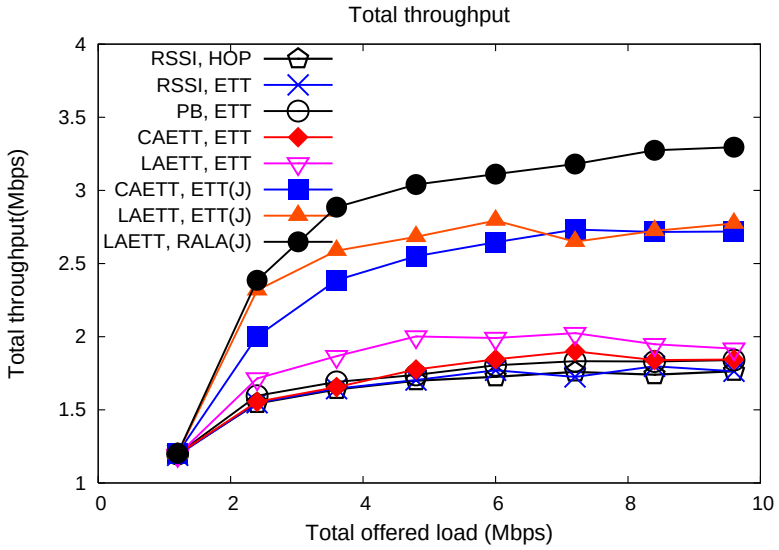

(a) Total end-to-end throughput

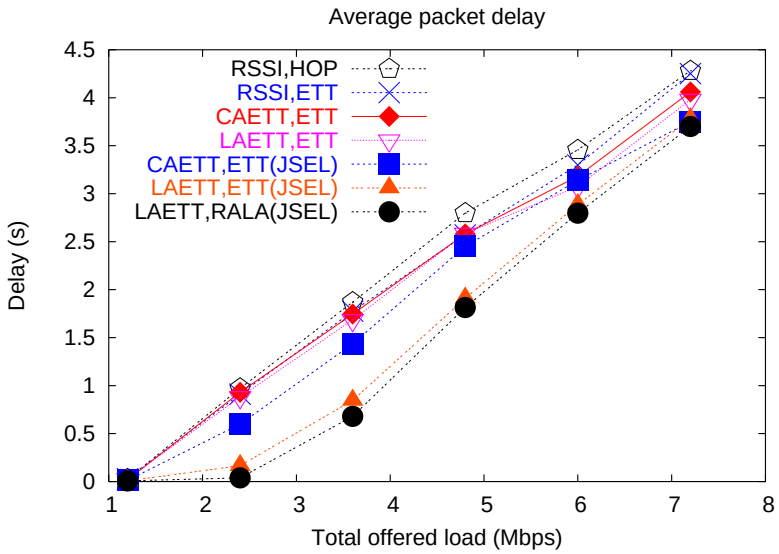

(b) Average transmission delay

Figure 2.10: 100% users are active: end-to-end throughput and delay

high-performance end-to-end path, without taking into account multi-rate capability, traffic load, MAC layer contention etc. If the users select MAPs only based on their access link quality without considering the backbone conditions, the end-to-end performance will not change much even if a better access link metric (PB, CAETT, LAETT) and/or an enhanced routing metric (ETT) is employed. The curves corresponding to "RSSI, HOP", "RSSI, ETT", "CAETT, ETT" and "LAETT, ETT" stay very close to each other. The reason is that the association is only based on the access link quality, not the end-to-end performance. When the MAP selection jointly considers the access link quality and the backbone path cost, we observe a significant increase in the throughput although we still use CAETT or LAETT as the access link metric, and ETT for the backhaul routing. For example, compared to "RSSI, HOP", "CAETT, ETT(J)" increases the aggregate throughput up to 60%. By considering the actual traffic load, "LAETT, ETT(J)" further improves the end-to-end performance in most cases. RALA is an enhanced routing metric that is radio and traffic load aware. It takes into account the link quality and traffic load on the candidate paths. "LAETT, RALA (J)" performs even better than "LAETT, ETT (J)", especially when the traffic load is high. Compared to "RSSI, HOP", "LAETT, RALA (J)" almost doubles the aggregate throughput and it achieves up to 20% gain on the aggregate throughput even compared to "CAETT, ETT(J)".

Chapter 3

Fair Bandwidth Allocation in Wireless Mesh Networks

Interference and collisions greatly limit the throughput and fairness of wireless mesh networks that use contention-based MAC protocols such as 802.11. It is widely believed that significantly higher throughput and fairness are achievable if bandwidth is carefully allocated and transmissions are scheduled. To study the performance limits of WMNs, and to find efficient algorithms achieving these performance limits, we optimally allocate channel bandwidth to individual flows and determine transmission schedule such that network throughput can be maximized while certain fairness is achieved. we first study the optimal performance of a WMN by jointly allocate bandwidth to each data flow without exceeding link capacities, and compute the corresponding user-router association and backbone routing solution. We then focus on the integral association, single-path routing case and investigate the optimal performance of a WMN on a given tree topology. An efficient scheduling algorithm is also developed for time-slotted WMN system to coordinate channel access as well as to enforce the allocated bandwidth.

3.1 Background and Related Work

Wireless Mesh Networks are envisioned to provide various attractive applications in the future, including broadband Internet access, distributed information sharing and storage, and different multimedia applications at very low costs. All of these potential applications demand the network to deliver a high volume of traffic efficiently. Hence, how to improve network throughput should be the most important design goal of WMNs. Moreover, every time when we talk about throughput, fairness must be taken into consideration, as otherwise we will end up with a serious bias on network resource allocation, which has been shown by previous research [104].

Therefore, an important goal of bandwidth allocation in wireless mesh networks is to maximize the utilization of network resources while sharing the resources in a fair manner among network flows. To strike a balance between fairness and throughput, the notion of max-min fairness [104] has been proposed and become a widely studied criterion in the network community. The majority of work on max-min fairness has been limited to the case where the routing of flows has already been defined and this routing is usually based on a single fixed routing path for each flow [104] [97] [50] [96] [12] [101] [63] [92].

Compared with wired networks, a wireless network normally has lower network throughput due to the existence of interference which prohibits simultaneous transmissions in a common neighborhood [36] [53]. In wireless networks, link is only a logical concept and links are correlated due to the interference with each other. Under the MAC strategies such as time-division multiple access and random access, these links contend for exclusive access to the physical channel. Unlike in the wired network where end-to-end flows compete for transmission resources only when they share the same link, here, flows that do not even share a wireless link in their paths can compete. Thus, in wireless networks the contention relations between links provide fundamental constraints for resource allocation.

The impact of wireless interference and corresponding interference-aware network solutions have attracted substantial attention from the networking research community. In their pioneering work [36], Gupta and Kumar study the capacity of wireless networks. In [53], the authors model the impact of interference using a conflict graph and derive upper and lower bounds on the optimal network throughput. In [40], the authors present a framework for multihop packet scheduling to achieve maximum throughput with both intra-flow and inter-flow contentions under consideration. Burkhart et al. propose topology control algorithms to compute interference-optimal connected subgraphs and spanners in [65]. Along this line, the authors in [54] present algorithms to compute a network topology in a wireless ad hoc network such that the maximum (or average) link (or node) interference of the topology is either minimized or approximately minimized.

In [49], the authors present routing algorithms to compute interference-minimum power bounded single or node-disjoint paths for multihop wireless networks using directional antennas.

Fairness has been well studied in both network layer and MAC layer. The classical max-min fairness problem ([15]) seeks bandwidth allocation for a set of given routes in a wired network. The problem of computing routes to provide max-min fair bandwidth allocation to a set of connections is much harder. Megiddo in [68] presents a polynomial time optimal algorithm to find LMM fractional flow routing solutions. Extending this work, the authors in [46] address the problem of finding integer flow routing solutions and propose approximation algorithms. In a recent paper [104], Hou et al. develop an elegant polynomial time algorithm, Serial LP with Parametric Analysis (SLP-PA), to calculate the LMM rate allocation under a network lifetime constraint in a two-tiered wireless sensor network. As in [104], [46], [68], our bandwidth allocation problem is implicitly coupled with a flow routing problem as well. Li [63] seeks bandwidth allocation for a set of flows on the given routes to achieve end-to-end max-min fairness. In [92], Gambiroza *et al.* develop a reference model and conduct extensive simulations to study the end-to-end performance and fairness in multihop wireless backhaul networks. Dong *et al.* [74] address fair bandwidth allocation in multi-hop WLANs. They demonstrate that a good tree structure can improve throughput without sacrificing fairness. In addition, max-min fair scheduling and fair queuing for TDMA-based or 802.11-based wireless ad hoc networks have also been addressed in [95], [39], [38], [62].

Although IEEE 802.11 is broadly used in current wireless mesh networks, scheduling-based MAC is believed to be a more suitable MAC solution for future WMNs [43] and adopted by the next generation wireless networking standard 802.16 [4].

3.2 System Model

As depicted in Figure 1.1, in a WMN only the gateway node is connected to the Internet; Mesh routers form a wireless backbone and rely on multi-hop routing to transfer their users traffic to and from the gateway. Each mesh router is equipped with two radios

used for router-router communications (relay) and user-MAP communications (access), respectively. We assume the two radios operate on orthogonal channels. A user is equipped with only one radio for access. Its operating channel is determined by the associated MAP. A MAP (the access radio) together with its associates users is called a Basic Service Set (BSS).

For the algorithm presented in this chapter, we assume that the wireless radios work in a half-duplex manner, i.e., they can only transmit or receive at a time. Only one channel is used for the mesh backbone. Channels are carefully assigned for the BSSs so that there is no inter-BSS interference. We assume that each node (mesh router or user) transmits with the same fixed transmission power, and therefore there is a fixed *transmission range* (D_T) and a fixed *interference range* (D_I) for each node, where $D_I = q \times D_T$ with $q \geq 1$.

We represent a wireless mesh network with M mesh routers and N users as a connectivity graph $G(V, L)$, where $V = V_m \cup V_s$ and $L = L_b \cup L_a$. Each node $v \in V_m$ represents a mesh router, while each node $u \in V_s$ represents a user station (STA). There exists a directed link $l = (v_1, v_2) \in L_b$ from $v_1 \in V_m$ to $v_2 \in V_m$ if $d(v_1, v_2) \leq D_T$, representing two mesh routers v_1 and v_2 can communicate directly (within one hop). There exists a directed link $(u, v) \in L_a$ from $u \in V_s$ to $v \in V_m$ if $d(u, v) \leq D_T$, implying that STA u is in the coverage of mesh router v. The capacity of a link $l = (i, j) \in L$ is represented by C_l or C_{ij}, which is the maximum transmission rate at which two nodes can communicate in one hop.

To model the interference in the mesh backbone, we use an undirected graph $G'(L_b, E_b)$, where L_b and E_b are the sets of vertices and edges of G', respectively. Each vertex in G' corresponds to a link in the connectivity graph G (and therefore they share the same notation L). There exists an edge in $G'(L_b, E_b)$ between $l_{xy} = (x, y) \in L_b$ and $l_{uv} = (u, v) \in L_b$, if the links l_{xy} and l_{uv} in G interfere with each other. That is, $d(x, v) \leq D_I$ or $d(u, y) \leq D_I$. We use $I_{l_{xy}}$ to denote the set of links interfering with link $l_{xy} = (x, y)$, i.e.,

$$I_{l_{xy}} = \left\{ l_{uv} \middle| (l_{xy}, l_{uv}) \in E_b \right\}.$$

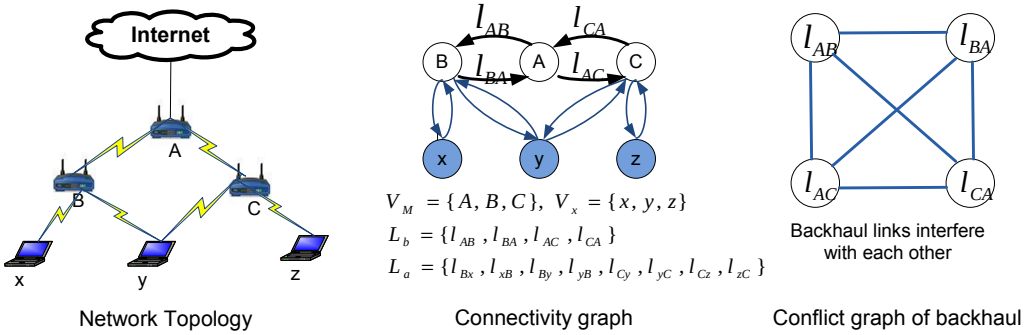

Figure 3.1: Network topology, connectivity graph and conflict graph

A *clique* is a set of links (vertices in G') which mutually conflict with each other. A maximal clique is a clique that is not contained in any other clique. To avoid conflict, at most one link in a maximal clique can be active at a time, implying that the total usage on these links should not exceed 1.

In Figure 3.1, we give an example of a network along with the corresponding connectivity graph and conflict graph.

3.3 Joint Optimization of Association, Routing and Bandwidth Allocation

In this section, we formulate the max-min fair bandwidth allocation problem, which is coupled with backbone routing and STA-MAP associations.

We use $\mathbf{r} = \{r_{ij}\}$ to denote a bandwidth allocation vector for STAs, where r_{ij} is the bandwidth allocated to STA i if it affiliates with MAP j. We use f_j to represent MAP j's traffic that is aggregated from its associated STAs and denote $\mathbf{f} = [f_1, f_2, ..., f_M]$. We denote with $\{R_{j,l}\}$ the corresponding flow routing solution in the backbone, where $R_{j,l}$ represents the amount of flow f_j that goes through link l.

3.3.1 Constraints

There are three sets of constraints that account for STA-MAP association feasibility, flow conservation and wireless interference, respectively. In the following, we use h(l)

and t(l) to denote the head (sender) and the tail (receiver) of a link l, respectively. gw stands for the gateway node.

$$\forall\ i \in V_s \quad , \quad \sum_{j:(i,j)\in L_a} \frac{r_{ij}}{C_{ij}} \leq 1, \tag{3.1}$$

$$\forall\ j \in V_m \quad , \quad \sum_{i:(i,j)\in L_a} \frac{r_{ij}}{C_{ij}} \leq 1. \tag{3.2}$$

$$\forall\ j \in V_m \quad , \quad \sum_{i:(i,j)\in L_a} r_{ij} = f_j, \tag{3.3}$$

$$\forall\ j \in V_m \setminus \{gw\} \quad , \quad \sum_{l:l\in L_b, \mathrm{h}(l)=j} R_{j,l} = f_j, \tag{3.4}$$

$$\forall\ j, v \in V_m \setminus \{j, gw\} \quad , \quad \sum_{l:\mathrm{h}(l)=v} R_{j,l} = \sum_{l:\mathrm{t}(l)=v} R_{j,l}, \tag{3.5}$$

$$\forall\ k = 1, ..., K \quad , \quad \sum_{l:l\in F_k} \sum_{j=1}^{M} \frac{R_{j,l}}{C_l} \leq 1, \tag{3.6}$$

(3.1) states that a STA may alternate in time affiliating with different MAPs. However, the total usage of the STA's radio to transmit on all these access links is at most 1. (3.2) represents that STAs which are associated with a given MAP mutually conflict with each other. Thus total usage of all the access links between the MAP and all its associated STAs is at most 1. (3.3) states that a MAP's traffic is the total traffic aggregated from its associated STAs. (3.4) shows that the total traffic on the outgoing links from MAP j is equal to f_j. (3.5) accounts for flow conservation. (3.6) requires that the total usage of the links in a maximal clique is at most 1, where K is the total number of maximal cliques in the network, and F_k is the k-th maximal clique.

With the above constraints, and a trivial constraint set that

$$\mathbf{r} \geq 0,\ \mathbf{R} \geq 0,\ \text{and}\ \mathbf{f} \geq 0, \tag{3.7}$$

we formulate the joint optimization problem next.

3.3.2 Bandwidth Allocation with Fractional Association and Multi-Path Routing

We first formulate a linear programming (LP) problem for joint optimization of user-MAP association, backbone routing, and bandwidth allocation. Here we allow fractional association and multi-path routing. With fractional association, a STA can associate with multiple MAPs at different times. The total bandwidth allocated to STA i is $r_i = \sum_{j:(i,j)\in L_a} r_{ij}$ and the network throughput is $S(\mathbf{r}) = \sum_{i=1}^{N} \sum_{j:(i,j)\in L_a} r_{ij}$. With multi-path routing, a traffic flow can be routed via multiple paths from the originating MAP to the gateway.

If the goal is simply to maximize the network throughput without regard to fairness, we can formulate the *Maximum Throughput Bandwidth Allocation* (MTBA) problem as:

$$\begin{aligned} \widehat{S} = \max \quad & S(\mathbf{r}) \\ \text{subject to:} \quad & \text{constraints (3.1)} \sim \text{(3.7)}. \end{aligned} \tag{3.8}$$

Sole consideration of throughput maximization may lead to a serious bias on network resource allocation. To achieve a good tradeoff between throughput and fairness, we adopt a max-min fairness model , and formulate a *Max-Min Fair Bandwidth Allocation* (MMBA) problem. The objective is to maximize the network throughput while ensuring max-min fairness. This problem is formulated in two steps:

Step 1:

$$r^* = \max \ r_{min} \tag{3.9}$$

$$\begin{aligned} \text{subject to:} \quad & \text{constraints (3.1)} \sim \text{(3.7) and,} \\ & \forall i \in V_s, \sum_{j:(i,j)\in L_a} r_{ij} \geq r_{min}, \qquad (3.10) \\ & r_{min} \geq 0. \end{aligned}$$

Step 2:

$$\widehat{S} = \max \quad S(\mathbf{r}) \tag{3.11}$$

subject to: constraints (3.1) $\sim$ (3.7) and,

$$\forall i \in V_s, \sum_{j:(i,j)\in L_a} r_{ij} \geq r^*. \tag{3.12}$$

In Step 1, we maximize the minimum bandwidth (r_{min}) allocated to individual STAs. Specifically, (3.10) states that the bandwidth allocated to any STA should be no less than r_{min}. The resulting bandwidth allocation from step 1 ensures the maximum minimum bandwidth value r^*, but it may not utilize the network resources efficiently. Hence, in Step 2, we maximize the network throughput while making sure that the amount of bandwidth allocated to each STA is at least r^*.

3.3.3 Bandwidth Allocation with Integral Association and Single-Path Routing

In order to limit path selection to single path routing and association to integral association, we introduce two sets of 0-1 variables, $p_{ij} \in \{0,1\}$ and $q_{j,l} \in \{0,1\}$. p_{ij} indicates whether or not STA i associates with MAP j, and $q_{j,l}$ indicates whether or not link l is used for routing traffic of f_j. The bandwidth allocation problem can be formulated by replacing r_{ij} in the above formulations with $p_{ij}r_{ij}$, $R_{j,l}$ with $q_{j,l}R_{j,l}$, and adding the following two constraints:

1. $\forall$ STA i, $\sum_{j:(i,j)\in L_a} p_{ij} = 1$, where $p_{ij} \in \{0,1\}$,
2. $\forall$ MAP k and f_j, $\sum_{l:h(l)=k} q_{j,l} \leq 1$, where $q_{j,l} \in \{0,1\}$.

The first constraint enforces that a STA associate with only one MAP. The second constraint represents that in a single-path routing, at any MAP k, there is at most one out-going link that carries flow f_j. Such problem formulation falls into mixed integer non-linear programming, which is NP-hard.

3.4 Bandwidth Allocation on A Given Tree Topology

To simplify the bandwidth allocation problem under integral association and single-path routing, we decouple the logical topology construction and bandwidth allocation in this section. A tree topology is first built using heuristic association and routing algorithms, and then bandwidth allocation is performed within the determined topology. This scheme is practical and easy to solve, but it gives sub-optimal solutions. We will compare its results with the optimal solutions in the performance evaluation section.

3.4.1 Construction of An Efficient Tree Topology

The logical topology is jointly determined by the STA-MAP association and the backbone routing algorithm. In the backbone, we use the tree-based routing of the hybrid mesh routing protocol defined in IEEE 802.11s [5] to establish paths between MAPs and the gateway. We define an interference-aware routing metric based on [102]. This metric reflects the amount of channel resources consumed by transmitting a packet over a particular link as well as the interference that the link may cause on other links. The cost for a link l consists of two components, the airtime cost $w_{l,a} = \frac{s}{C_l}\frac{1}{1-E_l}$ and the interference cost $w_{l,i} = |I| \times \frac{s}{C_l}$, where s is the test packet size, C_l is link l's capacity, E_l is the packet loss rate on link l, and $|I|$ is the size of the interference set of link l. The airtime cost $w_{l,a}$ reflects the amount of channel resources consumed by transmitting the packet over a particular link. The meaning of $w_{l,i}$ component is the aggregate channel time of the interfered links that transmission on link l consumes. Given $w_{l,a}$ and $w_{l,i}$, the cost of link l is the weighted sum of the two components, i.e., $w_l = \gamma w_{l,a} + (1-\gamma) w_{l,i}$. The cost of a path is simply the summation of the cost of the constituting links.

Unlike in single-hop wireless LANs, where APs are directly connected to a high-speed wired backbone (therefore the criteria for AP selection is the access link quality), traffic in mesh networks could be bottlenecked either by the access link or by the bandwidth-limited wireless backbone. Therefore, we use the end-to-end performance based association mechanism proposed in last chapter for STA-MAP association. In this mechanism, a MAP advertises its backbone path cost in its beacon and probe

response frames so that this information is available to the associating STA. The STA jointly considers the access link as well as the backbone path cost of a candidate MAP by using the composite association metric, *JSEL*, which is defined as:

$$JSEL = (1 - \beta)Q_{al} + \beta Q_{bp} \tag{3.13}$$

where Q_{al} is the access link metric that reflects the quality of the access link between the STA and the MAP; Q_{bp} is the cost of the backhaul path from the MAP to the gateway; $\beta \in [0, 1]$ is a tunable parameter that weights the impacts of access link and backbone path cost on the association.

3.4.2 Fair Bandwidth Allocation On the Given Tree Topology

Given the tree topology constructed by the heuristic association and routing algorithms described above, we perform max-min fair bandwidth allocation within this pre-determined topology. We call this bandwidth allocation problem MMBA-tree.

We use r_i to represent the bandwidth allocated to STA i and denote the vector $\mathbf{r} = [r_1, r_2, ..., r_N]$. We use $A(j)$ to represent the set of STAs that associate with MAP j, use $P(j)$ to represent the backbone path between MAP j and the gateway, and use f_j to represent the total traffic aggregated at MAP j from its associated STAs. Similar to MMBA, MMBA-tree is formulated as a two step problem:

Step 1:

$$r^* = \max\ r_{min} \tag{3.14}$$

subject to:

$$\forall\ j \in V_m, \quad \sum_{i:i\in A(j)} r_i = f_j, \tag{3.15}$$

$$\forall\ j \in V_m, \quad \sum_{i:i\in A(j)} \frac{r_i}{C_{ij}} \le 1, \tag{3.16}$$

$$\forall\ k = \{1,..,K\}, \quad \sum_{l\in F_k} \sum_{j:l\in P(j)} \frac{f_j}{C_l} \le 1, \tag{3.17}$$

$$\forall\ i \in V_s, \quad r_i \ge r_{min}, \tag{3.18}$$

$$\mathbf{r} \ge 0, \mathbf{f} \ge 0, r_{min} \ge 0; \tag{3.19}$$

Step 2:

$$\hat{S} = \max\ \sum_{i=1}^{N} r_i, \tag{3.20}$$

subject to: constraints (3.15) $\sim$ (3.17), and

$$\forall\ i \in V_s, \quad r_i \ge r^*, \tag{3.21}$$

$$\mathbf{r} \ge 0, \mathbf{f} \ge 0, \tag{3.22}$$

3.5 Maximal Clique Approximation

In the formulations of MTBA, MMBA and MMBA-tree, we need to find all the maximal cliques to construct the interference constraints. Searching all the maximal cliques itself, however, is NP hard. To alleviate the complexity, we propose to use the following *clique approximation*.

Instead of using the interference constraints given by (3.6) or (3.17) based on maximal cliques $\{F_k\}$, we form the constraints based on each link's interference set. Specifically, for a link $l \in L_b$, we define its extended interference set $I_l^+ = I_l \cup l$ to include the link itself. We require that the total usage of the links in I_l^+ is at most 1, for all

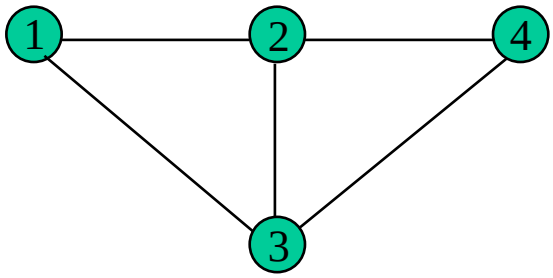

Figure 3.2: Maximal cliques and clique approximation: we use $I_2^+ = \{1, 2, 3, 4\}$ to approximate the two maximal cliques, {1, 2, 3} and {2, 3, 4}.

$l \in L_b$. We conclude that *a maximal clique F_k must be contained in at least one set among $I_l^+, l = 1, 2...|L_b|$*. To show this, suppose that link l belongs to a maximal clique F. According to the definition of maximal clique, the links in F must conflict with link l, and thus F is contained in I_l^+. In Figure 3.2, we give a simple example, where there are two maximal cliques: $\{1, 2, 3\}$ and $\{2, 3, 4\}$. They are both contained in link 2's extended interference set $I_2^+ = \{1, 2, 3, 4\}$.

In Figure 3.2's example, using I_2^+ to form the interference constraint requires that at most one link in I_2^+ is active at a time. This is over-strict, because link 1 and link 4 can actually be active simultaneously. In general, using the clique approximation makes the interference constraints more strict (due to the ignorance of spatial reuse), and yields a suboptimal result to the topology/bandwidth calculation. However, we will see in the next subsection that this performance loss can be at least partially recovered by the proposed scheduling.

3.6 Transmission Scheduling

We assume that the system is time-slotted. In this section we use MMBA-tree to illustrate the scheduling algorithm. Note, however, that the scheduling algorithm can be applied to all of the above schemes.

After solving the MMBA-tree formulated in Subsection 3.4.2, we have obtained $\{f_i\}$ and $\{r_i\}$, where f_i is MAP i's aggregate traffic and r_i is the bandwidth allocated to STA i. As shown in Figure 3.3, the algorithm receives $R(i, l)$ as input, which is the

bandwidth allocated to link l for transmitting flow i. $R(i,l)$ can be obtained from f_i and r_i as follows: when link l is a backbone link, $R(i,l) = f_i$ if link l is on the path between MAP i and the gateway, otherwise $R(i,l) = 0$; when link l is an access link, $R(i,l) = r_i$ if STA i is the sender of link l, otherwise $R(i,l) = 0$. (Note that $R(i,l)$ has been given explicitly in MTBA and MMBA.)

```
Input:  R(i,l) > 0 for link l and flow i,
        T: tentative scheduling cycle,

Set S(t) = Φ for t=1,2,...T, and set T* = 0,
Set x_{i,l} = T R(i,l)/C_l for each l and i,
For each pair (i,l)
    t = 1,
    SlotsToAssign = x_{i,l},
    while (SlotsToAssign > 0)
        if find an element in S(t) whose link interferes with l
            t = t+1,
        else
            Set S(t) = S(t) ∪ (i,l),
            SlotsToAssign = SlotsToAssign − 1,
        end
    end
    Set T* = max{T*, t},
end

Output: S(t), 1 ≤ t ≤ T*.
```

Figure 3.3: Conflict-free scheduling algorithm

Suppose that there are totally T time slots. The algorithm allocates $x_{i,l}$ time slots for link l to transmit flow i, where

$$x_{i,l} = T\frac{R(i,l)}{C_l}. \tag{3.23}$$

We assume that T is large enough so that $x_{i,l}$ is either integral or the rounding error is negligible. The algorithm greedily schedules a transmission to the first time slot such that it will not conflict with any transmission already scheduled in this slot. Scheduling non-interfering transmissions to the same slot accounts for spatial reuse. Note that when the bandwidth calculation is based on maximal cliques, all T time slots will be used and therefore the schedule cycle is T. However, when the bandwidth calculation is based

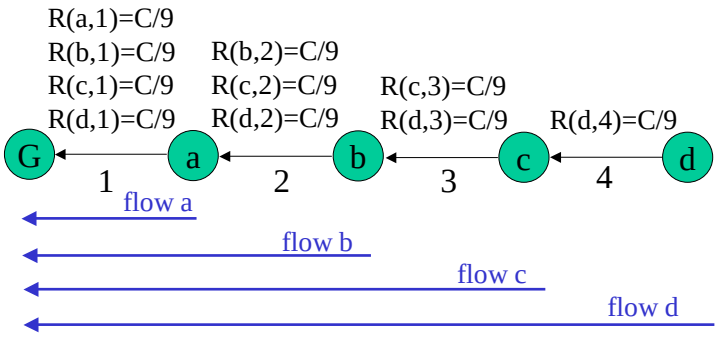

Figure 3.4: Link bandwidth allocation for a linear backbone network

on the maximal-clique approximation, a conservative solution is obtained and not all time slots will be used. Hence, the actual schedule cycle becomes $T^* < T$ (we omit the proof here). The scheduling saves $T - T^*$ slots and (at least partially) recovers the performance loss due to the clique approximation.

To illustrate the scheduling algorithm, we give a simple example in Figure 3.4, where we only show the wireless backbone. We assume that the capacity of each link is C, and that an end-to-end flow exists between each MAP and the gateway. The conflict graph of this network is given in Figure 3.2. By solving the optimal max-min bandwidth allocation (based on maximal cliques), we get $\{R(i,l)\} = C/9$ for all i, l, as shown in Figure 3.4. In contrast, by using the clique approximation (using $I_2^+ = \{1,2,3,4\}$), $R(i,l) = C/10$.

In Figure 3.5, assuming that the tentative scheduling cycle $T = 10$, we show the resulting schedule based on the clique approximation. This conflict-free schedule satisfies the bandwidth requirement. It uses only $T^* = 9$ slots during a scheduling cycle, so each MAP actually achieves the bandwidth of $C/9$. Hence, in this example, the performance loss due to clique approximation is fully recovered.

3.7 Performance Evaluation

In our system, a centralized topology-bandwidth server, collocated with the gateway, is responsible for constructing logical topology, allocating bandwidth, and scheduling link transmissions. The server works in the following three steps: first, it acquires the

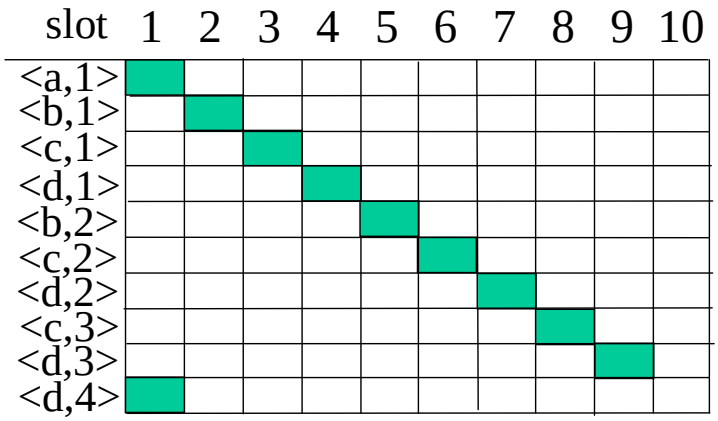

Figure 3.5: Slot assignment (T=10, T*=9): slot 1 is assigned to link 1 for transmitting flow a ($< a, 1 >$) and to link 4 for transmitting flow d ($< d, 4 >$); slot 2 is assigned to link 1 for transmitting flow b ($< b, 1 >$), and etc.

backbone information and the access link information; second, the server constructs the connectivity and conflict graphs based on the acquired information, and then solves the optimization problem for the logical topology and bandwidth allocation vector. Finally, the server uses the collision-free schedule to realize the above calculation.

For the performance evaluation, we consider a wireless mesh network with deployed backbone and randomly positioned STAs. This is often the case in practice, as randomly placed MAPs may lead to poor quality of backbone links and result in inefficient use of resources. In our setting, the backbone is deployed as a 5×3 grid in a rectangular area, with the gateway placed at the upper-right corner. 25 STAs are randomly placed in the area following the uniform distribution.

First, we vary β in (3.13) from 0 to 1 to study its effect on the performance of MMBA-tree scheme in terms of throughput and fairness. The results are presented in Figure 3.6. Figure 3.6(a) illustrates fairness, in which the x-axis is the sorted STA index and the y-axis shows the corresponding allocated bandwidth. We only present the results for 5 representative β values for readability purpose. We see that at $\beta = 0.6$, all the STAs are allocated equal bandwidth and at the same time the network throughput is maximized, as shown in Figure 3.6(b). This result shows that by finding a better logical topology (choosing an appropriate β), we can improve network throughput without sacrificing fairness.

Next we conduct two sets of performance comparison. First we compare the performance of MTBA, MMBA and MMBA-tree in terms of throughput and fairness. For MMBA-tree, we use $\beta = 0.6$. The three schemes construct the interference constraints based on the maximal cliques and thus provide the optimal solutions to the respective formulations. The bandwidth allocation vectors are shown in Figure 3.7(a) and the network throughput is given in Figure 3.8. MTBA provides the highest throughput, but it causes unfairness among STAs in which some of them get starved. MMBA provides perfect fairness, while decreases the throughput by about 20%. MMBA-tree further decrease the throughput and accordingly allocates less bandwidth to each STA. However, the difference between MMBA and MMBA-tree is not significant considering much lower complexity of the MMRA-tree algorithm.

As we described, the maximal clique approximation can alleviate the algorithm complexity, but leads to suboptimal solutions. However such performance gap can be recovered during scheduling where timeslot reuse is considered. To study the impact of clique approximation and scheduling, we compare the bandwidth allocation vectors obtained by solving MMBA-tree optimally and by solving it with clique approximation. We also compare these two vectors with the one that is obtained by first solving MMBA-tree with clique approximation and then performing time slot assignment based on the solution. Figure 3.7(b) gives the three bandwidth allocation vectors. We also show the network throughput of these three schemes in Figure 3.8.

As expected, bandwidth allocated to each STA decreases with clique approximation, so does the network throughput. The scheduling algorithm enables time slot reuse and recovers some performance loss due to clique approximation. As a result, most STAs can obtain the bandwidth equal to that in the optimal solution.

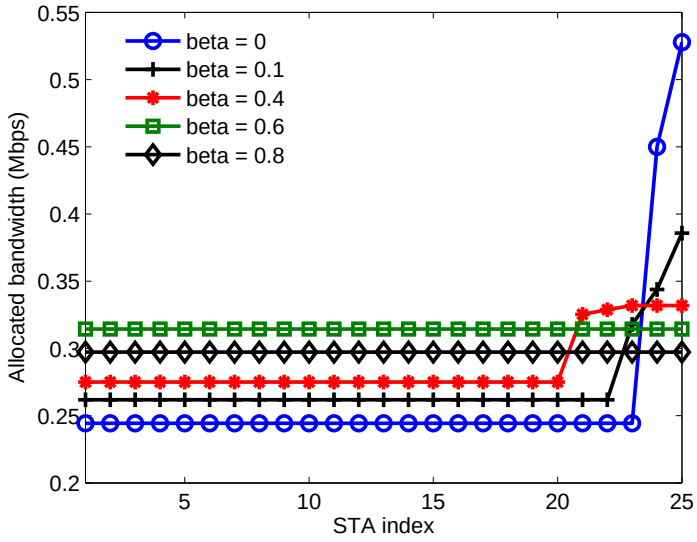

(a) Bandwidth allocation vector

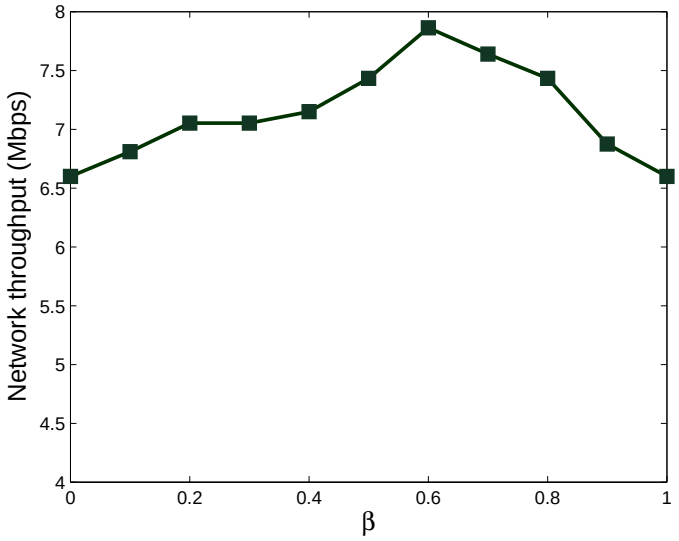

(b) Network throughput

Figure 3.6: Bandwidth allocation and network throughput of MMBA-tree with diff. β

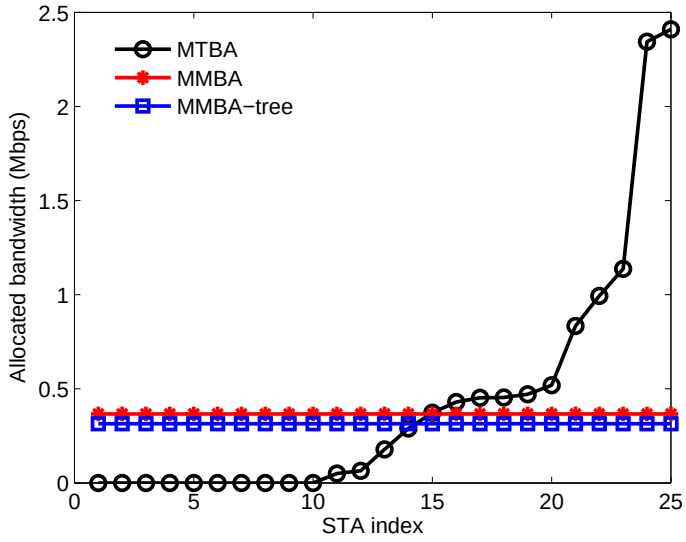

(a) Maximal clique based

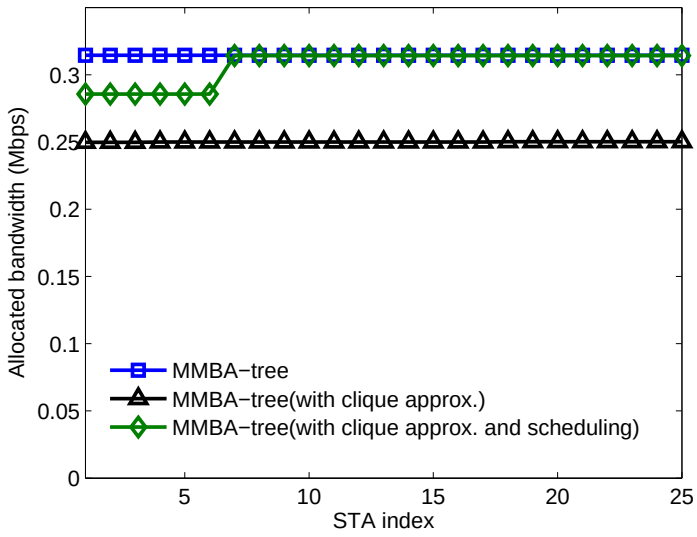

(b) Maximal clique approx. and scheduling

Figure 3.7: Bandwidth allocation vectors obtained by different schemes

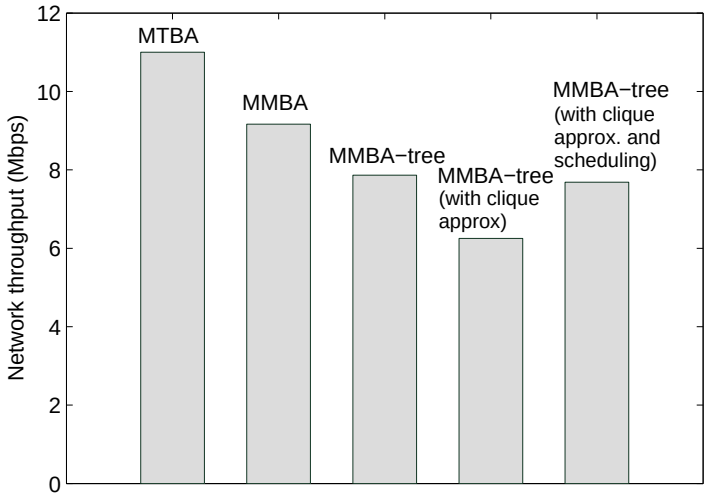

Figure 3.8: Network throughput obtained by different schemes

Chapter 4

Channel Assignment, Stream Control and Scheduling in Multi-Channel MIMO Wireless Mesh Networks

4.1 Background and Related Work

Compared with wired networks, a wireless network normally has lower network throughput due to the existence of interference which prohibits simultaneous transmissions in a common neighborhood. One effective approach for enhancing the network capacity is to use multiple channels. Past research results on wireless capacity (e.g., [36] [35]) that has typically considered a single channel is applicable to a multiple-channel network as well, provided that at each node there is a dedicated interface per channel. However in most cases it may not be feasible to have a dedicated interface per channel at each node. In [60], Kyasanur and Vaidya study how the capacity of multi-channel wireless networks scales with respect to the number of radio interfaces and the number of channels as the number of nodes grow. They have shown that when the number of interfaces per node is smaller than the number of channels, there is a degradation in the network capacity in many scenarios. However, one important exception is a random network with up to $O(\log n)$ channels, wherein even with a single interface per node, there is no capacity degradation. This implies that it may be possible to build capacity-optimal multi-channel networks with as few as one interface per node.

While multiple channels offer a way of minimizing interference, they raise an additional issue of channel assignment. The IEEE 802.11b standard and IEEE 802.11a standard [2] [3], for example, offer 3 and 12 non-overlapping channels respectively. Channel assignment deals with the assignment of 3 or 12 available channels to radio interfaces with the goal of minimizing the total network interference.

One kind of approaches to channel assignment is to change channels on-demand, e.g., on a per-packet basis [85] [70] [48] [83]. Such dynamic channel assignment schemes require frequent channel switchings within each node. This is known to cause delays on the order of a few milliseconds [20]. They also require high speed synchronization among nodes during transmission/receive over a particular channel, which is difficult to achieve without modifying the 802.11 MAC. Another commonly suggested approach is static channel assignment [9] [77] [67]. Although this approach is referred to as static, it can easily be extended to semi-dynamic by refreshing the channel assignment at regular fixed time intervals, depending on the network load stability and predictability. Hybrid approaches [82] [94] [59] apply semi-dynamic/static schemes to non-switchable interfaces and dynamic channel assignment schemes to switchable interfaces.

MIMO is another technology that has been widely accepted as a key technology to increase wireless capacity. MIMO employs multiple antenna elements to offer multiple Degrees of Freedom (DOFs) for communications in a node. A transmitting node can divide the incoming data flow into multiple independent data streams and transmit them simultaneously over multiple antenna elements, and the intended receiving node is able to separate and decode the received data streams based on their spatial signatures. This special feature is referred to as spatial multiplexing. In addition, in presence of interference, one or more antenna elements in a receiving node can also be used to suppress the interference from other links in a common neighborhood. Due to spatial multiplexing and interference suppression, MIMO links can significantly improve network throughput. It has been shown that dramatic capacity gains can be achieved by the use of multiple antennas at both transmit and receive sides in a point-to-point communication system [89] [32]. However, in a multiuser system, achieving link-level optimization does not always imply system-level optimization, especially for bursty packet data traffic. Kim *et al.* studied a maxmin optimization problem in [79] for multi-hop MIMO backhaul networks where they formulated a nonlinear optimization problem to maximize the fair throughput of the access points in the network under the routing, MAC, and physical layer constraints. The physical layer in [79] is based on minimum mean square error (MMSE) beamforming. In [21], Chu and Wang also

studied cross-layer algorithms for MIMO ad hoc networks where MMSE sequential interference cancelation technique (MMSE-SIC) was employed at the physical layer to maximize signal to interference and noise ratio (SINR). Some other works have simplified MIMO physical layer behavior so that tractable analysis can be developed for networking research. In [41], [17], a simplified MIMO cross-layer model was employed to study different throughput optimization problems. By using this model, the network throughput performance can be characterized simply by counting the number of degrees of freedom (DoF) in the network. In [42]- [47], various studies on MAC designs and routing schemes are given based on very simple MIMO models that do not fully exploit MIMO physical capabilities. While MIMO technologies promise greater data throughput and capacity, it raises another issue of stream control: how should the DOFs of each node be arranged (transmit, receive or suppress interference) at certain times?

Most of the current work on wireless mesh networks is mainly based on a layered approach. This layered architecture by providing modularity and transparency between the layers, led to the robust scalable protocols in the Internet and it has become the de facto architecture for wireless systems. However, the spatial reuse of the spectral frequency, the broadcast, unstable and error prone nature of the channel make the layered approach suboptimum for the overall system performance of WMNs. For instance, bad scheduling in MAC layer can lead to interference that affects the performance of the PHY layer due to reduced signal-to-interference-plus-noise-ratio (SINR) and ultimately deteriorates the overall network performance. Congestion control and MAC scheduling are two components that are crucial to the network performance. The congestion control component determines the rates at which users inject data into the network so as to ensure that they fall within the capacity region of the network, and the scheduling component decides which links should be active at what time and in what sequence to accommodate the rates allocated by the congestion control. In [11] an example was presented to show that due to adverse interactions between congestion control and MAC scheduling, the injection rates can not converge to the optimal solution. Motivated by the work of Kelly *et al.* [30] on fair resource allocation in wireline networks, researchers, therefore, have addressed this issue by considering algorithms for jointly combining

congestion control and scheduling [86] [29] [37] [64].

These are primarily why cross-layer design for improving the network performance has been a focus of much recent work. In a cross-layer paradigm, the joint optimization of control over two or more layers can yield significantly improved performance. In this chapter, we consider four design components in the multi-channel MIMO mesh networks: channel assignment, stream control, congestion control and scheduling. We first formulate a cross-layer framework to maximize aggregate utility under the MAC and physical layer constraints. Then we present a heuristic algorithm.

4.2 Preliminaries: MIMO Links

The term MIMO link is used to denote any transmitter-receiver pair such that (1) the receiver is within the transmitters transmission range, and (2) both the transmitter and receiver are equipped with multiple antennas.

4.2.1 MIMO Channel Model and Channel Information

MIMO Channel

In a MIMO link, signals emit from multiple antennas, propagate through the wireless channel and arrive at each of the receive antennas. There exists a path from each of the transmit antennas to each of the receive antennas, and the received signal power can vary from path to path. Therefore, the MIMO channel is always characterized in a form of (channel) matrix.

As long as the channel coherence time is larger than the reciprocal of the channel coherence bandwidth, the fading channels may be modeled as if they were frequency flat, through use of multiple narrow-band carriers (such as orthogonal frequency division multiplexing) [87]. This is the case for many practical environments and we assume it in the thesis. Under this assumption, each entries in the channel matrix is a scalar random variable (or a random process through time).

The received signal power (each entry in the channel matrix) varies due to three effects: mean propagation (path) loss, macroscopic fading and microscopic fading [78].

The propagation loss comes from signal attenuation along the path and is range dependent. Macroscopic fading results from blocking effects by buildings and natural features and is known as shadowing. Both path loss and shadowing can be considered to be the same for all the entries in the channel matrix. Microscopic fading results from the constructive and destructive combination of signal reflections, and is different for each entry in the channel matrix.

MIMO Signal Model

Here, we introduce the signal models for the cases of a point-to-point MIMO link and multiple interfering MIMO links.

In a point-to-point MIMO link, assuming there are K_t transmit antennas and K_r receive antennas, the overall channel is denoted by a $K_r \times K_t$ matrix $\sqrt{\frac{\rho}{K_t}}\mathbf{H}$, where ρ represents the mean received SNR of the channel, accounting for the effects of path loss and shadowing. For a typical fading scenario (Rayleigh fading), $\mathbf{H}$ is assumed to be a complex random matrix with each of its entries being i.i.d. Gaussian distributed [91] with zero mean and unit variance. We assume that the channel is slowly fading, and fixed for the duration of an entire signal burst. From now on we also assume that channel matrix is of full-rank.

In the absence of interference from nearby simultaneous transmissions, the input-output relation for a MIMO link is given by

$$\mathbf{y} = \sqrt{\frac{\rho}{K_t}}\mathbf{H}\mathbf{x} + \mathbf{n}, \tag{4.1}$$

where $\mathbf{x}$, $\mathbf{y}$ and $\mathbf{n}$ denote vectors of transmitted signal, received signal and white Gaussian noise with unit variance, respectively.

Now, let us consider a system with L MIMO links, where each link is subject to co-channel interference from the remaining $L-1$ links. We assume that the transmitting nodes are equipped with K_t antenna elements and receive nodes use K_r antennas. Although different nodes can be equipped with a different number of antennas in practice, our assumption of equal transmit/receive antennas is merely for ease of discussion.

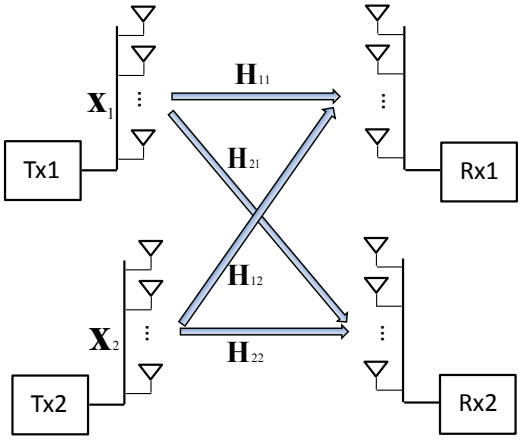

Figure 4.1: Signal model of two interfering MIMO links

The received vector corresponding to the i^{th} link ($i = 1, \ldots, L$) is given by

$$\mathbf{y}_i = \sqrt{\frac{\rho_{i,i}}{K_t}}\mathbf{H}_{i,i}\mathbf{x}_i + \sum_{j \neq i} \sqrt{\frac{\rho_{i,j}}{K_t}}\mathbf{H}_{i,j}\mathbf{x}_j + \mathbf{n}_i \tag{4.2}$$

where $\mathbf{x}_i$ and $\mathbf{x}_j$ are the signal vectors sent by the i^{th} and j^{th} transmitters, respectively, $\mathbf{H}_{i,j}$ and $\rho_{i,j}$ denote the channel gain matrices and mean signal-to-noise ratios (SNRs) between the transmitter of the j^{th} link and receiver of the i^{th} link; $\mathbf{x}_i$ denotes the transmit vector for the i^{th} link and $\mathbf{n}_i$ is the additive white Gaussian noise with zero mean and unit variance. Figure 4.1 depicts the signal model of two interfering MIMO links.

Acquisition of Channel Information

The channel matrix (matrices) can be estimated by the receiver(s) using training signals emitted by the transmitter(s) [72]. The estimation accuracy depends on the training signal energy, and the frequency of channel estimation depends on how fast the channel changes. In addition, the multiple transmit antennas will need additional training effort, since more parameters have to be estimated. The overhead is proportional to the number of transmit antennas.

Channel information can be acquired by the transmitter(s) via dedicated feedback channels from the receiver(s). In this approach, the forward link channel is estimated at

the receiver and is sent to the transmitter on the reverse link. The feedback will involve some delay, which may make the channel information outdated. In a fast changing channel, more frequent estimation and feedback are needed. The overhead becomes a headache when there are multiple interfering MIMO links. For example, in the system described by (4.2) where there are L links each with K_t transmit and K_r receive antennas, the overhead of each feedback is proportional to $K_t K_r L^2$. The resulting overhead on the reverse channel can be prohibitive when the channels change. Another approach of acquiring the channel at transmitter is using channel reciprocity, where the receivers send training signals for the transmitter to estimate. This approach is only applicable when the forward link and reverse link work in the same frequency band.

4.2.2 Transmission Modes and Benefits of MIMO

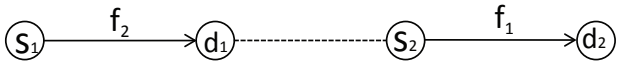

Figure 4.2: An illustrative network example

To illustrate the benefits brought by MIMO transmission, let's consider a very simple example of a multi-hop MIMO network in Figure 4.2, which consists of a set of 4 nodes denoted by $N = \{s_1, s_2, d_1, d_2\}$, and a set $L = \{(s_1, d_1), (s_2, d_2), (s_1, d_2)\}$ of MIMO links. For ease of discussion, we assume that the transmitters and the receivers are each equipped with 2 antennas. We consider a sufficient high SNR scenario, for which we can just discard the thermal noise terms as shown in (4.1) and (4.2). Furthermore, we assume all average SNRs denoted by ρ_{ji} are equal. As a result, ρ_{ji} are not included in the discussion, and the channel matrices between node s_i to node s_j are solely represented by $\mathbf{H}_{ji}$ for $i, j \in \{1, 2\}$.

Various schemes are available for MIMO transmission. In this section, for the purpose of illustration again, we assume a specific strategy, zero-forcing beamforming [72], is used at the receivers.

As shown in Figure 4.3, a MIMO transmission can allow a single stream or multiple streams to be transmitted at a time. In a single-stream transmission, each of the

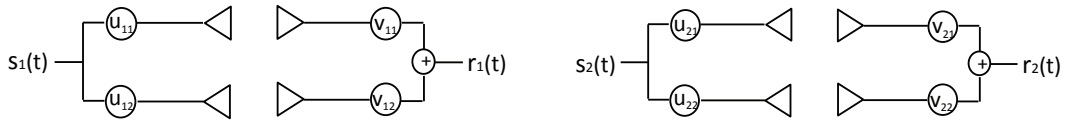

(a) One-stream signal

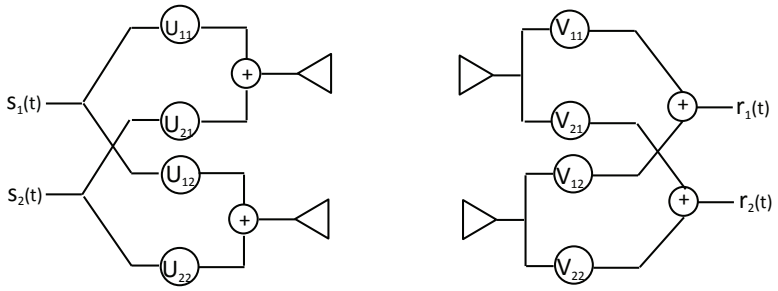

(b) Two-stream signal

Figure 4.3: Single-stream and Multi-stream MIMO transmissions

antennas at a transmitter transmits a linearly dependent copy of a signal; while in multi-stream transmission, each of the antennas transmits a different linear combination of multiple signals. For the particular example shown in Figure 4.2, these transmission modes results in two different benefits called *spatial reuse* and *spatial multiplexing*.

Spatial Reuse

Let's assume that, at a given time t, nodes s_1 and s_2 both decide to transmit signals to d_1 and d_2, respectively. Note that if each of the nodes is equipped with a single omni-directional antenna, then node s_2's transmission will interfere with node d_1's reception, and hence, node d_1 will not be able to successfully receive the signal from node s_1.

To transmit a signal $s_1(t)$ (or a single stream) over a 2-antenna array, node s_1 sends two weighted copies, $u_{1,1}s_1(t)$ and $u_{1,2}s_1(t)$, of the signal, one on each antenna; Similarly, node s_2 sends two weighted copies, $u_{2,1}s_2(t)$ and $u_{2,2}s_2(t)$, of the signal, one on each of its antennas; the vectors $\mathbf{u}_1 = [u_{1,1}\, u_{1,2}]^T$ and $\mathbf{u}_2 = [u_{2,1}\, u_{2,2}]^T$ are referred to as *transmission weight vectors*.

At the output of the channel, nodes d_1 and d_2 observe

$$\mathbf{y}_1(t) = \mathbf{H}_{11}\mathbf{u}_1 s_1(t) + \mathbf{H}_{12}\mathbf{u}_2 s_2(t),$$

and

$$\mathbf{y}_2(t) = \mathbf{H}_{21}\mathbf{u}_1 s_1(t) + \mathbf{H}_{22}\mathbf{u}_2 s_2(t),$$

respectively as the received signals.

Now the received signals at node d_1 is weighted with a *reception weight vector* $\mathbf{v}_1 = [v_{1,1}\, v_{1,2}]^T$ to generate $r_1(t)$, as illustrated in Figure 4.3(a). One can write

$$r_1(t) = (\mathbf{v}_1^T\mathbf{H}_{11}\mathbf{u}_1)s_1(t) + (\mathbf{v}_1^T\mathbf{H}_{12}\mathbf{u}_2)s_2(t).$$

Similarly, node d_2 uses a reception weight vector $\mathbf{v}_2 = [v_{2,1}\, v_{2,2}]^T$ to generate $r_2(t)$, as given by

$$r_2(t) = (\mathbf{v}_2^T\mathbf{H}_{21}\mathbf{u}_1)s_1(t) + (\mathbf{v}_2^T\mathbf{H}_{22}\mathbf{u}_2)s_2(t).$$

It turns out it is possible to choose weight vectors $\mathbf{u}_1, \mathbf{u}_2$, $\mathbf{v}_1$ and $\mathbf{v}_2$ to ensure that each of the receivers is able to recover its useful signal and successfully cancel the interfering signal (zero-forcing). This can be done by choosing the weight vectors satisfying $\mathbf{v}_1^T\mathbf{H}_{11}\mathbf{u}_1 = 1$, $\mathbf{v}_1^T\mathbf{H}_{12}\mathbf{u}_2 = 0$, $\mathbf{v}_2^T\mathbf{H}_{22}\mathbf{u}_2 = 1$ and $\mathbf{v}_2^T\mathbf{H}_{21}\mathbf{u}_1 = 0$. Here let's consider only the design of reception weight vectors $\mathbf{v}_1$ and $\mathbf{v}_2$ (zero-forcing beamforming at receiver only) by assuming the transmit weight vectors $\mathbf{u}_1$ and $\mathbf{u}_2$ are given. In this case, $\mathbf{v}_1$ and $\mathbf{v}_2$ can be solved from the simple linear equations

$$\mathbf{v}_1^T \begin{bmatrix} \mathbf{H}_{11}\mathbf{u}_1 & \mathbf{H}_{12}\mathbf{u}_2 \end{bmatrix} = \begin{bmatrix} 1 & 0 \end{bmatrix},$$

and

$$\mathbf{v}_2^T \begin{bmatrix} \mathbf{H}_{22}\mathbf{u}_2 & \mathbf{H}_{21}\mathbf{u}_1 \end{bmatrix} = \begin{bmatrix} 1 & 0 \end{bmatrix},$$

respectively.

We can see now that receivers can use their multiple antennas to suppress interferences caused by undesired nearby transmitters while successfully receiving their desired signals. Hence, multiple antennas are exploited to increase spatial reuse by allowing multiple simultaneous transmissions in the same vicinity.

Note that here we consider zero-forcing beamforming at receiver only. Likewise, transmitters can also null their signals at undesired nearby receivers (i.e., prevent their signals from reaching undesired nearby receivers) while ensuring acceptable signal gains at their desired receivers. However, we do not discuss transmit zero-forcing beamforming in this section.

Spatial Multiplexing

Multiple antennas can also be explored to send multiple-stream signals. Suppose node s_2 does not transmit at time t, then node d_1 can use both antennas to receive two streams of data concurrently from node s_1.

As shown in Figure 4.3(b), the transmitter can send two streams, $s_1(t)$ and $s_2(t)$, each weighted over both antennas using the transmission weight vector $\mathbf{u}_1 = [u_{1,1}\, u_{1,2}]^T$ and $\mathbf{u}_2 = [u_{2,1}\, u_{2,2}]^T$, respectively. At the receiver (node d_1), two separate streams, $r_1(t)$ and $r_2(t)$, are constructed by weighting the two received signals (one on each antenna) by two reception weight vectors $\mathbf{v}_1 = [v_{1,1}\, v_{1,2}]^T$ and $\mathbf{v}_2 = [v_{2,1}\, v_{2,2}]^T$. One can write

$$r_1(t) = (\mathbf{v_1}^T \mathbf{H}_{11} \mathbf{u_1}) s_1(t) + (\mathbf{v_1}^T \mathbf{H}_{11} \mathbf{u}_2) s_2(t),$$

and

$$r_2(t) = (\mathbf{v_2}^T \mathbf{H}_{11} \mathbf{u}_1) s_1(t) + (\mathbf{v_2}^T \mathbf{H}_{11} \mathbf{v}_2) s_2(t).$$

With an appropriate choice of all the weight vectors and under the assumption that $\mathbf{H}_{11}$ is of full-rank, one can ensure that $\mathbf{v_1}^T \mathbf{H}_{11} \mathbf{u}_1 = 1$ and $\mathbf{v_1}^T \mathbf{H}_{11} \mathbf{u}_2 = 0$ to correctly construct $s_1(t)$ from $r_1(t)$, and $\mathbf{v_1}^T \mathbf{H}_{11} \mathbf{u}_2 = 0$ and $\mathbf{v_2}^T \mathbf{H}_{11} \mathbf{u}_2 = 1$ to construct $s_2(t)$ from $r_2(t)$. Again, assuming that $\mathbf{u}_1$ and $\mathbf{u}_2$ are known, the reception weight vectors

$\mathbf{v}_1$ and $\mathbf{v}_2$ can be solved from a simple equation

$$\begin{bmatrix} \mathbf{v}_1^T \\ \mathbf{v}_2^T \end{bmatrix} H_{11} \begin{bmatrix} \mathbf{u}_1 & \mathbf{u}_2 \end{bmatrix} = \begin{bmatrix} 1 & 0 \\ 0 & 1 \end{bmatrix}.$$

Hence, multiple antennas can also be used to increase the transmission rates by exploiting the *spatial multiplexing* offered by the antennas. Note that now, node s_2 cannot transmit without causing interference at node d_1; spatial reuse cannot be increased when all antennas are used for spatial multiplexing.

4.2.3 Capacity of a Point-to-Point MIMO Link

In the illustrative example discussed above, we assume a very special (and somewhat unrealistic) channel model and a specific transmission scheme called zero-forcing beamforming. In this section, we discuss general channel models and consider the fundamental limit on the transmission rate that can be supported reliably in a MIMO link without constraining any transmission scheme.

The maximum error-free data rate that a channel can support is called the channel capacity. We assume that perfect channel knowledge is available at the receiver, and discuss the channel capacity for two different cases: channel known and channel unknown to the transmitter.

Channel Known to the Transmitter

When the channel is known to the transmitter, the capacity for the point-to-point MIMO link characterized by (4.1) is given by [88]:

$$C = \max_{Tr(\mathbf{Q})=K_t} W \log_2 \det(\mathbf{I}_{K_r} + \frac{\rho}{K_t}\mathbf{HQH}^\dagger) \tag{4.3}$$

where W represents the operating channel bandwidth; $Q = \varepsilon\{\mathbf{x}\mathbf{x}^\dagger\}$ is the input covariance matrix ; $\det(\cdot)$ represents a matrix determinant; $\mathbf{I}_{K_r}$ represents a $K_r \times K_r$ identity matrix.

The knowledge of channel $\mathbf{H}$ at the transmitter enables a neat and capacity-achieving scheme. First, we perform a singular value decomposition (SVD) of $\mathbf{H} = \mathbf{V}\Lambda\mathbf{U}^\dagger$, where $\mathbf{V}$ and $\mathbf{U}$ are both unitary matrices, and Λ is a diagonal matrix with the singular values of $\mathbf{H}$ on its main diagonal. The signal model can be written as $\mathbf{y} = \sqrt{\frac{\rho}{K_t}}\mathbf{V}\Lambda\mathbf{U}^\dagger s + \mathbf{n}$, By using $\mathbf{U}$ as the transmit weight matrix and $\mathbf{V}$ as the receive weight matrix, i.e., by letting $\mathbf{x} = \mathbf{U}^\dagger\mathbf{s}$, $\mathbf{r} = V^\dagger\mathbf{y}$ and $\tilde{\mathbf{n}} = V^\dagger\mathbf{n}$, the channel is

$$\mathbf{r} = \sqrt{\frac{\rho}{K_t}}\Lambda\mathbf{s} + \tilde{\mathbf{n}}, \tag{4.4}$$

which is equivalent to a set of parallel scalar channels. The number of non-zero singular values (i.e., non-zero diagonal entries in Λ) is $r \leq \min\{K_t, K_r\}$, i.e., the rank of $\mathbf{H}$. The rank of $\mathbf{H}$ is called *Degrees of Freedom* (DOF), which measures the number of independent signaling dimensions that are available in the channel.

By using $\mathbf{U}$ as the transmit weight matrix, the input covariance matrix is $\mathbf{Q} = \mathbf{U}\Sigma\mathbf{U}^\dagger$, where Σ is a diagonal matrix whose diagonal entries represent the allocation of total transmit power over each streams. The optimal power allocation scheme, called water-filling algorithm [90], is constructed based on the knowledge of $\mathbf{H}$. We refer the reader to [90] for more details.

Channel Unknown to the Transmitter

If the channel is completely unknown to the transmitter, the transmitted vector $\mathbf{x}$ may be chosen to be statistically non-preferential, i.e., $\mathbf{Q} = \mathbf{I}_{K_t}$. This implies that the signals are independent and equiv-powered at the transmit antennas. The capacity of the MIMO channel in the absence of channel knowledge at the transmitter is then given by [72]

$$C = W \log_2 \det(\mathbf{I}_{K_r} + \frac{\rho}{K_t}\mathbf{H}\mathbf{H}^\dagger). \tag{4.5}$$

Given that $\mathbf{H}\mathbf{H}^{\dagger} = \mathbf{V}\Lambda\mathbf{V}^{\dagger}$ (eigen-value decomposition) , the capacity of the MIMO channel can be expressed as

$$C = W \log_2 \det(\mathbf{I}_{K_r} + \frac{\rho}{K_t}\mathbf{V}\Lambda\mathbf{V}^{\dagger}), \tag{4.6}$$

which is equivalent to

$$C = W \log_2 \det(\mathbf{I}_{K_r} + \frac{\rho}{K_t}\Lambda) = W \sum_{i=1}^{r} \log_2(1 + \frac{\rho}{K_t}\lambda_i), \tag{4.7}$$

where r is the rank of the channel and λ_i are the eigenvalues of $\mathbf{H}\mathbf{H}^{\dagger}$.

In the absence of channel knowledge at the transmitter, the transmitter can use simple beamforming (identity) and power allocation (equal power) strategies, which do not depend on the channel matrix.

4.2.4 Degrees of Freedom and Stream Control

Based on the illustration given in Section 4.2.2, one can draw the following conclusion. At a given node, degrees of freedom (DOFs) can be exploited in one of the following three ways: (1) all DOFs are used to send a multiple-stream flow of data by exploiting the spatial multiplexing of the antenna array; (2) all DOFs are used to increase the spatial reuse of the spectrum by allowing multiple concurrent streams in the same vicinity; (3) some of DOFs are used to send a multiple-stream flow while the others are used to allow for concurrent streams in the same neighborhood.

The stream control problem is how to arrange the DOFs of each node (transmit, receive or suppress interference) at certain times.

4.2.5 Stream Control Via Antenna Selection

Stream control offers a lot of benefits in MIMO networks. Consider the network given in Figure 4.4, where the two transmissions on link (A, B) and link (C, D) interfere with each other. We assume each of the four nodes has $K = 4$ antennas. In TDMA scheme, only one transmission is allowed to take place in a given time slot but the

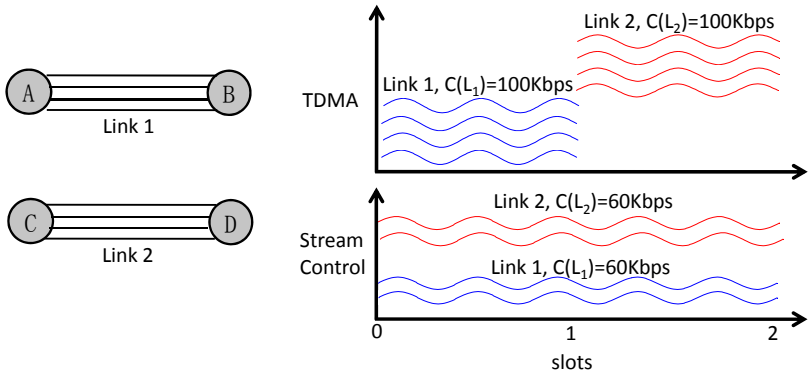

Figure 4.4: Illustration of the need for stream control

transmission proceeds with all four streams. On the other hand, stream control allows two transmissions to proceed simultaneously but the number of streams transmitted by each node is optimized (in this case to two streams) to give the maximum overall network throughput. For this simple two link topology, an improvement of 20% can be obtained in capacity over that of a TDMA scheme. In general, as the number of mutually interfering links (n) increases, the subset of streams used by each of the links decreases ($\frac{K}{n}$), which in turn increases the gain obtained from performing stream control.

Antenna selection provides an easy way for stream control. In the literature, a number of authors have considered MIMO with antenna selection as a means of providing spatial diversity to the streams in an isolated (no interference) MIMO links [34] [6] [33]. However, achieving optimal performance in the presence of co-channel interferers requires a mechanism to regulate the number of streams transmitted by each node, depending upon the strength and number of interfering streams. The authors of [31] and [18] suggested an optimal transmission scheme for OL-MIMO in an interference-free zone that puts independent data streams with equal power into the different antenna. However in an interference-limited environment, this may not be the best strategy. The author in [18] found that the system performance of OL-MIMO in presence of strong co-channel interferers is optimized when all power is put into a single antenna. The authors in [28] considered closed-loop MIMO (CL-MIMO) systems and proposed a distributed stream control mechanism wherein an additional stream is added if it leads

to an increment in the network throughput. The authors showed that MIMO nodes operating under this strategy greatly improve the overall network throughput compared to a time-division multiple access (TDMA) protocol, in which MIMO links operate in succession.

Although stream control works best when channel state information (CSI) is known to the transmitters, the overhead is significant, as the CSI for each pair of transmit-receive nodes has to be signaled back to the transmitters. Moreover, construction of transmission weight vectors and complicated power control also incur high overhead. On the other hand, stream control for OL-MIMO has significantly less complexity but still preserve the benefit of MIMO processing.

In this thesis, we assume that CSI is unknown to the transmitters. We present a simple stream control scheme based on antenna selection. The optimal stream control strategy for the case when the interference is weak is different from the one for the case when the interference is strong. In absence of interference at the receiver, the capacity given by (4.6) is maximized when equal power is put into all antennas. The transmit power correlation matrix (or the input covariance matrix) used by the transmitter of the i-th link in this case is simply a scaled identity matrix, $\mathbf{Q}_{ii} = \frac{E_s}{K_t}\mathbf{I}_{K_t}$. A similar strategy is followed in case of weak interference [18]. Thus in the case of weak interference, stream control is not that critical and near-optimal performance can be extracted by using all streams.

In the case of strong interference, the number of incident interfering streams becomes critical. When the number of interfering streams is greater than the number of receive antennas of the victim node, the optimal strategy is to excite just a single transmit antenna as in this case the receiver is already overloaded. However, when the number of interfering streams is less than the number of receiver antennas, the victim node can suppress interference using linear processing techniques [45]. In this case, the optimal strategy is to excite as many as K_i transmit antennas, where $K_r - K_i$ represents the number of incident interfering streams on the victim receiver i. The remaining antennas are powered off. The K_i transmitted streams are allocated equal power, and

an independent data stream is transmitted from each antenna. Such scheme can be regarded as a special case of spatial multiplexing with fixed (identity) transmission weight vectors. If we assume the first K_i antennas are selected, the transmit power correlation matrix is

$$\mathbf{Q}_{ii} = \frac{E_s}{K_i}\text{diag}(\underbrace{1, 1, ...1}_{K_i}, \underbrace{0, 0, ...0}_{K_t - K_i}) \tag{4.8}$$

where diag(.) denotes the diagonal matrix formed by the elements in its argument. The transmit power correlation matrix for other antenna selections is formed by reordering of diagonal elements in (4.8).

The benefits of this scheme is that no feedback of complex channel matrices are needed. The optimal values of the set of selected antennas are determined at the receiver(s) and sent back to the transmitter(s) over a very limited rate feedback channel.

4.2.6 Achievable Rates of Interfering MIMO Links

Now we consider two interfering MIMO links whereby we adopt antenna selection for stream control (refer to Figure 4.1). For ease of presentation, we assume nodes are equipped with same number of antennas, K. Assume K_i out of K antennas are selected for transmission at the i^{th} transmitter while the remaining antennas are powered off. With the total power constraint E_s, each selected antenna of transmitter i uses power $P_i = \frac{E_s}{K_i}$. In the following, when we refer to i and j at the same time, it is implied that $i \neq j$.

For a particular selection of antennas, the input-output relation for the two links are

$$\mathbf{y}_1 = \sqrt{\frac{\rho_{11}}{K_1}}\mathbf{H}_{11}\mathbf{x}_1 + \sqrt{\frac{\rho_{12}}{K_2}}\mathbf{H}_{12}\mathbf{x}_2 + \mathbf{n}_1$$

and

$$\mathbf{y}_2 = \sqrt{\frac{\rho_{21}}{K_1}}\mathbf{H}_{21}s_1 + \sqrt{\frac{\rho_{22}}{K_2}}\mathbf{H}_{22}\mathbf{x}_2 + \mathbf{n}_2$$

respectively. Here $\mathbf{H}_{ij}$ refers to the $K \times K_j$ channel matrix formed with K_j selected antennas at the j^{th} transmitter and K receive antennas at the i^{th} receiver. ρ_{ij} denotes the corresponding average SNR given the transmit power E_s.

We treat the interferer as noise and define $\tilde{\mathbf{n}}_i = \sqrt{\frac{\rho_{ij}}{K_j}}\mathbf{H}_{ij}\mathbf{x}_j + \mathbf{n}_i$. The covariance matrix of the newly defined noise $\tilde{\mathbf{n}}_i$ is

$$\begin{aligned}\mathbf{N}_i = E\big(\tilde{\mathbf{n}}_i\tilde{\mathbf{n}}_i^\dagger\big) &= E\left((\sqrt{\frac{\rho_{ij}}{K_j}}\mathbf{H}_{ij}\mathbf{x}_j + \mathbf{n}_i)(\sqrt{\frac{\rho_{ij}}{K_j}}\mathbf{H}_{ij}\mathbf{x}_j + \mathbf{n}_i)^\dagger\right)\\ &= \frac{\rho_{ij}}{K_j}\mathbf{H}_{ij}E[\mathbf{x}_j\mathbf{x}_j^\dagger]\mathbf{H}_{ij}^\dagger + E[\mathbf{n}_i\mathbf{n}_i^\dagger]\\ &= \frac{\rho_{ij}}{K_j}\mathbf{H}_{ij}\mathbf{H}_{ij}^\dagger + \mathbf{I}_K \qquad (4.9)\end{aligned}$$

The input-output relation can then be transformed into

$$\mathbf{r}_i = \sqrt{\frac{\rho_{ii}}{K_i}}\mathbf{N}_i^{-1/2}\mathbf{H}_{ii}\mathbf{x}_i + \hat{\mathbf{n}}_i,$$

where $\hat{\mathbf{n}}_i$ is normalized so that $E\{\hat{\mathbf{n}}_i\hat{\mathbf{n}}_i^\dagger\} = \mathbf{I}_K$. Using the capacity result for the point-to-point channel, the achievable rate of the i^{th} MIMO link in the presence of co-channel interferer j is given by

$$\begin{aligned}C_i &= W\log_2\det\big(\mathbf{I}_K + (\sqrt{\frac{\rho_{ii}}{K_i}}\mathbf{N}_i^{-1/2}\mathbf{H}_{ii})(\sqrt{\frac{\rho_{ii}}{K_i}}\mathbf{N}_i^{-1/2}\mathbf{H}_{ii})^\dagger\big)\\ &= W\log_2\det\big(\mathbf{I}_K + \frac{\rho_{ii}}{K_i}(\mathbf{N}_i^{-1/2}\mathbf{H}_{ii})(\mathbf{N}_i^{-1/2}\mathbf{H}_{ii})^\dagger\big)\\ &= W\log_2\det(\mathbf{I}_{K_i} + \frac{\rho_{ii}}{K_i}\mathbf{H}_{ii}^\dagger\mathbf{N}_i^{-1}\mathbf{H}_{ii}) \qquad (4.10)\end{aligned}$$

Inserting $\mathbf{N}_i$ we finally get

$$\begin{aligned}C_i &= W\log_2\det\big(\mathbf{I}_K + \frac{\rho_{ii}}{K_i}\mathbf{H}_{ii}\mathbf{H}_{ii}^\dagger(\mathbf{I}_K + \frac{\rho_{ij}}{K_j}\mathbf{H}_{ij}\mathbf{H}_{ij}^\dagger)^{-1}\big)\\ &= W\log_2\det\big((I_K + \frac{\rho_{ij}}{K_j}\mathbf{H}_{ij}\mathbf{H}_{ij}^\dagger + \frac{\rho_{ii}}{K_i}\mathbf{H}_{ii}\mathbf{H}_{ii}^\dagger)(\mathbf{I}_K + \frac{\rho_{ij}}{K_j}\mathbf{H}_{ij}\mathbf{H}_{ij}^\dagger)^{-1}\big)\\ &= W\log_2\frac{\det(\mathbf{I}_K + \frac{\rho_{ii}}{K_i}\mathbf{H}_{ii}\mathbf{H}_{ii}^\dagger + \frac{\rho_{ij}}{K_j}\mathbf{H}_{ij}\mathbf{H}_{ij}^\dagger)}{\det(\mathbf{I}_K + \frac{\rho_{ij}}{K_j}\mathbf{H}_{ij}\mathbf{H}_{ij}^\dagger)}\\ &= W\big[\log_2\det(I_K + \frac{\rho_{ii}}{K_i}H_{ii}H_{ii}^\dagger + \frac{\rho_{ij}}{K_j}H_{ij}H_{ij}^\dagger) - \log_2\det(\mathbf{I}_K + \frac{\rho_{ij}}{K_j}\mathbf{H}_{ij}\mathbf{H}_{ij}^\dagger)\big]\end{aligned}$$

4.3 Cross-Layer Optimization of Multi-Channel MIMO Mesh Networks

We first formulate a cross-layer optimization framework for maximizing an aggregate utility under the routing, MAC and physical layer constraints to seek the optimal network performance.

4.3.1 Network Model

We consider a wireless mesh network as shown in Figure 1.1 and assume the system is time-slotted. Each mesh node is equipped with one radio capable of switching channels on a per-slot basis. This determines that the channel assignment scheme falls into the kind of semi-dynamic approaches. Each node has multiple antenna elements and can form MIMO links with neighboring nodes if they operate on the same channel.

We model the target network as a direct graph $G = (V, E)$, where V represents the set of nodes in the network and E the set of directed links. If node u and node v are within the transmission range (denoted by R_T) of each other, they can communicate directly. The direct transmission from u to v is represented by a link, $u \rightarrow v$, with the link belonging to the set E, and the same for the direct transmission from v to u. The set of gateway nodes is denoted by $V_G \subseteq V$ and $V_M = V \setminus V_G$ represents the set of non-gateway mesh nodes. Each mesh node aggregates traffic for a large number of mobile users in its coverage.

We denote the interference range as R_I, where $R_I = qR_T$, $q \geq 1$. For a given link, interferer falls within the interference range is regarded as causing strong interference while interferer outside the interference range is regarded as causing no interference or weak interference. To avoid overloading the receiver, if two links are within the interference range of each other and operating on the same channel, the total number of streams they transmit should not exceed the receive antennas at the receivers. We denote by $I(e) \in E$ the set of links that are within the interference range of link $e \in E$. A *clique* is a set of links which mutually conflict with each other (if they operate on the same channel). A maximal clique is a clique that is not contained in any other clique. In

this thesis, we denote maximal cliques in the network as P_m, where $m = 1, 2, ..., M$ and M is the total number of maximal cliques in the network. Note that, in single-antenna systems, at most one link in a maximal clique is allowed to be active at a time on a given channel to avoid overloading receivers.

We assume that there are C orthogonal channels available in the network numbered from 1 to C. For example, with IEEE 802.11b/g networks $C = 3$ in the 2.4GHz band, and with 802.11a $C = 12$ in the 5GHz band. $F(u)$ denotes the set of channels assigned to node u and $|F(u)|$ is the number of channels in $F(u)$, i.e., the number of channels assigned to node u. A communication between two neighboring nodes u and v is possible only when there is a common channel between the sets $F(u)$ and $F(v)$.

We also assume the transmitter u and the receiver v of a MIMO link $e = (u, v)$ are equipped with K_u and K_v antenna elements, respectively. Thus there can be no more than $K_e = \min\{K_u, K_v\}$ concurrent MIMO streams over link e. The receiver can isolate and decode all incoming streams successfully as long as the total number of streams (including the data streams and the interference streams) is not greater than the receiver's degrees of freedom (DOF). For ease of exposition, we assume in this thesis that all the nodes have the same number of antennas, K. Therefore, to avoid conflict, at most K streams in a maximal clique is allowed to be active on a given channel at a time.

4.3.2 Performance Bound: Cross-layer Optimization

We let r_s be the injection rate into flow s and let $U_s(.)$ be a utility function that represents the "benefit to the system" achieved by a given flow rate. The goal of our optimization framework is to maximize the aggregate utility function $\sum_s U_s(r_s)$ by jointly determining channel assignment, MIMO stream control and MAC scheduling. Thus we need to seek: 1) a channel assignment specifying the channels assigned to each node $u \in V$, denoted by $F(u)$; 2) a network flow $f(e, i, j)$ for each link $e = (u, v) \in E$, on each channel i and with j MIMO streams ($1 \leq j \leq K$) over e; 3) a schedule that determines the set of simultaneous communications on each of the available channels

$i = 1, 2, ..., C$ and MIMO streams that is used at each time slot t, for $t = 1, 2, ..., T$ where T is the period of the schedule. Here $f(e, i, j)$ of $f(u, v, i, j)$ denotes the rate at which traffic is transmitted from node u to node v on channel i and using j streams.

In the following, we use $\delta(u)$ to denote the set of links that are incident (incoming or outgoing) on node $u \in V$. Among $\delta(u)$ the incoming links are denoted by $\delta^-(u)$ and the outgoing links are denoted by $\delta^+(u)$. For a link $e = (u, v) \in E$, let $X_t(e, i, j)$ be 1 if there is a communication (e, i, j) from u to v on channel i and using j streams at time slot t, and let $X_t(e, i, j)$ be 0 otherwise. The average flow throughput $f(e, i, j)$ over T time slots is thus given by $f(e, i, j) = \frac{1}{T} \sum_{t \in \{1,...,T\}} X_t(e, i, j) c_t(e, i, j)$ where $c_t(e, i, j)$ is the link capacity of $e = (u, v)$ at t-th slot when it works on channel i and transmits j independent streams. If channel is deterministic where link capacity is constant over all the time slots or if channel is varying but we use average or maximum link capacity instead of $c_t(e, i, j)$, then we can rearrange the terms and yield

$$\frac{1}{T} \sum_{t \in \{1,...,T\}} X_t(e, i, j) = \frac{f(e, i, j)}{c(e, i, j)} \tag{4.11}$$

Here $c(e, i, j)$ is a constant number representing the actual link capacity if channel is deterministic or average(/maximum) link capacity if channel is varying when e works on the i-th channel and transmits j independent streams.

With (4.11) we formulate the following aggregate utility maximization problem.

$$\max \sum_s U_s(r_s) \tag{4.12}$$

$$\forall\ u \in V_M, \sum_{e \in \delta^-(u), i, j} f(e, i, j) + \sum_{s: dst(s) = u} r_s = \sum_{e \in \delta^+(u), i, j} f(e, i, j) + \sum_{s: src(s) = u} r_s \tag{4.13}$$

$$\forall\ (e, i, j), f(e, i, j) \leq c(e, i, j) \tag{4.14}$$

$$\forall\ u \in V, \sum_{i=1}^{C} \sum_{e \in \delta(u)} \sum_{j=1}^{K} \frac{f(e, i, j)}{c(e, i, j)} \leq N(u) \tag{4.15}$$

$$\forall\ m \in [1, M], u \in V, \sum_{e \in P_m} \sum_{j=1}^{K} \frac{f(e, i, j)}{c(e, i, j)} j \leq K \tag{4.16}$$

Equation (4.13) is the flow conservation constraint, where $src(s)$ and $dst(s)$ denote the source and the destination of the flow s, respectively. It shows that at any node u, the total outgoing traffic plus the traffic destined to node u must equal the total incoming traffic plus the aggregate traffic sourced from node u. Equation (4.14) ensures that no link capacities are violated. Equation (4.15) is the radio constraint. Since radio is half-duplex, it can only be engaged in one activity at a time, either send or receive. Thus a node u can participate in at most $N(u)$ activities (send or receive) at a time, that is $\sum_{e\in\delta(u),i,j} X_{(e,i,j)}(t) \leq N(u)$. Averaging over all time slots:

$$\frac{1}{T}\sum_{t\in\{1,\ldots,T\}}\sum_{e\in\delta(u),i,j} X_{(e,i,j)}(t) \leq N(u) \tag{4.17}$$

and from (4.11) the radio constraint (4.15) is derived.

The last constraint (4.16) is the interference constraint. There is interference between a pair of links that operate on the same channel and are within the interference range of each other. With MIMO spatial reuse, two interfering links can transmit simultaneously on the same channel if the receiving nodes have sufficient degrees of freedom to suppress interference. The constraint (4.16) ensures that in each maximal clique P_m, there can be no more than M active streams.

It is worthwhile pointing out that we used point-to-point link capacity instead of actual transmission rate in the above formulation. This results in more loose performance bound. When two interfering links transmit simultaneously on the same channel by taking advantage of MIMO processing, the transmission rate is expected to be lower than the point-to-point link capacity conditioned on the same channel and the same number of streams. The smaller the impact of interference, the closer is the transmission rate to the link capacity and thus the closer is the system performance to the bound. The performance bound would be even more loose if maximum instead of average link capacity is used as $c(e,i,j)$.

4.4 Stream Controlled Multiple Access (SCMA)

In this section, we present a scheduling algorithm responsible for selecting links to transmit in every time slot. The scheduling algorithm proceeds in two stages: channel assignment for scheduling a set of non-interfering links and link pairing for taking advantage of MIMO stream control to improve performance. The algorithm also incorporates a congestion control for source node to determine whether or not to inject a packet so as to prevent congestion in the network. In the following, we assume the routing is pre-determined. we first present the congestion control scheme, and then detail the scheduling algorithm.

4.4.1 Congestion Control

In [86] a Greedy Primal-Dual algorithm is introduced for combined congestion control and scheduling. A per-destination queue (PDQ) is maintained at each node. The per-destination queue for destination d at node i, denoted Q_d^i, stores all the packets at node i that have address d as their destination. Let q_d^i be the amount of data in this queue. Let $n(i,d)$ be the next hop for the destination-d bound traffic after it leaves node i. Each PDQ has an associated concept of urgency weight. The urgency weight for the queue Q_d^i is denoted by w_d^i and is defined by $w_d^i = [q_d^i - q_d^{n(i,d)}]r_{i,n(i,d)}$, i.e., the urgency weight is set to be the difference of the PDQ size at the current node minus the associated PDQ size at the downstream node, multiplied by the transmission rate between these nodes. Actually the urgency weight is a link oriented concept as it involves the two end nodes of a link.

We take the congestion control component from GPD as our congestion control scheme. It is very simple. We use r_s to denote an exponentially filtered average of the injection rate into flow s, i.e. r_s is multiplied by a factor $1-\beta$ in each time step and is increased by βl_p whenever a packet of size l_p is injected into flow s. If flow s is an elastic flow with source and destination nodes $src(s)$ and $dst(s)$ then in each time step it injects a packet if and only if $U_s'(r_s) - \beta q_{dst(s)}^{src(s)} > 0$, where $\beta > 0$ is some (small) parameter and $U_s'(.)$ is the first derivative of $U_s(.)$. In the case that flow s is semi-elastic

(and hence has a minimum rate requirement R_s^{min}) the congestion control component injects a packet whenever $g(\beta T_s) + U'(r_s) - \beta q_{dst(s)}^{src(s)} > 0$, where $g(.)$ is some (sharply) increasing function and T_s is a *token counter* that keeps track of whether or not flow s is meeting its minimum rate requirement. In particular, T_s receives tokens at rate R_s^{min} at all times. Whenever a packet of size l_p is injected into flow s, T_s is decremented by an amount l_p (but is never allowed to drop below zero).

The main theoretical result of [86] is that as β approaches zero, the flow rates produced by the GDP algorithm approach the optimal solution.

4.4.2 Channel Assignment

The MAC scheduling in each time slot t is performed in two stages. The first stage is channel assignment in which channels are assigned to the links in the decreasing order of urgency weights. The second stage is link pairing whereby we attempt to achieve higher throughput by taking advantage of MIMO stream control. In the first stage, some links may not obtain an idle channel, and cannot be scheduled to be active for transmission because of the limited number of available channels and the interference constraint (another link in the interference range has been scheduled). However, with MIMO antenna technique, an unassigned link may share a channel with a neighboring link that has been scheduled in the first stage. Specifically, in the link pairing stage, it is determined whether or how a link unassigned in the first stage can share a channel with an active link (i.e. a link assigned a channel in the first stage). After this stage, the two interfering links may be active simultaneously on the same channel under the constraint that the total number of streams is not greater than the effective degrees of freedom at respective receivers.

Specifically, the following procedure is performed to assign channels in time slot t.

1. Form a set S of all link-channel pair (e, i). We and use $h(e)$ and $t(e)$ to denote the head (transmitter) and tail (receiver) of link e, respectively. Then we define the weight of (e, i) to be $w_{(e,i)} = \max_d [q_d^{h(e)} - q_d^{t(e)}] r_e^i$, where $[q_d^{h(e)} - q_d^{t(e)}]$ represents the difference of the PDQ (for packets destined to d) sizes at the end nodes of link

e and r_e^i is the transmission rate of link e when working on channel i, calculated as in section 4.2.3 in which all of DOFs are used for transmission. We start with an empty schedule $M^i(t)$ for each channel i.

2. Search for the link-channel pair (e, i) with the largest weight $w_{(e,i)}$. Add link e to $M^i(t)$, meaning that link e will be scheduled on i^{th} channel in the t^{th} time slot. we correspondingly assign channel i to the end nodes of link e, i.e. node u and node v where $e = (u, v)$. In other words, we update $F(u)$ and $F(v)$ to include the newly assigned channel i, $F(u) = F(u) \cup \{i\}$ and $F(v) = F(v) \cup \{i\}$.

3. Remove from the set of S all link-channel pairs (e', i), where $e' \in I(e)$. Since $e' \in I(e)$ and i^{th} channel has been assigned to link e, e' can no longer use channel i or interference will occur between e and e'.

4. If $|F(u)| \geq N(u)$, which means node u has used up all its radios, then remove from S all the link-channel pairs (e', i') where e' is any link incident on node u, and i' is a channel not included in $F(u)$. Do the same for the receiving node v.

5. Repeat the above steps until S is empty.

In the channel assignment stage, all effective DOFs are assumed to be used for the intended transmissions. Therefore, if a link is scheduled on the i^{th} channel, no other links in the same neighborhood can operate on the same channel without causing interference to this link. The channel assignment stage results in a schedule in which interfering links can be all active only if each of them can be exclusively assigned a channel. Otherwise, they have to be scheduled in different time slots. We refer to such scheduling algorithm as TDMA in the sequel. By taking advantage of MIMO stream control, we could achieve better performance by scheduling interfering links on the same channel each using partial number of DOFs to transmit and the remaining DOFs for interference suppression. We refer to this latter scheme as SCMA (Stream Control Multiple Access). SCMA adds link pairing stage on top of channel assignment.

4.4.3 Link Pairing

The links that are not scheduled in the channel assignment stage because no more channels are available (some links in its interference range have higher weights and used up all available channels) are referred to as unassigned links at this point. If nodes are equipped with multiple radios, an unassigned link represents a link between two nodes each of which has at least one unassigned/unused radio. For an unassigned link e', we denote an assigned link in its neighborhood as e. If e and e' both use partial number of DOFs for their respective transmissions and set aside enough DOFs for suppressing interference from the other, then e' can be scheduled in the same slot on the same channel as e. Note that if this happens e can no longer transmit as many streams as its DOFs which is assumed in the channel assignment stage. Stream control determines which transmission strategy we should use, letting e transmit with all its DOFs while keeping e' silent, or allowing e' and e transmit simultaneously each using partial number of DOFs? The answer is whichever generates the better performance. Also if e' and e are both scheduled, how many and which antennas should be selected at each transmitter? The answers to these two questions are determined by link pairing stage, which proceeds as follows.

1. All the unassigned links form a set U.

2. Search for the unassigned link e with the highest workload (queue size) in the set U. On each available channel perform the following step 3 and step 4.

3. On channel i, find a candidate pairing link e' for link e. A pairing link candidate e' must satisfy the following two conditions: (a) e' is the only link within the interference range of link e that has been scheduled on channel i in the channel assignment stage; (b) no neighboring link (links within the interference range) of e' has been paired with link e' earlier in the link pairing stage.

4. There is at most one candidate on each channel. If no candidate link exists, continue with the next available channel. Otherwise, determine the set of antennas to be used at each transmitter of the two links. As described in section 4.2.5, we

use the stream control strategy based on antenna selection. We define $w_{(e,i)}^{A(e)} = \max_d[q_d^{h(e)} - q_d^{t(e)}]r_e^{(A(e),i)}$ as the urgency weight of the link-channel pair (e,i) with $A(e)$ being the set of antennas selected at the transmitter of e. Here $r_e^{(A(e),i)}$ denotes the transmission rate of link e on channel i when the sets of antennas selected by the transmitters of e and e' are $A(e)$ and $A(e')$, respectively. As before, $q_d^{h(e)} - q_d^{t(e)}$ is the difference of PDQ (for packets destined to d) sizes at the end nodes of link e. The criterion for antenna selection is to jointly optimize the total urgency weight of (e,i) and (e',i), i.e., to $\max_{|A(e)|+|A(e')|\leq K_r}\{w_{(e,i)}^{A(e)} + w_{(e',i)}^{A(e')}\}$. At the transmitter of e, An independent data stream is transmitted from each selected antenna with the transmit power correlation matrix being $P_e = \frac{E_s}{|A(e)|}diag(\underbrace{1,0,...1,...0}_{|A(e)|\text{ 1's}})$. Similar transmission mode applies to e'.

5. Link e may find qualifying candidates on multiple channels. For each candidate link, we have determined the sets of selected antennas on both transmitters and stored the corresponding maximal total weight in step 3 and step 4. We then select the most qualifying candidate, i.e., the candidate which results in the largest maximal total weight, and pair link e with this selected link, i.e., scheduling e and e' simultaneously on the same channel each using the transmission mode determined in step 4.

6. Assume the selected candidate link e' operates on channel i, we then assign channel i to node u and node v where u and v are the end nodes of link e. Update $F(u) = F(u) \cup \{i\}$ and $F(v) = F(v) \cup \{i\}$.

7. Add link e to $M^i(t)$, meaning that in the t-th time slot link e can be active on channel i using the MIMO mode determined in step 4. Also update the selected pairing link e' that has been added in $M^i(t)$ in the channel assignment stage with the new MIMO mode determined in step 4. After pairing, link e' may not be able to transmit K_t MIMO streams as assumed in the first stage because it has to share the same channel with link e. The total number of MIMO streams transmitted by link e and link e' should not exceed the degree of freedom at respective receivers,

which in most cases equals the number of antenna elements K_r.

8. Update the queue size of link e and link e'.

9. If $|F(u)| \geq N(u)$ which implies node u has used up all its radios, remove from U all the links incident on u.

10. If $|F(v)| \geq N(v)$ which implies node v has used up all its radios, remove from U all the links incident on v.

11. It is possible that link e cannot find a link to pair with. If so, link e is not scheduled in this time slot and removed from the set U.

12. Repeat from step 2 until the set U becomes empty.

4.4.4 Centralized and Distributed Implementations of SCMA

SCMA can be implemented either centralized or distributed, each has its own advantages and disadvantages.

In the centralized implementation, we assume there is a central scheduler in the network to collect channel state and PDQ size information and to schedule link transmissions in each time slot. Since the central scheduler has the complete information about the network, channel assignment and stream control are very easy tasks. The disadvantages of the centralized implementation include single point of failure and poor scalability. At the beginning of each slot, the CSI and the PDQ size for each pair of transmit receive nodes have to be signaled back to the central scheduler, which may incur very high overhead especially for large or dense networks.

Distributed implementation addresses the issues associated with the centralized version but may lose some performance. The distributed scheme consists of 3 components: signaling, contention resolution and scheduling.

- *Signaling*: in the channel assignment stage, links are assigned channels in the decreasing order of urgency weight that is calculated from PDQ size and transmission rate. First of all, on each physical link, the receiver needs to calculate the

transmission rate base on its collected channel state information and send it back to the transmitter. Sent along with the rate information is the PDQ size at the receiver so that the transmitter has the information of PDQ size difference between itself and the receiver. Then transmitter computes the urgency weight and propagate the urgency weight information to its neighbors. The second stage, link pairing, only involves two links, so it is a local concept. Even in the centralized scheme, it can be done without involving the central scheduler.

- *Contention Resolution and Scheduling*: As described the scheduling and contention resolution decisions are based on the urgency weights associated with the PDQs. The scheduling decisions are made in two stages. First, there is an intra-node scheduling procedure in which each transmitter decides which packet it will transmit whenever it is next allowed to make a transmission. Next, there is the contention resolution (or inter-node) scheduling phase in which transmissions that interfere compete among themselves to determine who should transmit next.

  The intra-node scheduling phase is extremely simple. Whenever a node has completed a transmission it determines the PDQ Q_d^i for which w_d^i is maximum. It then removes a packet from that PDQ and joins in a contention resolution competition that aims to determine which among a competing set of transmissions should next be allowed to transmit.

  For inter-node scheduling, it is clear from the definition of the ideal algorithm that its exact implementation would require the solution of a max-weight independent set problem which is not only NP-hard but also hard to approximate. Our inter-node contention resolution protocol is based on the following heuristic. Each node determines the urgency weights of all transmissions with which it will potentially interfere. If it has the maximum urgency weight among those transmissions then it decides to transmit. Note that the inter-node scheduling described here is mainly used in the channel assignment stage of our heuritic algorithm.

4.5 Performance Evaluation

We consider a time-slotted multi-hop wireless mesh network with n static mesh nodes. We present simulation results to compare the performance of TDMA and SCMA for different network scenarios. We assume nodes are equipped with only one radio capable of switching channels on a per-slot basis and have the same number of antennas K. In TDMA, interfering MIMO links either operate in succession or operate on different channels in the same time slot. Which links are to be scheduled is determined by and only by the channel assignment (the first stage of SCMA). When getting its turn, a link uses all the effective DOFs for transmit/receive. SCMA consists of channel assignment stage and link pairing stage. Via link pairing, two interfering MIMO links may simultaneously transmit K_1 and K_2 streams on the given channel, where $0 \leq K_i \leq K (i = 1, 2)$ and $K_1 + K_2 \leq K$. Due to its MIMO awareness, SCMA provides more flexibility than does TDMA since it can choose an appropriate number of streams so as to maximize network throughput. In our system, we also assume that all the mesh nodes have the same total transmission power constraint and receiving sensitivity, resulting in a same maximum transmission range by a certain path loss model. Two nodes can form a link only when the distance between them is not greater than the maximum transmission range. Wireless channels are coarsely characterized by its path loss exponent only in our simulations and we do not consider other channel characteristics such as shadowing. Pathloss describes the attenuation experienced by a wireless signal as a function of distance. Specifically the received signal power at a given distance d is given by

$$P_{dBm}(d) = P_{dBm}(d_0) - 10\alpha \log_{10}(\frac{d}{d_0})$$

where α is the pathloss exponent and d_0 is the reference distance. The prior work [78] suggested that the pathloss exponent can range from 2 to 5 for outdoor urban environment. We use $\alpha = 4$ in our model. Also we take $d_0 = 10m$ as the reference distance and assume $P(d_0) = 40dB$. We also assume the channel bandwidth is 10MHz. Our performance evaluation is based on the centralized implementation of the TDMA and

the SCMA algorithms. We case study the max-min fairness.

4.5.1 Performance in A Simple 4-Link Network

First we consider a simple network which consists of 4 MIMO links, as shown in Figure 4.5, where each receiver is interfered by all the other senders. The four MIMO links are close to each other, so there is mutual interference if they work on the same channel. The distance between the end nodes of each link is 150 meters. Routing is easily determined in this network as 4 one-hop paths from the source to the destination of each flow (flow from 1 to 2, 3 to 4, 5 to 6 and 7 to 8). This simple network makes it possible for us to trace the underlying operations of our schemes and verify their correctness.

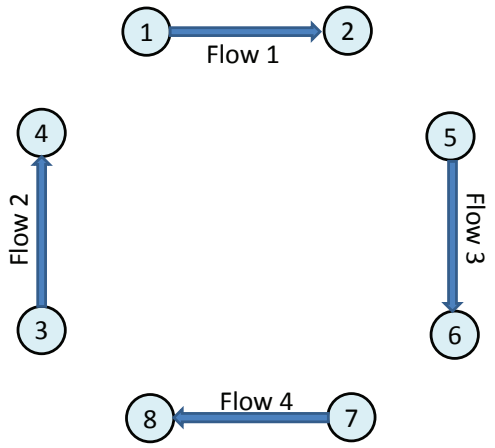

Figure 4.5: A network with 4 MIMO links

We assume there are two available channels in the network and each node has two antenna elements. In TDMA, two and only two links can be active in a time slot, each working on a different channel. In SCMA, two links are assigned different channels in the channel assignment stage; the third and the fourth link may be paired with one of the assigned links and scheduled in the same slot through MIMO stream control. We compare the performance of TDMA and SCMA schemes with derived performance bound in terms of per-flow throughput. We repeat the experiment 100 times, in each of which channel matrices are randomly generated. We then take the average of the

experiment results. Figure 4.6 presents the average throughput each flow receives. The X-axis is flow index. We can see that by taking advantage of MIMO stream control, SCMA outperforms TDMA in fairness as well as in network throughput and its performance is close to the optimal.

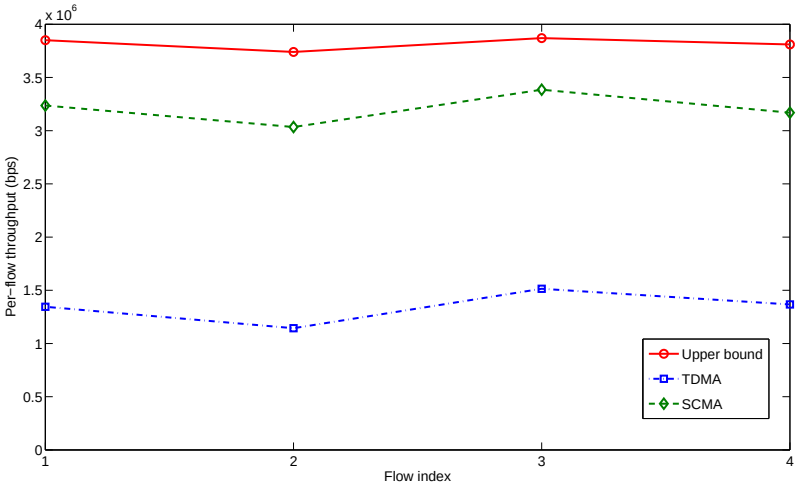

Figure 4.6: Per-flow throughput of 4-link network

4.5.2 Performance in A Tree Network

Next we consider tree networks which are often used in backhaul WMNs. Figure. 4.7 shows a regular two-tier ternary tree network used in our experiment. The root node 0 is an Internet gateway while the other nodes are mesh routers. All links are of a distance of 200m, resulting in the same pathloss. In addition the network topology here is symmetric, so the links on the same tier experience the same level of interference. We randomly generate channel matrix between each node pair with each of its entries being i.i.d. Gaussian distributed with zero mean and unit variance. We assume there is a traffic flow from each mesh router to the gateway. Under the described topology and traffic pattern, it is easily seen that the three links incident on the gateway node form a bottleneck area for the traffic flows, since all the traffic has to go through this area. It is expected that all the traffic flows will be allocated equal channel resources if max-min fairness is seek.

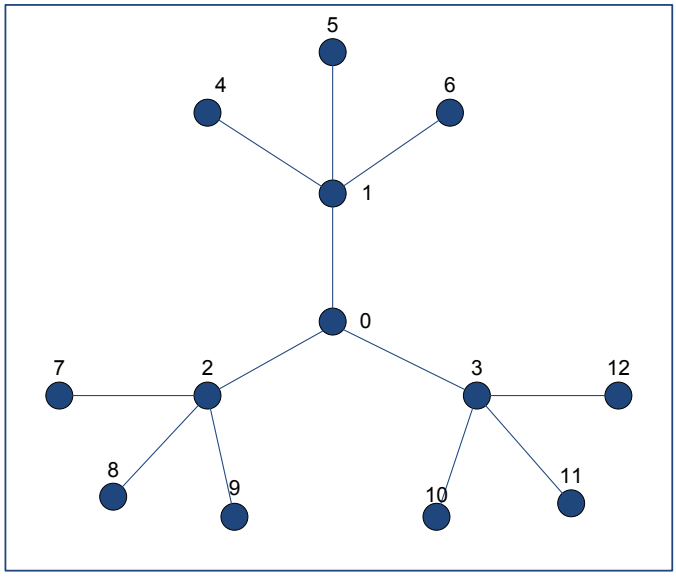

Figure 4.7: Tree network

First we assume there are two available channels in the network and each mesh node has two antennas. We repeat the experiment 100 times, each with randomly generated channel matrices. We average the per-flow throughput on the 100 experiments (100 channel realizations) and present the results in Figure 4.8. We see that channel resources are fairly allocated to 12 flows, but SCMA achieves much higher throughput than TDMA and its performance is very close to the optimal. It is worth noting that the performance gap between the SCMA and the optimal is smaller in the tree network than in the 4-link network. This is due to the impact of interference. As we mentioned, the performance bound is achieved assuming the transmission rate is equivalent to the single link capacity in the absence of interference. We note that the impact of interference in the tree network is much smaller than in the 4-link network. For example, in the 4-link network, node 5, an interferer of node 2, is much closer to node 2 even than node 2's desired sender, node 1. In the tree network, the interferers of a node are all two hops away from the node, which is approximately twice the distance between the intended sender-receiver pair. The strength of interfering streams is thus far weaker than that of the intended transmissions.

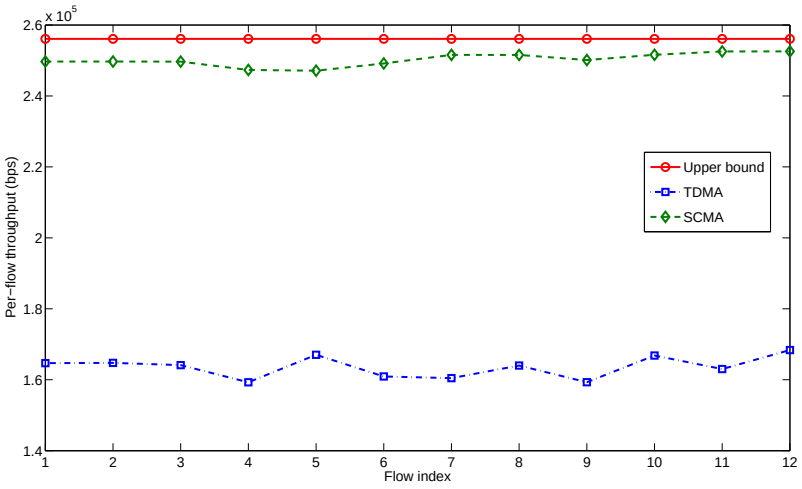

Figure 4.8: Per-flow throughput of the tree network, 2 channels, 2 antennas

Next we investigate the impact of the number of antennas on the network performance. When there are still two available channels, we now assume each node has 4 antenna elements. As above, we repeat the experiment 100 times, each with randomly generated channel matrices. The average throughput of each flow is shown in Figure 4.9. We see that compared to the results of 2-channel 2-antenna case, the throughput performance is significantly improved while preserving fairness when 2 more antenna elements are used.

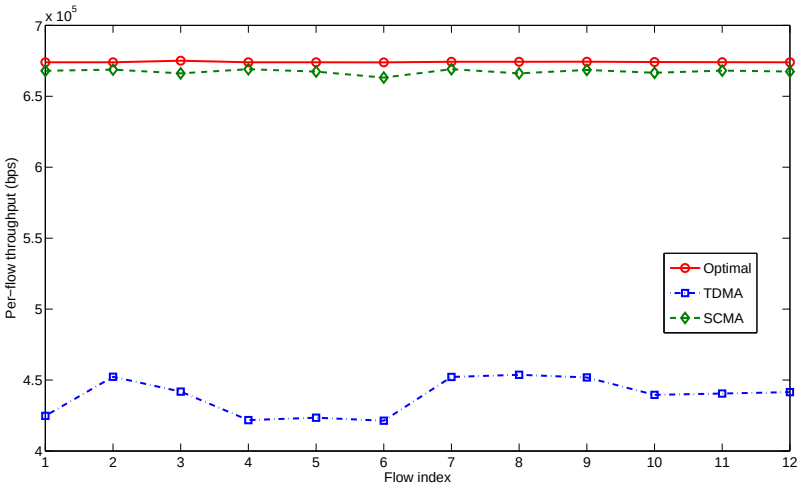

Figure 4.9: Per-flow throughput of the tree network, 2 channels, 4 antennas

To see more clearly how the number of antennas affects throughput and fairness, we vary the number of antennas from 2 to 6, and present the minimum flow throughput and total network throughput in Figure. 4.10. We see that in SCMA, the minimum flow throughput is very close to the average flow throughput (total network throughput over number of flows), showing that it fairly allocates the wireless resources among flows. We observe that the throughput is nearly a linearly increasing function of number of antennas. In addition, SCMA achieves very close to optimal performance.

Last we study the impact of number of available channels on network performance. We vary the number of available channels from 1 to 3 (more than 3 channels would be redundant for this topology). We present the minimum flow throughput and total network throughput in Figure. 4.11. Both minimum flow throughput and total network throughput are increasing with the number of available channels. SCMA outperforms TDMA and goes very close to the optimal. To see more details, we give the throughput of each flow for 3-channel, 4-antenna case in Figure 4.12. We see that wireless resources are almost equally allocated to 12 flows.

4.5.3 Performance in A Random-Topology Network

Last we evaluate the performance of TDMA and SCMA in a network with random topology. We randomly place 20 wireless nodes in a square area of $800 \times 800m^2$. We generate 8 data flows with sources and destinations randomly selected. We show the network topology and flows in Figure. 4.13, where 8 flows are represented by 8 different colors with arrows showing their directions. We repeat the experiment 20 times, in each of which channel matrices are randomly generated. The flow throughput averaged on 20 experiments is given in Figure.4.14. We observe that SCMA outperforms TDMA in this scenario. The performance gap between the SCMA and the performance bound is a little bit larger in this random network than in the tree network due to greater impact of interference.

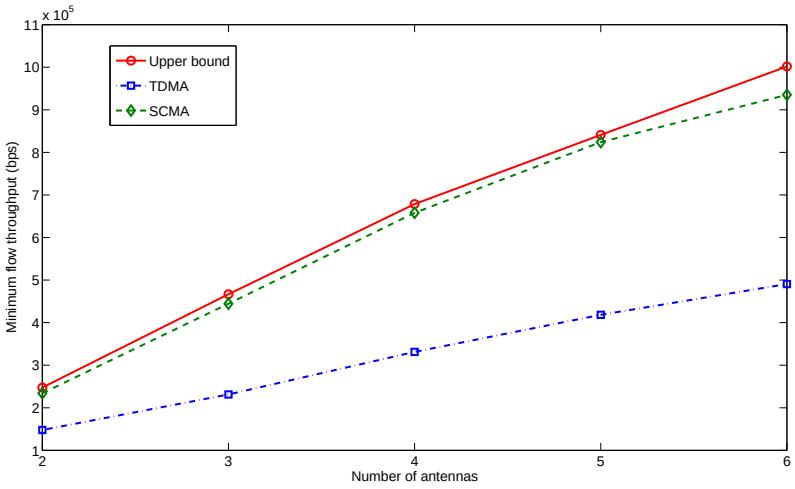

(a) Minimum flow throughput vs. number of antennas

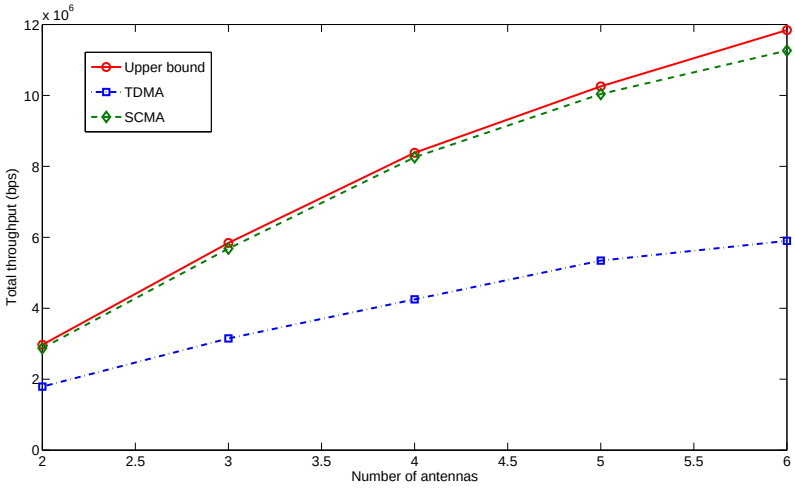

(b) Total network throughput vs. number of antennas

Figure 4.10: Minimum flow throughput and total throughput vs. number of antennas

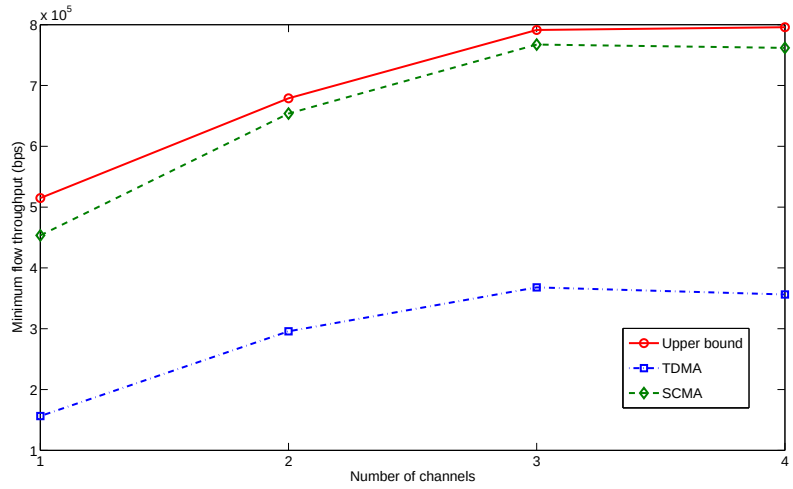

(a) Minimum flow throughput vs. number of channels

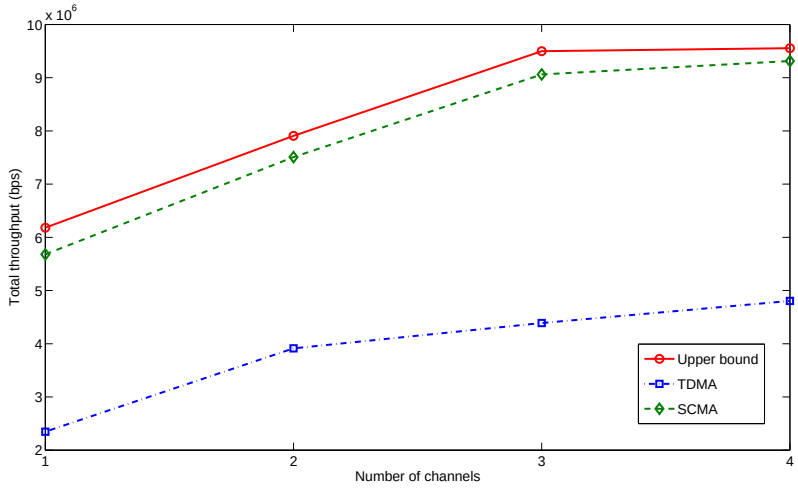

(b) Total network throughput vs. number of channels

Figure 4.11: Minimum flow throughput and total throughput vs. number of channels

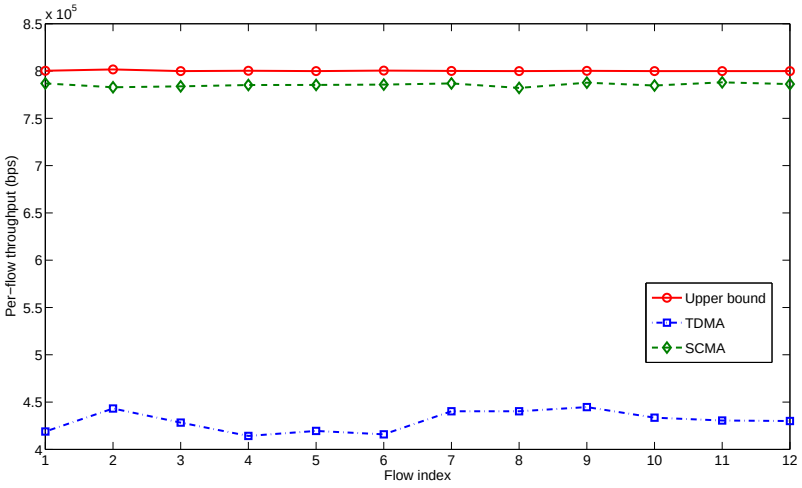

Figure 4.12: Per-flow throughput of the tree network, 3 channels, 4 antennas

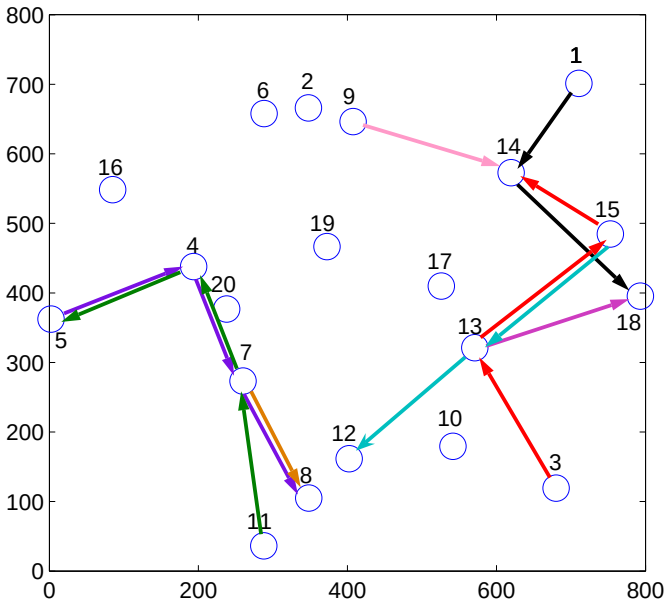

Figure 4.13: Random topology

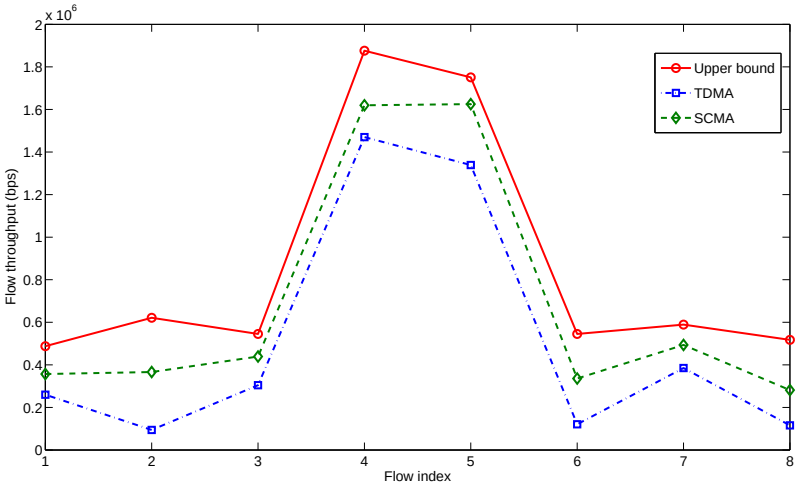

Figure 4.14: Flow throughput of 20-node random network

Chapter 5

Conclusion and Future Work

In this thesis, we have studied association, routing and scheduling algorithms for enhancing throughput and fairness in wireless mesh networks (WMNs). First we have proposed a new cross-layer association control framework for wireless mesh networks. In this framework, we have first introduced two access link metrics that can be applied as association metrics for WLANs and WMNs. The two metrics take into consideration channel quality, channel access contention as well as AP load. We then extend such schemes by combining information about the links between the users and the candidate mesh routers as well as the information about the routing of the packets from those routers to the gateway. In such a way, the association is based on the end-to-end transmission capability of a candidate mesh router, and thus it has the promise to increase the overall throughput of the mesh network. We have conducted extensive simulations and shown that the proposed association mechanism can significantly improve the network performance in terms of throughput and delay by up to 100%. However, the proposed association mechanism still falls short of balancing the network load effectively as the network load increases. Therefore, in the future, we plan to develop an additional mechanism working together with our association scheme to achieve the load balancing in the network. Also we plan to extend our association scheme to be more general, e.g., when inter-cell interference is present or multiple channels are used in the mesh backbone.

We then addressed the optimality which lays an upper bound for the system performance, by optimally allocating channel bandwidth to individual flows and determining transmission schedule such that network throughput can be maximized while certain fairness is achieved. We first study the optimal performance of a WMN by jointly

allocating bandwidth to each data flow without exceeding link capacities, and computing the corresponding user-router association and backbone routing solution. Two scenarios have been considered: (1) fractional association and multi-path routing; (2) integral association and single-path routing. We then focus on the integral association, single-path routing case and investigate the optimal performance of a WMN on a given tree topology. To alleviate the complexity for constructing the wireless interference constraints, we have proposed to use links' extended interference sets to approximate maximal cliques in the network. In addition, we have developed a scheduling algorithm for time-slotted WMN systems to coordinate channel access and to enforce allocated bandwidth. As a bonus, our scheduling algorithm enables spatial reuse and thus can recover some performance loss due to the maximal clique approximation. This has been confirmed by our evaluation. Our evaluation has also shown that association and routing have a great impact on bandwidth allocation, namely constructing a good topology by an efficient algorithm can improve throughput while enhancing fairness. In the future, we plan to study the bandwidth allocation problem in the networks where multiple channels are used in the backbone and inter-cell interference can not be completely eliminated. We also plan to develop a distributed scheduling algorithm to maximize network throughput while preserving fairness.

Last we have studied multi-channel MIMO wireless mesh networks. We have first formulated a cross-layer optimization framework for maximizing an aggregate utility by jointly allocating link bandwidth for data flows, and determining channel assignment and MIMO stream selection. The solution to this optimization framework has provided an upper bound on the performance of multi-channel MIMO WMNs. We then presented an efficient MIMO-aware scheduling algorithm called stream controlled multiple access (SCMA). SCMA determines a baseline schedule in the channel assignment stage where a set of non-interfering links are scheduled on each channel. The second stage of SCMA, link pairing, takes advantage of the performance gain of MIMO stream control. SCMA also incorporates a congestion control scheme for the traffic sources so as to prevent the network from being overloaded. Simulation results have shown that the MIMO-aware scheduling algorithm leads to much higher throughput while preserving fairness than

the MIMO-oblivious algorithm. SCMA achieves performance very close to the optimal in certain scenarios. In our current implementation, we have assumed there is a central scheduler responsible for scheduling. In the future, we plan to relax this assumption and implement a distributed scheme for scheduling.

References

[1] *NS2network simulator*. http://www.isi.edu/nsnam/ns.

[2] Wireless LAN medium access control (MAC) and physical layer (PHY) specification, 1997.

[3] Wireless lan medium access control (mac) and physical layer (phy) specifications - amendment 1: High-speed physical layer in the 5 ghz band, 1999.

[4] Air interface for fixed broadband wireless access systems, 2004.

[5] Wireless lan mesh networking, 2006.

[6] M. Z. Win A. F. Molisch and J. H. Winters. Capacity of mimo systems with antenna selection. In *Proc. IEEE Int. Conf. Communications*, pages 570–574, St.-Petersburg, Russia, 2001.

[7] D. Miorandi A. Kumar, E. Altman and M. Goyal. New insights from a fixed point analysis of single cell ieee 802.11 wlans. In *Proc. of IEEE INFOCOM'05*, Miami, FL, March 2005.

[8] M. Chen B. Noble A. Nicholson, Y. Chawathe and D. Wetherall. Improved access point selection. In *Proc. ACM MobiSys06*, Appsala, Sweden, 2006.

[9] K. Gopalan A. Raniwala and T.-C. Chiueh. Centralized channel assignment and routing algorithms for multi-channel wireless mesh networks. *ACM Mobile Computing and Communications Review (MC2R)*, 8(2):50–65, 2004.

[10] U. Akyol. Effect of physical layer models on wireless network simulations. Master's thesis, Rutgers University.

[11] M. Andrews and A. Slivkins. Oscillations with tcp-like flow control in networks of queues. In *Proc. of IEEE INFOCOM'06*, Barcelona, Spain, 2006.

[12] B. Awerbuch and Y. Shavitt. Converging to approximated max-min flow fairness in logarithmic time. In *Proc. of IEEE INFOCOM'98*, San Francisco, CA, August 1998.

[13] A. Chaintreau K. Papagiannaki B. Kauffmann, F. Baccelli and C. Diot. Measurement-based self organization of interfering 802.11 wireless access networks. In *Proc. IEEE Infocom07*, Anchorage, Alaska, May 2007.

[14] Y. Bejerano and R. Bhatia. Mifi: A framework for fairness and qos assurance in current ieee 802.11 networks with multiple access points. In *Proc. IEEE INFOCOM'04*, Hongkong, 2004.

[15] D. Bertsekas and R. Gallager. *Data Networks*. Prentice-Hall, 1987.

[16] R. Bhatia and L. Li. Throughput optimization of wireless mesh networks with mimo links. In *Proc. IEEE Infocom07*, pages 2326–2330, Anchorage, Alaska, May 2007.

[17] R. Bhatia and L. Li. Throughput optimization of wireless mesh networks with mimo links. In *Proc. of IEEE INFOCOM'07*, pages 2326–2230, Anchorage, AK, May 2007.

[18] R. S. Blum. Mimo capacity with interference. *IEEE Journal on Selected Areas in Communications*, 21:793–801, June 2003.

[19] E. Belding-Royer C. Perkins and S. Das. Ad hoc on-demand distance vector (aodv) routing. RFC 3561, Internet Engineering Task Force, 2003.

[20] R. Chandra and P. Bahl. Multinet: Connecting to multiple ieee 802.11 networks using a single wireless card. In *Proc. of IEEE INFOCOM'04*, Hongkong, China, 2004.

[21] S. Chu and X. Wang. Opportunistic and cooperative spatial multiplexing in mimo ad hoc networks. In *Proc. of ACM Mobihoc'08*, pages 63–72, Hongkong, China, May 2008.

[22] Cisco. *Data sheet of cisco aironet 1200 series*, 2004.

[23] J. Bicket D. De Couto, D. Aguayo and R. Morris. High-throughput path metric for multi-hop wireless routing. In *Proc. of ACM MOBICOM'03*, San Diego, CA, 2003.

[24] M. F. Kaashoek D. G. Andersen, H. Balakrishnan and R. Morris. Resilient overlay networks. *ACM SIGOPS Operating Systems Review*, 35(5), December.

[25] R. Murty D. Larson and E. Qi. An adaptive approach to wireless network performance optimization. *Technology@Intel Magazine*.

[26] G. Chandrasekaran D. Lee and P. Sinh. Optimizing broadcast load in mesh networks using dual-association. In *Proc. IEEE WiMesh05*, Santa Clara, CA, 2005.

[27] M. Sridharan D. Lee, G. Chandrasekaran and P. Sinha. Association management for data dissemination over wireless mesh networks. *Elsevier Computer Networks*, 2007.

[28] M. F. Demirkol and M. A. Ingram. Stream control in networks with interfering mimo links. In *Proc. of IEEE Wireless Communications and Networking Conference*, volume 1, pages 343–348, New Orleans, LA, 2003.

[29] A. Eryilmaz and R. Srikant. Fair resource allocation in wireless networks using queue-length based scheduling and congestion control. In *Proc. of IEEE INFOCOM'05*, Miami, FL, March 2005.

[30] A. Maulloo F. Kelly and D. Tan. Rate control for communication networks: shadow prices, proportional fairness and stability. *Journal of the Operations Research Society*, 49(3):237–252, 1998.

[31] G. J. Foschini and M. J. Gans. On limits of wireless communications in a fading environment when using multiple antennas. *Wireless Personal Communications*, 6.

[32] G. J. Foschini and M. J. Gans. On limits of wireless communications in a fading environment when using multiple antennas. *Wireless Personal Commun.*, 6(3):311–335, 1998.

[33] A. Ghrayeb and T. M. Duman. Performance analysis of mimo systems with antenna selection over quasi-static fading channels. *IEEE Trans. Vehicular Tech.*, 52:281–288, March 2003.

[34] D. A. Gore and A. J. Paulraj. Mimo antenna subset selection with space-time coding. *IEEE Trans. Signal Processing*, 50:2580–2588, October 2002.

[35] M. Grossglauser and D. Tse. Mobility increases the capacity of ad-hoc wireless networks. In *Proc. of IEEE INFOCOM'01*, Anchorage, Alaska, 2001.

[36] P. Gupta and P. R. Kumar. The capacity of wireless networks. *IEEE Information Theory*, 46(2):388–404, March 2000.

[37] P. Gupta and A. Stolyar. Optimal throughput allocation in general random-access networks. In *Proc. of IEEE CISS'06*, Princeton, NJ, March 2006.

[38] J. Cheng S. Lu H. Luo, P. Medvedev. A self-coordinating approach to distributed fair queueing in ad hoc wireless networks. In *Proc. of IEEE INFOCOM'01*, Anchorage, Alaska, 2001.

[39] S. Lu H. Luo. A topology-independent fair queueing model in ad hoc wireless networks. In *Proc. of IEEE ICNP'00*, Osaka, Japan, November 2000.

[40] Y. Fang H. Zhai, J. Wang. Distributed packet scheduling for multihop flows in ad hoc networks. In *Proc. of IEEE WCNC'04*, Atlanta, GA, 2004.

[41] B. Hamdaoui and K. G. Shin. Characterization and analysis of multihop wireless mimo network throughput. In *Proc. of ACM Mobihoc'07*, pages 120–129, Montreal, Quebec, Canada, September 2007.

[42] M. Hu and J. Zhang. Mimo ad hoc networks: Medium access control, saturation throughput, and optimal hop distance. *Special Issue on Mobile Ad Hoc Networks, Journal of Communications and Networks*, pages 317–330, December 2004.

[43] X. Wang I.F. Akyildiz and W. Wang. Wireless mesh networks: a survey. *Computer Networks*, 47(4):445–487, 2005.

[44] E. Madruga D. Beyer J. Garcia-Luna-Aceves, C. Fullmer and T. Frivold. Wireless internet gateways (wings). In *Proc. IEEE MILCOM 97*, Monterey, CA, November 1997.

[45] J. Salz J. H. Winters and R. D. Gitlin. The impact of antenna diversity on the capacity of wireless communication systems. *IEEE Transactions on Communications*, 40(2).

[46] Y. Rabani J. M. Kleinberg and E. Tardos. Fairness in routing and load balancing. In *Proc. of IEEE FOCS'99*, New York, NY, October 1999.

[47] M. Gerla J.-S. Park, A. Nandan and H. Lee. Space-mac: Enabling spatial reuse using mimo channel-aware mac. In *Proc. of IEEE ICC'05*, pages 3642–3646, Seoul, Korea, May 2005.

[48] T. Salonidis J. Shi and E. Knightly. Starvation mitigation through multi-channel coordination in csma based wireless networks. In *Proc. of ACM MOBIHOC'06*, pages 214–225, Florence, Italy, May 2006.

[49] C. Chandler W. Zhang J. Tang, G. Xue. Interference-aware routing in multi-hop wireless networks using directional antennas. In *Proc. of IEEE INFOCOM'05*, Miami, FL, March 2005.

[50] J. M. Jaffe. Bottleneck flow control. *IEEE/ACM Transaction on Communications*, pages 954–962, 1998.

[51] G. Judd and P. Steenkiste. Fixing 802.11 access point selection. *ACM SIGCOMM Computer Communication Review*, 2002.

[52] H-S Park K-J Myoung, S-Y Shin and W-H Kwon. Ieee 802.11b perforamnce analysis in the presence of ieee 802.15.4 interference. *IEICE Trans, Commun*, E90-B(1), January.

[53] V. Padmanabhan K. Jain, J. Padhye and L. Qiu. Impact of interference on multihop wireless network performance. In *Proc. ACM Mobicom '03*, pages 66–80, San Diego, CA, 2003.

[54] X. Y. Li K. Moaveninejad. Low-interference topology control for wireless ad hoc networks. *Journal of Ad Hoc and Sensor Wireless Networks*, 1.

[55] G. Chandranmenon-S. Miller K. Almeroth K. Ramachandran, M. M. Buddhikot and E. Belding-Royer. On the design and implementation of infrastructure mesh networks. In *Proc. of IEEE WIMESH05*, Santa Clara, CA, 2005.

[56] M. A. Ingram K. Sundaresan, R. Sivakumar and T-Y. Chang. Medium access control in ad hoc networks with mimo links: optimization considerations and algorithms. *IEEE Transactions on Mobile Computing*, 3(4):350–365, 2004.

[57] A. Khanna and J. Zinky. The revised arpanet routing metric. In *Proc. of ACM SIGCOMM'89*, Austin, TX, 1989.

[58] A. Kumar and V. Kumar. Optimal association of stations and aps in an ieee 802.11 wlan. In *Proc. NCC 05*, January 2005.

[59] P. Kyasanur and N. Vaidya. Routing and interface assignment in multichannel multi-interface wireless networks. In *Proc. of IEEE WCNC'05*, pages 2051–2056, New Orleans, LA, 2005.

[60] P. Kyasanur and N. H. Vaidya. Capacity of multi-channel wireless networks: Impact of number of channels and interfaces. In *Proc. of ACM MobiCom'05*, Cologne, Germany, August 2005.

[61] B. Anepu I. Seskar L. Raju, S. Ganu and D. Raychaudhuri. Beacon assisted discovery protocol (bead) for self-organizing hierarchical ad-hoc networks. In *Proc. IEEE Globecom '04*, pages 1676– 1680, Dallas, TX, November 2004.

[62] S. Sarkar L. Tassiulas. Maxmin fair scheduling in wireless networks. In *Proc. of IEEE INFOCOM'02*, New York, NY, 2002.

[63] B. Li. End-to-end fair bandwidth allocation in multi-hop wireless ad hoc networks. In *Proc. ICDCS'2005*, Columbus, Ohio, June 2005.

[64] X. Lin and N. Shroff. The impact of imperfect scheduling on cross-layer rate control in multihop wireless networks. In *Proc. of IEEE INFOCOM'05*, Miami, FL, March 2005.

[65] R. Wattenhofer A. Zollinger M. Burkhart, P. von Rickenbach. Does topology control reduce interference. In *Proc. of ACM MobiHoc'04*, Tokyo, Japan, May 2004.

[66] G. Berger-Sabbatel M. Heusse, F. Rousseau and A. Duda. Performance anomaly of 802.11b. In *Proc. of IEEE INFOCOM'03*, San Francisco, CA, March 2003.

[67] M. Marina and S. Das. A topology control approach for utilizing multiple channels in multi-radio wireless mesh networks. In *Proc. of IEEE BroadNet'05*, Boston, MA, October 2005.

[68] N. Megiddo. Optimal flows in networks with multiple sources and sinks. *Mathematical Programming*, 7(3):97–107, 1974.

[69] V. Mhatre and K. Papagiannaki. Using smart triggers for improved user performance in 802.11 wireless networks. In *Proc. MobiSys 06*, Appsala, Sweden, 2006.

[70] R. Chandra P. Bahl and J. Dunagan. Connecting to multiple ieee 802.11-based networks using a single wireless card. In *Proc. of IEEE INFOCOM'04*, pages 882–893, Hongkong, China, 2004.

[71] I. Papanikos and M. Logothetis. A study on dynamic load balance for ieee 802.11b wireless lan. In *Proc. COMCON'2001*, 2001.

[72] A. Paulraj, R. Nabar, and D. Gore. *Introduction to space-time wireless communications*. Cambridge University Press, 2003.

[73] J. P. Pavon and S. Choi. Link adaptation strategy for ieee 802.11 wlan via received signal strength measurement. In *Proc. of IEEE ICC'03*, pages 11–15, Anchorage, AL, May 2003.

[74] S. Banerjee Q. Dong and B. Liu. Throughput optimization and fair bandwidth allocation in multi-hop wireless lans. In *Proc. IEEE Infocom '06*, Barcelona, Spain, 2006.

[75] J. Padhye R. Draves and B. Zill. Comparison of routing metrics for static multi-hop wireless networks. In *Proc. of ACM MOBICOM'04*, Philadelphia, PA, 2004.

[76] J. Padhye R. Draves and B. Zill. Routing in multi- radio, multi-hop wireless mesh networks. In *Proc. of ACM MOBICOM04*, Philadelphia, PA, 2004.

[77] A. Raniwala and T.-C. Chiueh. Architecture and algorithms for an ieee 802.11-based multi-channel wireless mesh network. In *Proc. of IEEE INFOCOM'05*, Miami, FL, March 2005.

[78] T. S. Rapport. *Wireless communications principles and practice*. Prentice-Hall, 1996.

[79] X. Wang S.-J. Kim and M. Madihian. Cross-layer design of wireless multihop backhaul networks with multiantenna beamforming. *IEEE Trans. Mobile Comput.*, 6(11):1259–1269, November 2007.

[80] E. Altman S. Shakkottai and A. Kumar. The case for non-cooperative multihoming of users to access points in ieee 802.11 wlans. In *Proc. IEEE INFOCOM 06*, Barcelona, Spain, 2006.

[81] C. Diot-J.Kurose S. Vasudevan, K. Papagiannaki and D. Towsley. Facilitating access point selection in ieee 802.11 wireless networks. In *Proc. ACM Sigcomm IMC '05*, Berkeley, CA, October 2005.

[82] C. Lin S. Wu, Y. Tseng and J. Sheu. A multi-channel mac protocol with power control for multi-hop mobile ad hoc networks. *IEEE Computer Journal*, pages 419–424, 2002.

[83] Y. Tseng S. Wu, C. Lin and J. Sheu. A new multi-channel mac protocol with on-demand channel assignment for mobile ad hoc networks. In *Proc. of IEEE ISPAN'00*, Dallas, TX, December 2000.

[84] B. Schrick and M. Riezenman. Wireless broadband in a box. *IEEE Spectrum Magazine*.

[85] J. So and N. H. Vaidya. Multi-channel mac for ad hoc networks: Handling multi-channel hidden terminals using a single transceiver. In *Proc. of ACM MobiHoc'04*, pages 222–233, Tokyo, Japan, May 2004.

[86] A. Stolyar. Maximizing queueing network utility subject to stability: Greedy primal-dual algorithm. *Queueing Systems*, 50(4):401–457, 2005.

[87] X. Tang and Y. Hua. Optimal design of non-regenerative mimo wireless relays. *IEEE Transactions on Wireless Communications*, 6(4):1398–1407, Apr. 2007.

[88] E. Telatar. Capacity of multi-antenna gaussian channels. *European Transactions on Telecommunications*, 10(6).

[89] I. E. Telatar. Capacity of multi-antenna gaussian channels. *European Trans. Telecommun.*, 10(6):586–595, 1999.

[90] Joy A. Thomas Thomas M. Cover. *Elements of Information Theory*. Wiley-Interscience, 1991.

[91] A. M. Tulino and S. Verdu. *Random Matrix Theory and Wireless Communications*. now Publishers Inc., 2004.

[92] B. Sadeghi V. Gambiroza and E. W. Knightly. End-to-end performance and fairness in multihop wireless backhaul networks. In *Proc. ACM Mobicom '04*, Philadelphia, PA, 2004.

[93] A. Mishra W. Arbaugh and M. Shin. An empirical analysis of the ieee 802.11 mac layer handoff process. In *Proc. ACM SIGCOMM 03*, Karlsruhe, Germany, August 2003.

[94] K. Law W. Hung and A. Leon-Garcia. A dynamic multi-channel mac for ad hoc lan. 2002.

[95] B. Bensaou X. L. Huang. On max-min fairness and scheduling in wireless ad hoc networks: Analytical framework and implementation. In *Proc. of ACM MobiHoc'01*, Long Beach, CA, October 2001.

[96] Y. Mansour Y. Afek and Z. Ostfeld. Phantom: a simple and effective flow control scheme. *Computer Networks*.

[97] Y. Mansour Y. Afek and Z. Ostfeld. Convergence complexity of optimistic rate based flow control algorithms (extended abstract). In *Proc. of ACM Symposium on Theory of Computing*, pages 89–98, Philadelphia, PA, May 1996.

[98] M. Hilsdale-R. Musaloiu-Elefteri Y. Amir, C. Danilov and N. Rivera. Fast handoff for seamless wireless mesh networks. In *Proc. ACM MobiSys06*, Appsala, Sweden, 2006.

[99] S. Han Y. Bejerano and L. Li. Fairness and load balancing in wireless lans using association control. In *Proc. ACM MobiCom'04*, Philadelphia, PA, 2004.

[100] T. Abe Y. Fukuda and Y. Oie. Decentralized access point selection architecture for wireless lans. In *Proc. IEEE WTS '04*, pages 137–145, Pomona, CA, May 2004.

[101] H. H.-Y. Tzeng Y. T. Hou and S. S. Panwar. A generalized max-min rate allocation policy and its distributed implementation using abr flow control mechanism. In *Proc. of IEEE INFOCOM'98*, San Francisco, CA, August 1998.

[102] J. Wang Y. Yang and R. Kravets. Designing routing metrics for mesh metworks. In *Proc. IEEE WiMesh '05*, Santa Clara, CA, 2005.

[103] M. Wu D. Li Y. Zhu, H. Liu and S. Mathur. Implementation experience of a prototype for video streaming over wireless mesh networks. In *Proc. IEEE CCNC '07*, Las Vegas, NV, January 2007.

[104] Y. Shi Y.T. Hou and H.D. Sherali. Rate allocation in wireless sensor networks with network lifetime requirement. In *Proc. of ACM MobiHoc'04*, pages 67– 77, Tokyo, Japan, May 2004.

[105] A. Hunag Z. Zhang, S. Liu and A. Zhang. Performance analysis of cck modulation under multipath fading channel. In *Proc. of IEEE NORSIG'04*, pages 276–279, Meripuisto, Espoo, Finland, June 2004.

Curriculum Vita

Lin Luo

2003-2010 Ph.D. in Wireless Information Network Laboratory (WINLAB), Electrical and Computer Engineering (ECE), Rutgers University

2003-2006 M.S. in Wireless Information Network Laboratory (WINLAB), Electrical and Computer Engineering (ECE), Rutgers University

2000-2003 M.S. in Electrical Engineering (EE), University of Electronic Science and Technology of China

1996-2000 B.S. in Electrical Engineering (EE), University of Electronic Science and Technology of China

2004-2010 Graduate Assistant, WINLAB, ECE, Rutgers University

2007 Research Intern, Thomson Corporate Research Lab, Princeton, NJ

2006 Research Intern, Thomson Corporate Research Lab, Princeton, NJ

2003-2004 Teaching Assistant, ECE, Rutgers University

Publications

- L. Luo, D. Raychaudhuri, H. Liu, M. Wu and D. Li, "End-to-End Performance Aware Association Mechanism for Wireless Municipal Mesh Networks", *Elsevier Computer Communications Journal*, vol. 31/8, pp. 1602-1614, May 2008.
- M. A. Ergin, M. Gruteser, L. Luo, D. Raychaudhuri and H. Liu, "Available Bandwidth Estimation and Admission Control for QoS Routing in Wireless Mesh Networks", *Elsevier Computer Communications Journal*, vol. 31/7, pp. 1301-1317, May 2008.
- L. Luo, D. Raychaudhuri, H. Liu, "Channel Assignment, Stream Control, Scheduling and Routing in Multi-Radio MIMO Wireless Mesh Networks", in *Proc. of International Workshop on the Network of the Future*, held with *IEEE ICC*, Jun. 2009.
- L. Luo, D. Raychaudhuri, H. Liu, M. Wu and D. Li, "Joint Association, Routing and Bandwidth Allocation for Wireless Mesh Networks", in *Proc. of IEEE Globecom*, New Orleans, LA, Dec 2008.

- L. Luo, M. Gruteser and H. Liu, "Achieving Temporal Fairness in Multi-Rate 802.11 WLANs with Capture Effect", in *Proc. of IEEE ICC*, pp. 2496-2501, Beijing, China, May 2008.
- L. Luo, D. Raychaudhuri, H. Liu, M. Wu and D. Li, "Improving End-to-End Performance of Wireless Mesh Networks through Smart Association", in *Proc. of IEEE WCNC*, Las Vegas, NV, April 2008.
- L. Luo, D. Raychaudhuri, H. Liu, M. Wu and D. Li, "End-to-End Performance Aware Association in Wireless Municipal Mesh Networks", in *Proc. of IEEE Globecom, workshop on wireless mesh and sensor networks*, pp. 1-6, Washington DC, Nov 2007.
- L. Luo, M. Gruteser, H. Liu, D. Raychaudhuri, K. Huang, S. Chen, "A QoS Routing and Admission Control Scheme for 802.11 Ad Hoc Networks", in *Proc. of Mobicom DIWANS workshop*, pp. 19-28, Los Angeles, CA, Sept 2006.